Distribution Agreement

The role of calcineurin in the recovery of cognitive function following isoflurane anesthesia

By

Iris Ann Speigel
Doctor of Philosophy

Graduate Division of Biological and Biomedical Sciences
Neuroscience

____
Paul S. García, MD PhD
Advisor

____
Andrew Jenkins, PhD
Advisor

____
Jennifer L. Gooch, PhD
Committee Member

____
Randy A. Hall, PhD
Committee Member

____
William R. Tyor, MD
Committee Member

____
James Q. Zheng, PhD
Committee Member

Accepted:

____
Lisa A. Tedesco, Ph.D.
Dean of the James T. Laney School of Graduate Studies

____
Date

The role of calcineurin in the recovery of cognitive function following isoflurane anesthesia

By

Iris Ann Speigel
B.S., University of Maryland, 2010

Advisor: Paul S. García, MD PhD
Advisor: Andrew Jenkins, PhD

An abstract of
a dissertation submitted to the Faculty of the
James T. Laney School of Graduate Studies of Emory University
in partial fulfillment of the requirements for the degree of
Doctor of Philosophy

Graduate Division of Biological and Biomedical Sciences
Neuroscience
2017

Abstract

The role of calcineurin in the recovery of cognitive function following isoflurane anesthesia

By Iris Ann Speigel

General anesthesia, while indispensable for modern healthcare, is suspected as a factor in cognitive dysfunction. Elevated hippocampal surface expression of the $\alpha_5\beta_3\gamma_2$ $GABA_A$ receptor ($GABA_AR$) subtype is implicated in memory and synaptic plasticity impairments that persist over a week beyond a brief exposure to isoflurane anesthesia in rodent models. The exact mechanism is unknown, but neuroinflammation has been implicated.

Calcineurin (CN), a calcium-dependent phosphatase that is active during isoflurane exposure, has been mechanistically linked to neurodegeneration and neurotoxicity. CN is also directly involved in synaptic plasticity as a regulator of $GABA_AR$ trafficking as well as activity-dependent changes in gene expression and protein synthesis. Calcineurin inhibitors such as cyclosporine A (CSA) are standard of care for immunosuppressive therapy, but the potential for chronic use to affect recovery from anesthesia is unclear.

We explored the potential impact of CSA on cognitive outcomes following isoflurane anesthesia. In an *in vivo* model, mice given thirty minutes of isoflurane within a chronic CSA treatment paradigm have aberrations in the production and surface expression of α_5 containing receptors in their hippocampus, and behaviorally have significant deficits in visuospatial learning. Further analysis of protein expression also revealed a decrease in GAD-67 and α_5 total protein, suggesting that changes in inhibitory signaling occur alongside altered $GABA_AR$ surface expression. *In vitro* experiments in primary hippocampal neurons measuring $GABA_AR$ surface expression in response to isoflurane demonstrate no acute effect with a one-hour exposure, regardless of CSA pretreatment, suggesting that *in vivo* memory-impairing aberrations in surface expression manifest post-operatively (e.g during or after emergence).

Our results confirm the work of others that isoflurane induces changes to inhibitory network function and exclude CN inhibition as an intervention. Rather, these findings identify calcineurin inhibitors as a previously unknown risk-factor for the development of post-operative cognitive dysfunction, and identify patients receiving CSA for immunosuppression (e.g. prior to organ transplantation) as a vulnerable group.

The role of calcineurin in the recovery of cognitive function following isoflurane anesthesia

By

Iris Ann Speigel
B.S., University of Maryland, 2010

Advisor: Paul S. García, MD PhD
Advisor: Andrew Jenkins, PhD

A dissertation submitted to the Faculty of the
James T. Laney School of Graduate Studies of Emory University
in partial fulfillment of the requirements for the degree of
Doctor of Philosophy

Graduate Division of Biological and Biomedical Sciences
Neuroscience
2017

Table of Contents

Index of Figures and Tables

Index of Abbreviations

ACSF	artificial cerebro-spinal fluid
AMPA	α-amino-3-hydroxy-5-methyl-4-isoxazolepropionic acid
ANOVA	analysis of variance
APV	(2R)-amino-5-phosphonovaleric acid
BCA	bicinchoninic acid assay
BIS	Bispectral index
β-ME	β-mercaptoethanol
BZD	benzodiazepine
CA1/3	cornu ammonis subfields 1/3
CN	Calcineurin
ΔCN-48	Calcineurin 48 kD truncated protein
CNQX	6-cyano-7-nitroquinoxaline-2,3-dione
CNS	central nervous system
CREB	cAMP response element-binding protein
CSA	Cyclosporine A
DAG	diacylglycerol
DIV	days *in vitro*
DG	dentate gyrus
DMSO	dimethyl sulfoxide
EEG	electroencephalography
ER	endoplasmic reticulum
GABA	γ-Aminobutyric acid

$GABA_AR$	γ-Aminobutyric acid receptor, type A
GAD-67	glutamic acid decarboxylase, 67 kilodalton isoform
GAPDH	glyceraldehyde 3-phosphate dehydrogenase
HBS	HEPES-buffered saline
HBSS	Hanks' balanced salt solution
HCN1	K^+/Na^+ hyperpolarization-activated cyclic nucleotide-gated channel 1
HEK	human embryonic kidney cells
HEPES	(4-(2-hydroxyethyl)-1-piperazineethanesulfonic acid
IL-1 β	interleukin-1 beta
IL-2	interleukin-2
IP3R	inositol trisphosphate receptor
IPSC	inhibitory post-synaptic current
ISO	isoflurane
LORR	loss of righting reflex
LTP	long-term potentiation
MAC	minimal alveolar concentration
MAP-Kinase	mitogen-activated protein kinase
MCS	minimally conscious state
MEF-2	myocyte enhancer binding factor 2
MEM	minimal essential media
MPTP	mitochondrial transition pore permeability
NFATc	nuclear factor of activated T-cells, cytoplasmic
NMDA	N-Methyl-D-aspartic acid receptor

PIP2	phosphatidylinositol 4,5-bisphosphate
PKC	protein kinase C
POCD	post-operative cognitive dysfunction
PVS	partially vegetative state
REM	rapid-eye movement
RIPA/PI	radioimmunoprecipitation assay buffer with proteinase inhibitor
RM 2-way ANOVA	repeated measures two-way ANOVA
SDS- PAGE	sodium dodecyl sulfate polyacrylamide gel electrophoresis
SEP	super-ecliptic pHluorin
STAT3	signal transducer and activator of transcription 3
TBS	tris-buffered saline
tdTomato	tandem tomato
TMN	tuberomammillary nucleus
TRESK	potassium channel subfamily K^+ member 18
TRIS	tris(hydroxymethyl)aminomethane
VEH	vehicle
VGA	volatile gas anesthetic
WRAM	water radial arm maze

Chapter 1:
Introduction

A portion of this chapter was prepared for submission as “The anesthetic implications of anatomical specificity and pharmacologic influence of $GABA_AR$ Subtype expression” by I Speigel and PS García.

1.1 Introduction to neuroscience research in anesthesia

Millions of medical procedures are performed with general anesthesia every year [1], with an estimated 60,000 recipients per day in the US alone in 2010 [2]. Although modern healthcare is absolutely dependent on anesthetic agents, their long-term impact on cognitive function is unclear. Clinical and experimental studies have begun to suggest relationships between the use of anesthetics and the development of adverse cognitive changes –however both patients and animal models exhibit variable penetrance. Currently, pediatric and geriatric populations appear to be the most vulnerable.

One important motivation among neuroscience researchers interested in anesthesiology mechanisms is to understand the full physiological and cognitive consequences that occur after the cessation of anesthesia. What is becoming quickly apparent in anesthesia research is that the brain does not deal with recovery from anesthesia passively, and that trajectories for recovery of cognitive function following anesthesia are complex and heterogeneous between individual patients. Emergence from anesthesia increasingly appears to be an active and dynamic process whereby the brain "reboots" after unconsciousness [3]. Within individual neurons, there is evidence that anesthetics induce changes in the intracellular signaling pathways that control cellular function and survival, including neurotransmitter receptor expression. There increasing evidence that anesthetic agents have the potential to cause long-lasting changes in neurophysiology, which has serious implications for basic and clinical sciences alike. A comprehensive understanding of these processes will be necessary for predicting how persistent adverse effects in neurological function arise, and determining what factors underlie resilience to the effects of anesthetics.

In this thesis, I explored the impact of Cyclosporine A, a commonly prescribed immunosuppressant drug, on cognitive outcomes following isoflurane anesthesia. To preface these studies, this introductory chapter will describe several concepts that contextualize anesthesia research. First, I will review the phenomenology of loss of consciousness from anesthesia, describing current theories of neurophysiological and pharmacological mechanisms of general anesthetic action, and their relation to understanding consciousness at large. Next, I will describe how anesthesia arises from the pharmacological actions on neuronal ion channel function, and the importance of $GABA_AR$ receptor ($GABA_AR$) functional diversity and subtype specificity in generating the behavioral endpoints of anesthesia. Then, I will summarize our current understanding of the intracellular mechanisms of $GABA_ARs$ trafficking, how these mechanisms are recruited by external stimuli and physiological conditions, and how these trafficking changes impact behavior. This summary will include a discussion of how $GABA_AR$ subtype heterogeneity underlies important subtype-specific functional and trafficking properties relevant to anesthesia. To introduce the rationale of our experiments, I will discuss evidence for the role of inflammation in the development of cognitive dysfunction following anesthesia, including mechanisms impacting $GABA_AR$ trafficking. Finally, I define the hypotheses and the experiments of this thesis and outline the structure of the rest of this document.

1.2 The study of consciousness: specific challenges and experimental approaches

The study of consciousness can be viewed as two different problems. First, there is the “hard problem”, of how exactly our internal conscious experience arises from the firing patterns of neurons, or why is there a subjective experience of external events [4]. Prior to the development of modern neuroscience, this was mainly debated philosophically, in the form of the mind-body problem, of how the seemingly non-physical mind is related to the physical body. Thomas Nagel famously cast this issue as a rhetorical question: what is it like to be a bat, and why? He himself argued that its fundamentally impossible to imagine what it is like to be a bat, even with perfect knowledge of the brain [5].

In light of such a challenge, most researchers focus instead on the so-called "easy problems" of how nervous systems operate, which are comparatively more tractable with modern experimental techniques. In principle, an increased understanding of the "easy problems" should inform the "hard problem": consciousness, whether it is an emergent property of complex systems or unique to humans, is a phenomenon that must be based in physiological processes, specifically arising from the structure and connectivity of the brain. Thus an increased mechanistic understanding of the brain and other components of conscious nervous systems should allow us to *infer* what consciousness is *like*. In terms of understanding what is qualitatively like to be a bat, we could use information about the sensory functions and cognitive capacity of the animal to infer components of its conscious experience. This rationale justifies the use of animal models, which enable the reductionist approaches that have been instrumental for understanding the functional circuitry/neurophysiology of brain regions that are critical for various aspects of consciousness.

To approach consciousness from a human-specific perspective instead, some researchers investigate the "neural correlates of consciousness"- the minimum neural mechanisms required for the subjective experience of consciousness, in awake human subjects[6]. Much of this research has relied on correlating functional measures of brain activity (e.g. fMRI) with self-reported internal states during cognitive tests or illusions. The difficulty with this model is that the act of reporting private subjective information requires its own processes (e.g. introspection or self-reflecting on emotional processes, metacognition, or thinking about thinking, and verbal communication or language usage), so correlated functional data may over-represent the most fundamental conscious neural processes. For this reason, "no-report" models, whereby indirect physiological responses such as pupil dilation are measured instead, are gaining favor as alternatives that potentially control for these variables [6, 7]. For a more direct approach, anesthetics allow researchers a means to experimentally manipulative consciousness as a independent variable within functional studies [8]. The principal aim is to identify the neural correlates of consciousness by identifying brain activity changes that correspond with transitions between conscious states, e.g. at the anesthetic loss of consciousness. To adjust the temporal resolution of imaging during state transition, the rate of drug delivery can be precisely controlled, e.g. administering intravenous anesthetics as a slow transfusion. Example results of one such study are discussed later in section 1.2.5: Neurophysiology of anesthetic loss of consciousness, and shown in **Figure 1.2.** Thus, anesthetics have the potential to be an important research tool for studying the neurobiology of consciousness.

Like other branches of neuroscience, consciousness (and unconsciousness) research has had great insight from human patients. Neurological phenotypes of interest include seizure disorders, patients in a persistent vegetative state or a minimally conscious state, patients during or after brain injury/ operations, and patients under anesthesia. A conceptual representation of these various states of consciousness, each having differences in recovery, is shown in **Figure 1.1**. As depicted, one fundamental determinant of the conscious state is the level of arousal, which refers to the physiological state generated by the combined effects of endocrine, brainstem neuromodulators, and autonomic influence on the forebrain. Behaviorally, it is often quantified as the magnitude of the stimulus necessary to evoke some response, e.g. eliciting a response from an awake, attentive person requires less provocation than someone who is asleep or drowsy. The persistent vegetative state, or more accurately, unresponsive wakefulness, does exhibit some features of arousal such as circadian rhythms and recognizable sleep cycles. Minimally conscious states show more cognitive function and more meaningful responsiveness to stimuli, with fluctuating levels of lucidity. Because of the difficulty of discerning purposeful versus reflexive behavioral responses, these distinctions can be unclear even with the aid of functional brain imaging [9]. Regardless, from these medical conditions it is clear that arousal, wakefulness, and responsiveness, are dissociable phenomena with overlapping and integrated but non-redundant neural systems. Living and post-mortem neuroanatomical study have demonstrated the critical importance of several projection systems (e.g. the thalamo-cortical loop and the reticular activating system) and their associated nuclei (e.g. tuberomamillary, ventral-lateral pre-optic nucleus, thalamus etc.) with the maintenance of consciousness [10]. Perhaps unsurprisingly, many of these regions have been revealed as targets of anesthetics, as reviewed later in this chapter in section 1.8 Specific $GABA_AR$ subtypes in neuroanatomical regions important to anesthesia.

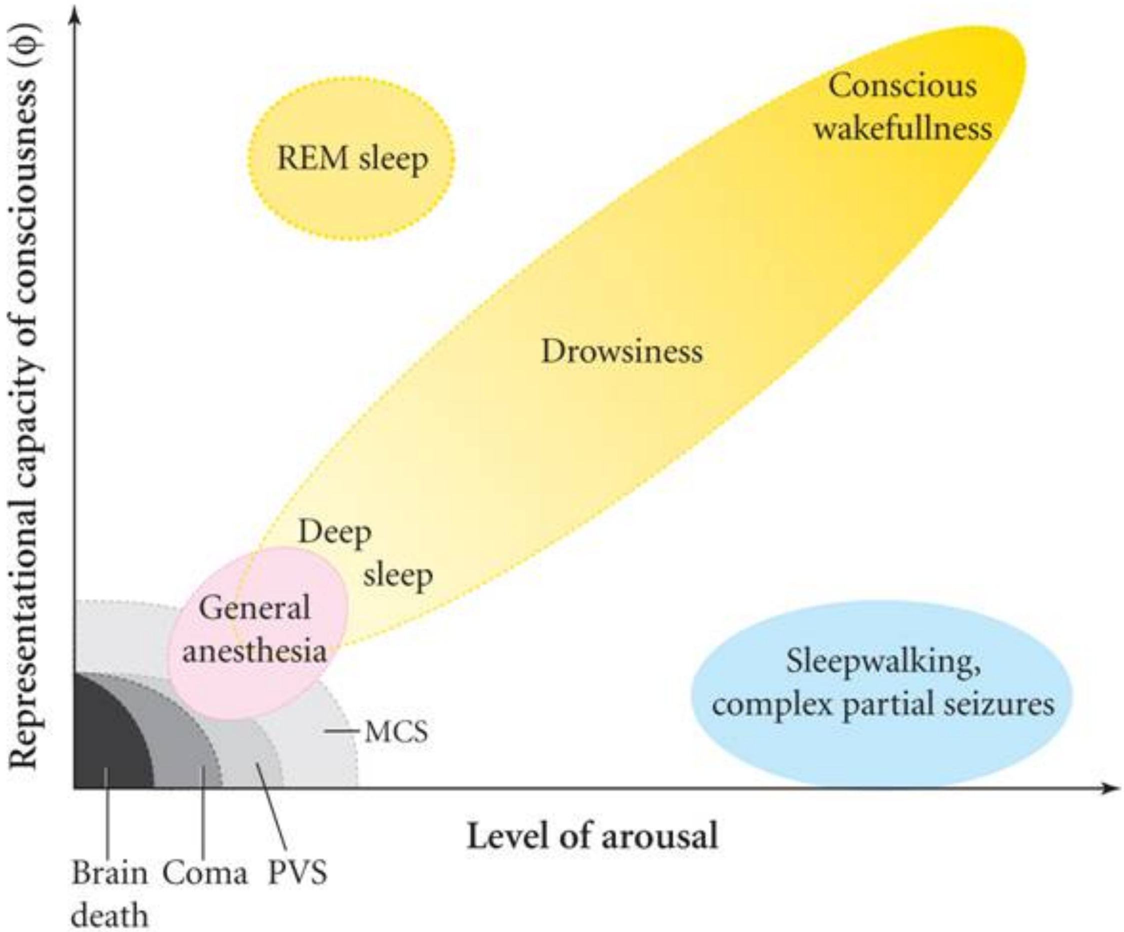

Figure 1.1 Theoretical representation of conscious states Figure from Laureys, 2005 [9]. The yellow states are naturally occurring and reversible. The state of general anesthesia (pink) is iatrogentically induced and reversible. The blue states are potentially pathological but generally reversible. The grey/black states are pathological and rarely reversible.

Figure 1.1 Theoretical representations of conscious states from Laureys, 2005 [9], illustrates a spectrum of conscious states that manifest during health and disease. Arousal level (**X-axis**) is a physiological feature from several neurochemical influences on the forebrain (e.g. cortisol and neuromodulators) with correlates in metabolic or brain activity. Representational capacity of consciousness (**Y-axis**) describes informational content, which theoretically accounts for the richness or vividness of experience. Proponents of the information theory of consciousness (fully described in the following section) have suggested that this idea can be described with a computational metric called the perturbational complexity index (ϕ). When calculated using a weighted measure of cortical TMS and EEG based recordings of signal differentiation and integration, ϕ measures can distinguish between dissociative states brought about by certain drugs and anesthetics like ketamine, which allow for extremely rich and elaborated but disorganized sensory perceptions that lack the dimensions of the environment and the sense of self within it or "self-consciousness".

Arousal and conscious content (however described) are clearly dissociable. For example, REM sleep is characterized by both wake-like dreams (experience) and reduced arousal. Conversely, episodes of parasomnia or complex partial seizures can include complex behaviors, even to the extent of interacting with and maneuvering through the external environment, with little or no recall of the experience. The clearest examples of "consciousness disorders" are in patients diagnosed with persistent vegetative state (PVS) or a minimally conscious state (MCS), although clinical distinctions can be difficult.

1.2.1 Anesthetics and theories of consciousness

The most fundamental problem in understanding mechanistically how anesthetics affect consciousness is the difficulty in describing how consciousness itself works. For this section, I will introduce two current leading theories of consciousness in order to contextualize how anesthetics are thought to disrupt consciousness. Naturally, there will be a bias for theories that fit with what we currently know about the neurophysiological properties of anesthetic drugs.

One hypothesis for a cognitive framework for consciousness is the global workspace theory popularized by Baars and colleagues [11], which essentially proposes a decentralized information sharing system, based on neural networks anatomically distributed throughout the brain and especially the cortex [6]. The global workspace concept itself originates from artificial intelligence, and refers to a transient memory domain that is simultaneously accessed by various specialized programs- not dissimilar to random access memory in a computer. This theory is robust because it is consistent with what we know about the cortex and about higher-order cognitive processes, but it is not inherently specific about how these processes are generated by the electrochemical behavior of neurons.

Another prominent paradigm is the integrated information theory (Tononi & Edelman), which proposes that the levels of consciousness held by a nervous system or neural network is instantaneously dictated by the number of possible informational states it has and how tightly integrated those states are, which in principal can be mathematically calculated as a value phi (ϕ)[12]. This theory does have the capacity to explain several counterintuitive features of consciousness. For example, consciousness is lost during a seizure although neural activity increases, potentially because the number of possible neuronal informational states (e.g. diversity of neuron firing patterns) decreases.

Neurophysiologically, each of these frameworks would be dependent on sustaining high amounts of activity through extensively recurrent synaptic connections between frontal and sensory cortices [6]. This type of activity is termed reverberatory, because initial sensory stimuli are echoed, or are repeatedly circulating throughout the brain in some processed form. This activity is supported by “background neurophysiological mechanisms”. Some of these mechanisms serve physiological minimal requirements, such as the metabolic need for an appropriate supply of glucose and oxygen to maintain neurotransmission and basic cellular function. For example, brain anoxia causes unconsciousness but oxygen levels *per se* are not part of our subjective experience. There are also factors that are necessary to keep neuronal activity within an operational range for conscious processes including neuromodulators, and excitatory drive to the cortex from thalamic and cortical afferent inputs.

The predominant theory of how anesthesia collapses these connections is by disrupting cortico-cortico and cortico-thalamic information processing. Here, I will give a description of how we think anesthetics induce unconsciousness in terms of neuronal information processing. The neurophysiology of these processes is greatly simplified here but will be explained in depth later in this chapter. Anesthetics do not specifically inhibit consciousness itself, but instead appear to destabilize the background neurophysiological mechanisms that in turn disrupt larger networks of functional integration, which maintain consciousness. Anesthetics act directly to hyperpolarize neurons by modulating the ion channels that control neuronal excitability, thereby initiating a cascade of neurophysiological changes that follow lead to unconsciousness. Pharmacological depression of excitation itself promotes further neuronal deactivation by diminishing excitatory drive from afferent inputs to cortical and cortico-thalamic networks. The “tipping point” is thought to be when oscillatory bursting and then highly synchronized slow-wave high-amplitude activity (characteristic of non-REM sleep) replaces the highly active and desynchronized low-voltage population activity. Because of their intrinsic electrophysiological properties, like hyperpolarization-gated conductances, thalamic neurons that project to the cortex are particularly prone to being recruited into this process [13].

The theoretical significance is that this transition in firing behavior reduces the amount, complexity, and transfer of information, possible in the neural network. Signal complexity among individual neurons simplifies, as stereotyped patterns of firing provide a narrower range of post-synaptic electrical patterns. In addition to a theoretical loss of computational power for synaptic integrations, experimental measures of information transfer suggest that anesthesia depresses communication between cortical regions [14]. Of the many studies of functional connectivity measured during anesthetic induction, this feature of cortical disconnect seems to be a mechanism common to many pharmacologically distinct anesthetics (very recently and thoroughly reviewed in [15]). However, the local functions of smaller cortical circuits persist. During anesthesia, deep sleep, and minimally conscious or vegetative states, evoked EEG potentials can be measured from primary sensory cortices; representing the first-order brain response to incoming sensory information potentially because these local circuits are “idling”.

Processes going on in deeper brain regions, especially subcortical structures and the hippocampus remain a mystery. Empirically, less is known because scalp EEG recordings from patients effectively only measure potentials immediately below the skull, specifically an over-representation of the ensemble electric potentials summed at the apical dendrite of cortical layer five pyramidal neurons. Activity in deeper brain regions can only be inferred by how they affect these cortical neuron potentials. Animal models, where intracranial electrodes can be placed in these regions, are naturally limited in their capacity to report consciousness through surrogate measures. During the process of anesthesia, the release of arousal neuromodulators from their origin nuclei onto their projection targets in the forebrain is attenuated, along with activity in these regions. The exact order and causal relationships between activity changes in the thalamus, cortex, and brainstem, as they occur during anesthesia, are not completely resolved.

In summary, one salient characteristic of consciousness is that it is reversible with anesthetics. Within the neural networks that underlie consciousness, anesthetics do not stop neuronal activity altogether but rather modulate it. This results in a temporary fragmentation of higher-order processing, leading to a dissociation of information processing among brain regions. Understanding the process by which anesthetics alter the signaling among these regions may hold the key to understanding and treating disorders of consciousness. However, one limitation to a better understanding of anesthetized neural states is an imperfect understanding of the underlying pharmacologic mechanisms of anesthetic agents.

1.2.2 A history of clinical anesthesia

In order to put anesthesia pharmacology in context, I will present a brief history of clinical anesthesia. Perhaps because serendipity and empiricism determined the innovations of anesthesia, many mysteries of producing unconsciousness and regaining consciousness remain elusive. For most of human existence, surgery was uncommon and painful. The earliest attempts to interfere with consciousness in preparation for an operation were plant-based extracts containing psychoactive compounds. These locally sourced treatments varied greatly in efficacy. For example, the Incas' use of coca leaf solution was prescient in the use of cocaine as a local anesthetic [16].

Early formulations for general anesthesia were often dangerous but contained powerful compounds with recognizable pharmacology. Examples include plants like belladonna, wolsbane, and nightshades, like mandrake, which are sources of cholinergic drugs like atropine, scopolamine, and alkaloids. Hanaoka Seishu performed the first documented cancer resection surgery with anesthesia, a partial mastectomy, with a more comprehensive version of this mixture in Japan, in 1804 [17]. In the west, sponges soaked in similar herbal mixtures (supplemented with opium and poison hemlock) could be attached to the face for inhalation. However, these drugs are also potent neurotoxins, so death by overdose was common. Until the mid 1800s, the standard of care in the industrialized western world was alcohol with opium or morphine.

This process was revolutionized in the 1840s by ether. At the time, ether was a popular recreational substance, and for some, these "ether frolics" were rationalized as an alternative to alcohol. After its initial synthesis in 1540 from ethanol and sulfuric acid, ether was used for entertainment purposes for hundreds of years before being applied to surgery. Crawford Long was the first clinician to use of ether for anesthesia in 1842 in Jefferson, Georgia [18]. Despite the success of these experiments, he declined to widely publicize his findings. Some attribute this to his moral concern about contributing to ether addiction, other believe it was out of a fear of repercussions for treating slaves with advanced techniques [19].

In parallel, William Morton introduced ether into his own dental practice after preliminaries studies on himself and his pet terrier. In 1846, he performed the first public demonstration of a successful painless operation with ether at the Massachusetts General Hospital in Boston [18]. Within a month of his exhibition, ether was in regular use in other US cities and in Great Britain. Around this time, another commonly abused inhalant, nitrous oxide, was also introduced for intraoperative pain relief. Nitrous oxide produces euphoria and analgesia, but not unconsciousness or immobility. The apocryphal origin story is that Gardner Quincy Colton was inspired by a “friend” who was sustained a serious leg injury during intoxicated dancing, but registered no pain and continued [20]. These qualities render it a useful drug even today for many types of procedures.

The reinvention of ether from a drug of abuse to an essential medicine revolutionized surgery, but as a drug it had imperfections. Ether reacts with air and light or heat to form explosive peroxides, and operating room fires and explosions were a serious problem [18]. Chloroform, which was less flammable and less nauseating, briefly replaced ether until its cardiac and hepatic toxicity became apparent. Another breakthrough came with the mastery of intravenous anesthetic agents (sodium thiopental) by Lundy and Waters in 1930s, the advantage of which being its rapidity of induction. Today, anesthesia is typically initiated by the intravenous agent propofol.

The other main pharmacological component of the modern anesthetic drug plan came in a series of discoveries spanning 1950-1990. Breakthroughs in fluorine chemistry, stemming from the Manhattan project, enabled the synthesis of halogenated (non-flammable) ether analogues, including halothane and several drugs that are used today: isoflurane, desflurane, sevoflurane [18]. The discovery process for this generation of volatile agents was a thorough and systematic screening program that synthesized and tested >700 candidate novel compounds [21]. Today, fluorescent and photosensitive anesthetics and anesthetic analogues have enabled the introduction of high-throughput small-molecule assays as a means of discovering new anesthetic compounds, and may also accelerate large scale discovery of their protein targets [22, 23].

Monitoring the end-target organ of anesthesia has a more modern history. In the 1980s and 1990s, brain-monitoring technology started to enter routine clinical anesthesia practice[24]. Forehead scalp electroencephalogram (EEG) can non-invasively measure the spontaneous brain activity from the superficial layers of the cortex and the changes that occur during surgery. Hans Berger first described the characteristic effects of general anesthetics on the EEG shortly after his development of the technology in the 1920s. Through advances in computer miniaturization and neuroscientific knowledge, the EEG was introduced to the operating room in the 1980s. The first commercially available device to help approximate depth of anesthesia was introduced in 1992. Although this Bispectral index (BIS) monitor currently has the largest market, share several competitor devices exist and the routine use of such devices as a “standard” monitor remains controversial [25]. At its simplest, the Bispectral index is a statistical analysis of several forebrain EEG waveform features that reports an awareness level as a single dimensionless number between 0 and 100. The BIS algorithm was developed with recordings from over a thousand patients collected throughout the course of anesthetic induction. The theoretical advantage of the BIS index is to titrate intra-operative hypnosis, however, other studies have determined that brain function monitors help minimize the amount of anesthetic delivered and decrease the time required for clinical emergence and recovery [25]. Many creative uses have been attempted or suggested for the BIS and other similar devices, ranging from monitoring the critically ill to the humane administration of lethal injections, the subject continues to be openly debated.

1.2.3 A history of anesthetic theories and mechanism

The first long-reigning hypothetical mechanism of anesthesia was the Meyer-Overton "lipid partition" theory, based on the observed linear correlation between an anesthetic agent's potency on an animal (tadpole) and its lipid solubility, specifically the olive-oil/ water partition coefficient [18]. Perhaps inspired by the contemporary discovery of the role of lipids in the dynamic fluidity of the plasma membrane, the idea was that anesthetic agents work by dissolving into the neuron cell surface and altering its functional properties somehow. This theory existed for decades before being soundly repudiated. Briefly, the main problems were that at clinically relevant concentrations, the actual effect on lipids is actually very small, that higher temperatures decreases anesthetic potency, and that for chiral agents there was stereo-selectivity [26].

The lipid paradigm was overthrown by a series of experiments demonstrating that specific binding to cavities within proteins was an alternate and superior hypothesis. As a proof of principal, a variety of anesthetics were shown to bind and inhibit the firefly lucerifase enzyme, with an inhibitory potency that correlated with anesthetic potency just as well as lipid solubility. In effect they had reproduced the Meyer-Overton correlation with a random soluble protein [27]. Also damning was the "cut-off effect" which showed that when considering the anesthetic potency of a series of chemically homologous agents made of increasingly longer carbon chains, the potency positively correlates with size, until its anesthetic effect is lost altogether. This is difficult to explain with a model of solubility, but sensible when the model is instead a protein cavity with a set size.

The $GABA_AR$ emerged as a target following the discovery that barbiturate anesthetics allosterically enhance native chloride currents [26]. With the advent of heterologous expression systems, $GABA_AR$ subunit-specific sensitivities to GABA and anesthetics could be characterized for all the possible subunits and pentameric receptor combinations. This system also opened the door for the direct testing of anesthetic binding sites using site-directed mutagenic experiments. Using this approach, the putative binding sites for the intravenous anesthetics propofol and etomidate [28] were first identified.

Identifying structure-function relationships of the volatile agents and their protein targets is inherently more difficult for several reasons. It is technically more challenging to deal with gases for *in vitro* experiments (described in detail in chapter 5). The volatiles also exhibit much less pharmacology potency and more off-target effects due to promiscuous interactions at many proteins. Using a chimeric α_1 receptor containing regions imported from a rare $GABA_AR$ subtype (rho) that is naturally insensitive to volatile anesthetics, two critical amino acids for allosteric modulation were identified within two different transmembrane domains, far remote from the GABA ligand-binding site [29]. Because data suggests that volatile anesthetic binding itself does not change protein conformation, the classical lock and key model is limited in explaining the biophysical means of allosteric modulation. Kinetic and structural modeling suggests that instead, anesthetics alter the way in which the entire heteromeric protein undergoes conformational change in response to ligand binding. The movement in the flexible extracellular loops that connect the transmembrane alpha helices is suspected [26].

A landmark *in vivo* demonstration that anesthesia is unambiguously dependent on the physical interaction of anesthetic agents binding to discrete locations on $GABA_A$Rs, was the generation of a transgenic mouse resistant to intravenous but not volatile anesthetics. A single point mutation in the β_3 subunit (N265M) can abolish propofol and etomidate hypnosis, while largely preserving the enflurane and halothane response [30]. This experiment demonstrates that extremely specific interactions between the $GABA_A$R and anesthetic agents are fundamental for anesthesia, an outcome predicted by $GABA_A$R site-directed mutagenesis experiments in recombinant systems [29].

1.2.4 Neurophysiology of anesthetic loss of consciousness

Anesthesia can be defined as a pharmacologically induced state intended to reduce or eliminate both conscious awareness of the environment and the perception of unpleasant sensory stimuli. Anesthesia is usually associated with a clinical environment, such as surgery. Administration of anesthetic drugs results in a temporary disruption of normal cognitive processing. Although many exogenous and endogenous factors can produce perceptual disturbance via a promotion of abnormal brain activity (e.g. seizures, or pharmacologic interference with information transfer among brain areas) most anesthetic agents in common use, depress neuronal activity among cortical and non-cortical areas through an augmentation of inhibitory signaling.

Neuronal information transmitted among different brain regions typically involves long-range excitatory projections that synapse onto neuronal populations heavily interconnected with local inhibitory interneurons. As inhibition increases, propagation of neuronal information decreases and information critical for forming consciousness is lost. Additionally, specific brain regions exhibit a reduction in the complexity of their firing patterns with increased inhibition and begin to organize into synchronous patterns of burst firing observable as EEG oscillations. After achieving a sufficient brain concentration of anesthetic drug, the subject is considered to be unconscious, and unable to process sensory input. At this point the brain exists in a very low energy state. This can be observed as a global reduction in cortical metabolism and a state that phenotypically resembles natural sleep (**Figure 1.2**). Because of the obvious similarities, this facet of anesthesia is sometimes referred to as hypnosis. However, important distinctions are observed between sleep and anesthesia (see later sections).

Anesthetic drugs that do not exert their main clinical effects through increases in inhibitory signals (e.g., ketamine, nitrous oxide, xenon) result in observed clinical behavior that does not closely mimic natural sleep [31]. These drugs disrupt neuronal communication but do not result in low energy states for the brain. The result is a different anesthesia phenotype, where the patient is unaware of themselves and their surroundings, but not entirely quiescent, thus is has been described as a dissociative anesthetic state. The use of drugs that produce this type of anesthesia are comparatively rare and will not be given much consideration in this research description.

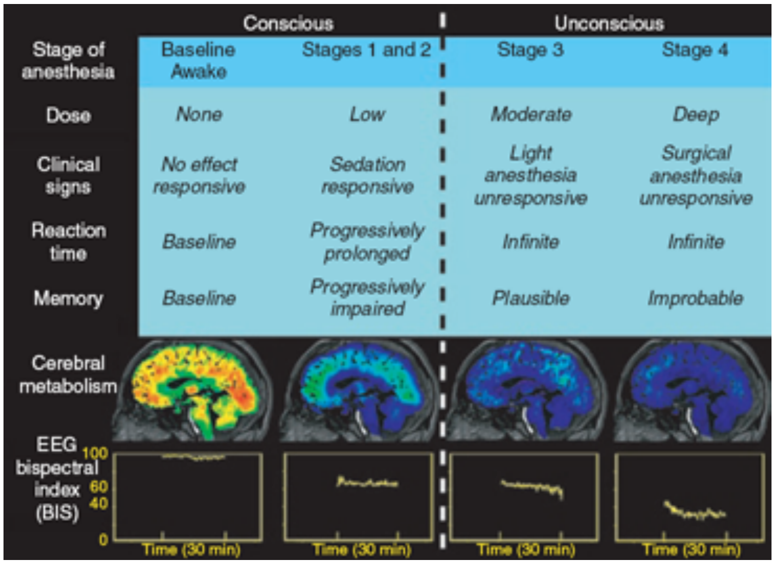

Figure 1.2 Cerebral metabolism during the progressive induction of anesthesia.

Figure 1.2 Cerebral metabolism during the progressive induction of anesthesia. Figure from Alkire, 2008 [32]. Behavior at four clinical stages of anesthesia, with paired 13C glucose PET scans. The fully conscious state (**left**) requires a high level of brain energy. The main metabolic cost is neurotransmission, specifically action potential generation and glutamate neurotransmitter cycling. The deeply anesthetized brain (**right**) is in a comparatively low-energy state. When PET and BOLD fMRI measures of relative changes in activity are calibrated using spectroscopy of 13C glucose metabolites, both suggest ~50% reduction during anesthetic loss of consciousness [13]. In the bottom row, the output from a common processed EEG signal, the bispectral or BIS index value, is shown for each stage and brain. Note the relative similarity between Level 2 (conscious but unresponsive) and level 3 (unconscious and unresponsive). Perhaps not unsurprisingly, the neurophysiological correlates for this transition are difficult to parse even with complex statistical modeling.

1.3 Anesthesia considerations for surgery

Since its inception, the field of anesthesia changed medical care because it allowed us to deal with physical pain in a radically different way. To describe the revolutionary effects of ether, Oliver Wendell Holmes was inspired by classical linguistics as to create a new name for this type of consciousness "Anaesthesia", or without sensation in Greek. However, unconsciousness is just one facet of the anesthetized state that is typically requested for a preferred surgical experience. Clinical anesthesiologists must contend with the physiological consequences of their anesthetic drugs, provide optimal conditions for surgery, and respond quickly to restore homeostasis in response to surgical manipulation or underlying pathology. In addition to unconsciousness, there needs to be analgesia, immobility, and intra-operative (retrograde) amnesia. Physiologically, this is caused by a progressive depression of the central nervous system by mechanisms specific to the anesthetic agent [10, 33]. Analgesia or loss of pain is produced by inhibition of neurons in the spinal cord, particularly dorsal horn nociceptors. Immobility, or the suppression of motor and autonomic somatosensory reflexes, is produced by inhibition of the spinal reflex pathways [34]. Amnesia is a result of the disruption of hippocampal learning and memory circuits.

Typically, an intravenous agent is used to induce unconsciousness, and then an inhalational agent is used to maintain a depth of anesthesia appropriate for the procedure, one of the most common combinations being propofol followed by isoflurane. At its simplest, the depth of anesthesia is measured based on clinical vital signs and autonomic responses including heart rate, blood oxygen saturation, respiratory patterns, and blood pressure. However, these measures are indirect with respect to the brain. To increase control of the depth of anesthesia, these physiological measures are augmented by the use of monitoring functional brain activity using EEG recordings or monitors that process these EEG recordings (see BIS discussion above), usually from the forebrain scalp.

Emergence from anesthesia, or return of consciousness, occurs after agent delivery is stopped. The simplest explanation for this phenomenon is pharmacokinetics: the effect of hypnosis leaves as the drugs are cleared from the nervous system. However, there is evidence that emergence is a more active neurological process whereby the brain transitions between discrete activity states in a reproducible sequence [3]. Recent advances in receptor pharmacology have also allowed us to actively modulate this period with anesthetic reversal agents such as flumazenil [35], methylphenidate (Ritalin)[36], and neostigmine [37].

1.3.1 The overlap between sleep, coma, and anesthesia as EEG patterns

Sensory information from the external world is integrated in specific thalamic nuclei before complex processing by the cortex. The interaction between the thalamus and cortex is critical for behaviors we consider evidence of consciousness. During slow-wave sleep, hyperpolarized thalamic relay neurons cause slow oscillations that entrain cortical neurons. This pattern is indicative of a reduction of complex processing of thalamic information by cortical neurons and is observable as delta (0.5-4 Hz) and/or alpha oscillations (8 – 12 Hz) in encephalopathy, slow-wave sleep and in anesthesia. During anesthesia, EEG recordings of anesthetized patients typically show either these slow waves or "burst suppression" spectral patterns where high frequency activity is interleaved with periods of very slow or flat-lined “isoelectric” electrical activity [2] [38].

These isoelectric EEG epochs, characteristic of comatose brains, are never found in natural sleep patterns and thought to be an effect of very deep anesthesia. Despite use of the euphemism “going to sleep” to describe the start of anesthesia, this process is not restorative or refreshing, and the increasing evidence suggests that anesthesia is a neurological challenge. These EEG patterns are illustrated in **Figure 1.3.**

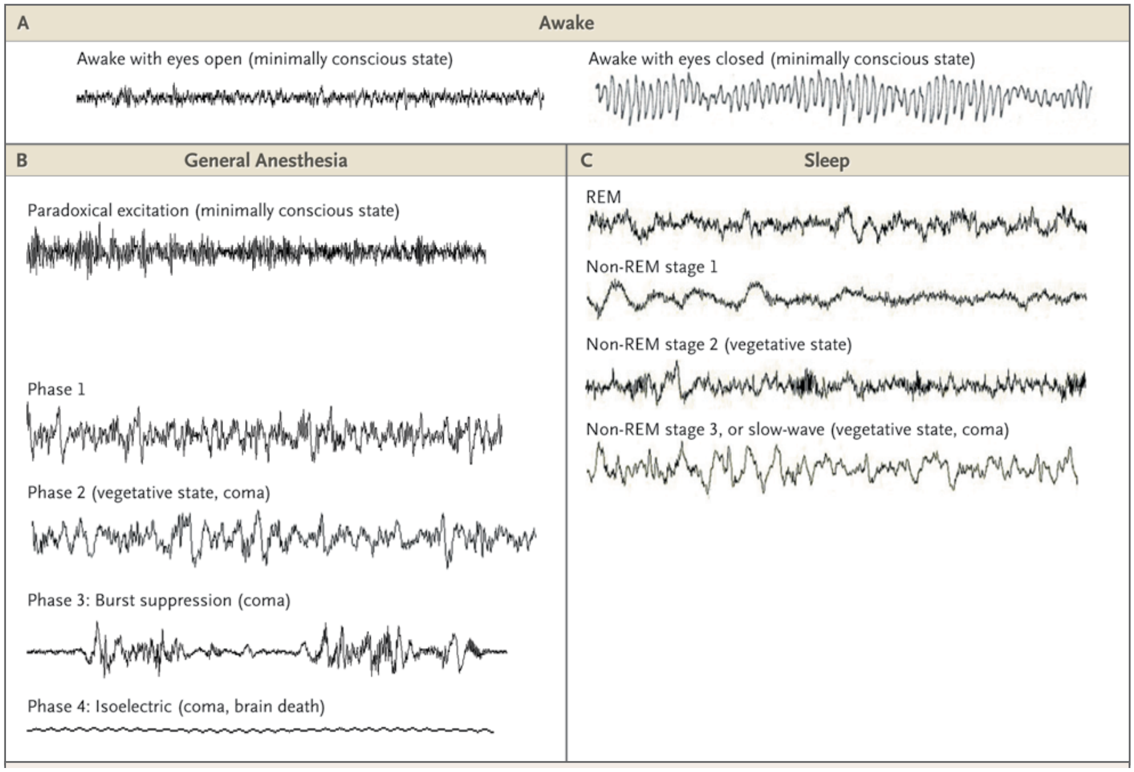

Figure 1.3 EEG patterns characteristic to conscious and unconscious states.

Figure 1.3 EEG patterns characteristic to conscious and unconscious states.

Figure from [2]. Parentheses denote a pattern that can be observed in a state of impaired consciousness (e.g. coma). Awake-brain EEG patterns are shown in panel A. The left trace (awake with eyes open) has low-voltage, fast, varied, and desynchronized activity, reflecting an attentive and actively concentrating mind; the main spectral component is the range of the β rhythm (14 – 40 Hz). When awake and relaxing with the eyes closed (right trace), the EEG is dominated by the α wave. The first EEG recorded looked like this, hence the name. One theory is that the α wave is a result of the occipital cortex "idling". Panel B depicts EEG patterns that manifest with increasing depths of anesthesia. The lightest stage of anesthesia, paradoxical excitation, is a result of the neuronal disinhibition, when low doses of anesthetics suppress inhibitory networks. Behaviorally it can result in euphoria, dysphoria, and purposeless movements, probably from striatal-thalamic pathways. Consciousness is still present and the waveform is still relatively desynchronized. As more anesthetics are administered- with intravenous agents usually increasing rapidly over 10-15 seconds as a bolus, longer and higher amplitude waveforms take over, similar to sleep. The burst suppression pattern is unique to anesthesia and coma, and is not seen in sleep. With even greater doses of anesthesia, periods of silence between bursts will increase until activity more or less ceases altogether. In comparison, panel C depicts the EEG patterns of various sleep stages. REM is similar to waking EEG, probably because of the process of dreaming. These active EEG patterns are generated by strong cholinergic excitatory inputs onto the cortex and thalamus.

1.3.2 Neurologic problems related to modern anesthesia

Intraoperative awareness

Intraoperative awareness is one of the more enigmatic and feared complications from anesthesia. It is estimated that one or two people in a thousand experience, and form memories of, being aware and sensate but paralyzed during a session of anesthesia that outwardly presents as sufficient by clinical measures [39]. Often the remembrance is in the form of vague or implicit (non-declarative) memory, but lucid awareness with accurate recall does happen. Quality-wise, the sensations vary but typically include sound, pain or pressure. For simplicity, intraoperative awareness is defined here strictly as awareness with some form of memory that can be quantifiably assessed.

At its simplest, there are two fundamental problems. First, many operations require paralytic agents which block or blunt the most elementary pain responses such as autonomic or motor reflexes. Second, there is no direct biomarker for consciousness. Unresponsiveness can be dissociated from unconsciousness, so testing even physical reactions to given commands can be misleading. Monitoring of the raw or processed EEG in combination with other diagnostic criterion can be helpful [40], but ultimately these are all indirect measures that have to be evaluated in the context of overall patient physiology.

Anesthetics normally prevent memory by preventing experience and preventing memory formation. In strict terms of anesthetic endpoints, intraoperative awareness occurs when immobility is achieved but amnesia and hypnosis are incomplete or unstable. If there were a unitary mechanism for anesthesia, this phenomenon would be surprising because the effective dose for amnesia is lower than the effective dose for unconsciousness. However, distinct neurophysiological processes that occur in the circuits of the hippocampus and thalamus (specifically thalamo-cortical circuits) generate these two anesthetic endpoints. Experimentally, amnesia and loss of consciousness are dissociable in various transgenic mouse models of mutated $GABA_A$ receptors [41]. How anesthetic agents interact with specific $GABA_AR$ subtypes within these regions to alter hippocampal and thalamic function are elaborated later in this chapter (1.8 Specific $GABA_AR$ subtypes in neuroanatomical regions important to anesthesia). Additionally, unconsciousness does not preclude memory or synapse formation. The cellular correlates of learning and memory are inhibited, but viable, in the presence of anesthesia. For example, the rabbits used in the Bliss and Lomo experiments to identify plasticity in the perforant-path to dentate gyrus synapse were heavily anesthetized [42].

Despite these complications, it should be reiterated that anesthetics are some of the most powerful memory-impairing drugs available. Even at sub-anesthetic doses, they have profound effects on working memory and can induce retrograde and even anterograde amnesia.

Post-Operative Cognitive Dysfunction

General anesthetics are suspected in the development of cognitive dysfunction following surgery. Their potential to cause or exacerbate neurodegenerative processes has been openly debated for over fifty years, yet a clear cellular mechanistic link remains unclear and complicated. The reported deficits are primarily in executive and memory functions including working memory, attention, and concentration. Collectively, attributing poorer performance in neurocognitive tests to a previous experience of surgery with general anesthesia come to be referred to as post-operative cognitive dysfunction (POCD)[43-46]. The primary risk factor is patient age, with occurrence and persistence being greatest in patients over the age of 65 [47]. In young and middle-aged adults, symptoms are more typically transient and resolve within days or weeks (37% age 18-36 at discharge, 6% at 3 months after surgery), whereas elderly presentations are more persistent (41% at discharge, 13% at 3 months after surgery).

Duration of anesthesia is another risk factor, and concerns about drug titration have motivated the use of functional brain monitoring to guide anesthetic agent delivery, which may decrease the occurrence of POCD compared to the use of autonomic and vital signs alone [48]. There are several other identifiable risk factors including: lower educational level, alcohol abuse, epilepsy, presence and severity of pre-existing cognitive impairments (e.g. forgetfulness), and neurodegenerative disease (e.g. Alzheimer's, Parkinson's). As revisited later, changes in inhibitory networks are suspected because altered $GABA_AR$ expression is a feature of many of these conditions.

Epidemiologically, POCD has not been resolved as a distinct disorder. Some consider it as a risk factor for natural incidental age-related dementia or cognitive loss, as an unmasking of pre-existing cognitive fragility that manifests from the combination of surgery and anesthesia, or as a statistical artifact. No direct correlations between cognitive decline/neurological symptoms and the use of general anesthetics has been unambiguously demonstrated in human populations, possibly because this research question has unique challenges, even for human studies. Surgery and its associated physiological consequences occur (usually) because of some serious condition, and the hospitalization experience itself is challenging; distress, discomfort, and poor sleep can affect cognition. Pre-operative assessment of cognitive baseline is not yet routine or standardized at most institutions, so data collection and the meaningful assessment of cognitive loss throughout treatment have been problematic. The pharmacology of the anesthetic plan varies per the subjectively assessed needs of the patient and surgical procedure, and can be complex. Typically, anesthetics are co-administered with sedatives, opiates, and neuromuscular junction blocking drugs, in addition to the course of medication dictated by condition and treatment plan (e.g. immunosuppression).

Despite the difficulty in demonstrating a clear statistical relationship between anesthetics and cognitive outcome in patients, POCD has received intense focus in anesthesiology research because of pre-clinical data suggesting adverse effects of volatile anesthetics on learning and memory in aged animals [49-51]. However, to date POCD remains un-defined as a clinical entity with no clear pathophysiology demonstrated so far [52].

1.4 Anesthetic agents modulate ion channels in the CNS

The modern anesthetic agents as a group are chemically heterogenous structures: most of the inhaled vapors are halogenated derivatives of ether, thus small hydrophilic molecules, while the intravenous agents are more structurally diverse [53]. Both volatile and intravenous agents vary in their effect on many ligand-gated ion channels involved in determining neuronal excitability, including $GABA_A$, glycine, acetylcholine, serotonin, AMPA, kainate and NMDA receptors [31, 53]. Of these pharmacological interactions, the most prominent contribution to the anesthetized state is likely the enhancement of $GABA_AR$ neurotransmission by allosteric potentiation of channel function [54]. Several other ion channels important for neuronal excitability are also influenced by anesthetics including HCN1, TRESK, and voltage gated calcium and sodium channels [55].

While anesthetics primarily generate unconsciousness by actions on ion channels in the central nervous system, they have molecular targets on many other proteins in the body [56]. The molecular promiscuity of these agents and the existence of off-target effects may be unsurprising given that the first anesthetic-protein interaction identified was the binding of halothane to firefly luciferase [27]. In neurons, affected processes include cellular housekeeping systems such as mitochondrial transition, calcium homeostasis, and actin polymerization [55]. “Off-target” effects can underlie catastrophic patient reactions, such as the hypersensitivity of skeletal muscle ryanodine receptor channel function to volatile agents in malignant hyperthermia [57]. Subtler effects with latent complications are suspected in the anesthetic contribution to several neurodegenerative diseases, namely Alzheimer’s via β-Amyloid [58]. Later, we review anesthetic-protein interactions in the second messenger signaling protein pathways known to control $GABA_AR$ trafficking. Of non-ion channel proteins, there are no obvious structural motifs of the intracellular protein targets of anesthetics. One basis for molecular promiscuity at clinically relevant doses is that these drugs, especially the volatile anesthetics, have a low pharmacological potency and low therapeutic induces and must be used at very high doses to achieve a satisfactory level of anesthesia [26].

1.5 $GABA_A$ receptor diversity and distribution

The crystallized $GABA_AR$ structure was reported in 2014 [59]. $GABA_ARs$ are structurally related to serotonin and nicotinic acetylcholine receptors, all members of the Cys-loop superfamily of ligand-gated ion channels, which share similarities with the prokaryotic gleobacter ligand gated ion channel [60]. $GABA_ARs$ are assembled as heteropentamers from 19 different possible subunits that are classified by protein sequence homology as α1-6, β1-3, γ1-3, δ, ρ1-3, π, θ ε1-3. Most naturally occurring receptors contain two α, two β, and either a δ or γ subunit (**Figure 1.4, top**), with $\alpha_1\beta_2\gamma_2$ being the most abundant subtype in the mammalian CNS [61]. Only nine different configurations are unambiguously expressed in abundance in the mammalian brain [62]. **Table 1.1** describes some of the known research of these configurations. Individual subunit combinations are unique with respect to their pharmacology [62], distribution among different brain regions [63] and subcellular localization (see below)[64, 65]. Recombinant studies have demonstrated that the subunit composition contributes to biophysical difference in GABA sensitivity, as heterologously expressed $\alpha_1\beta_2\gamma_2$ receptors show a lower affinity than $\alpha_4\beta_2\gamma_2$ [66]. In most of the brain, intrasynaptic receptors contain α1-3 subunits whereas extrasynaptic receptors contain α4-6 subunits [64].

The endogenous ligand is GABA, which causes neuronal inhibition by opening the chloride-permeable ion channel pore and hyperpolarizing the membrane potential to dampen or shunt neuronal excitation. At clinically applied doses, most anesthetics act as positive allosteric modulators, increasing channel function by binding to protein cavities remote from the ligand binding site and causing conformational changes in structure that increase and prolong the response to GABA [31]. Several putative interaction sites for volatile agents on the $GABA_A R$ have been identified through mutagenic and biophysical experiments [29, 67]. Similarly, sites for intravenous agents have been identified [22, 59, 68]. On the intracellular face of the receptor, each subunit contains a small cytoplasmic loop between the first and second transmembrane domains and a larger cytoplasmic loop between the third and fourth transmembrane domain (**Figure 1.4, bottom**). This larger loop domain has the largest sequence variability between subtypes [62], and contains several sites for protein-protein interactions. In addition to conferring some of the subtle biophysical properties that lead to specific pharmacology among the subunits, this intracellular loop is also the main site for regulatory control of membrane trafficking by intracellular signaling pathways.

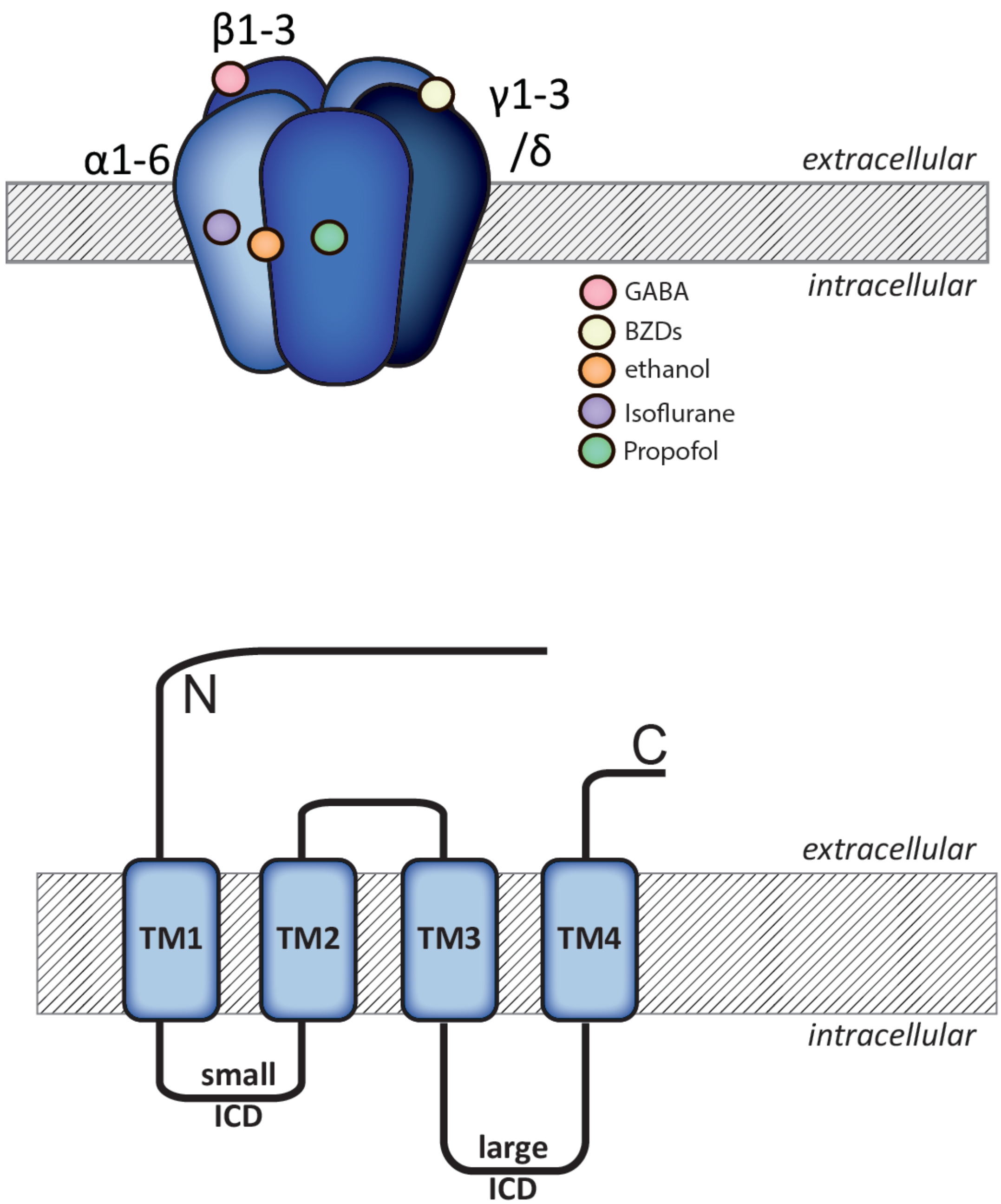

Figure 1.4 GABA$_A$ receptor structure

Figure 1.4 $GABA_A$ receptor structure. The vast majority of $GABA_A$ receptors are heteromeric pentamers, with subunit stoichiometry following a 2:2:1 ratio of α(1-6), β(1-3), and then a γ (1-3) or a δ subunit respectively. GABA and benzodiazepines bind sites on the extracellular domain, whereas isoflurane, ethanol, and propofol bind to regions within the plasma membrane (**top**). The individual subunits have a common transmembrane organization of four transmembrane domains with two intracellular domains (ICDs) that are targeted by regulatory proteins (**bottom**). The N-terminus is the larger component of the extracellular domain.

Subtype configuration	Subcellular localization	CNS region of importance	Pharmacology notes	References
$\alpha_1\beta_2\gamma_2$	Intrasynaptic	ubiquitous	BZD sensitive	[63]
$\alpha_2\beta_2\gamma_2$	Intrasynaptic-Axon Hillock	striatum, cortex, hippocampus	BZD sensitive, selective agonists in development	[69]
$\alpha_4\beta_x\delta$	Extra-synaptic	reticular thalamus, dentate gyrus, cortex (L2/3)	BZD insensitive Neurosteroid sensitive	[70-72]
$\alpha_4\beta_x\gamma_2$	Intrasynaptic	thalamus	Aberrant, appears after ethanol intoxication	[73] [74] [66]
$\alpha_5\beta_3\gamma_2$	Extra-synaptic	Hippocampus Cortex	Increased BZD / VGA sensitivity	[75, 76]
$\alpha_6\beta_x\delta$	Extra-synaptic	cerebellum	Furosemide sensitive	[65]

Table 1.1 $GABA_AR$ subtype diversity and anatomical distribution.

Table 1.1 $GABA_A R$ subtype diversity and anatomical distribution of common subtype configurations**.** Generally, the main intrasynaptic receptor for most regions is $\alpha_1\beta_2\gamma_2$ whereas the extrasynaptic receptor subtype that mediates tonic current varies the most between brain regions. The thalamus, hippocampus, and cerebellum use $\alpha_4\beta_x\delta$, $\alpha_5\beta_3\gamma_2$, and $\alpha_6\beta_x\delta$ extrasynaptic receptors respectively.

1.6 Intrasynaptic and extrasynaptic $GABA_A$Rs generate phasic and tonic current

GABA-ergic neurotransmission evokes two distinct forms of inhibitory currents (**Figure 1.5**). The basis for these two types of currents lies in receptor subunit composition and subcellular location. Phasic currents are primarily mediated by low-affinity intrasynaptic receptors, which generate brief and quickly-desensitizing inhibitory post-synaptic currents (IPSCs) in response to interneuronal input [64, 65]. Intrasynaptic receptor clustering is based on the construction of the GABA-ergic synapse, which is made of post-synaptic density of several proteins organized opposite to the presynaptic terminal [77]. Intrasynaptic receptors are typically are made of large clusters of α_1, α_2 or α_3 containing subtype configurations anchored to the post-synaptic cytoskeleton by the scaffold protein gephyrin [78]. Inside the synapse, these receptor clusters are transiently exposed to high (~mM) concentrations of GABA from synaptic vesicular release, and generate phasic currents that terminate after GABA is cleared from the synapse. Even before clearance by glial or neuronal pumps, phasic currents rapidly desensitize, generating the characteristic decayed shape of the ISPC.

Tonic currents are mediated by receptors located extrasynaptically, which generate long sustained conductances in response to smaller (~nM-μM) amounts of GABA existing in the intercellular space [79]. The extrasynaptic receptors have a higher affinity for GABA and ideal for detection of small amounts of neurotransmitter. An additional difference is that extrasynaptic receptors exhibit little or no accommodation to saturating concentrations of GABA, a phenomenon known as desensitization. The GABA that evokes tonic current is thought to arise from two overlapping sources, ambient and spill-over GABA. Ambient GABA describes the minute amount preexisting in the extracellular space. Measurements from *in vivo* microdialysis suggest peri-synaptic GABA is between 30-300nM, depending on brain region [80, 81]. Notably, GABA levels can change with physiological and behavioral states, such as active exploration [82]. Spill-over GABA is released by synaptic transmission and diffuses away to have paracrine action on remote receptors, e.g. on other neurons. These terms have conceptual overlap and do not demarcate two types of GABA, but rather distinguish effects in spatiotemporal relation to synaptic transmission. High levels of phasic inhibition can drive spillover and raise local ambient GABA. For example, an increase in inhibitory activity can encourage sleepiness in part due to the accumulation of ambient GABA due to spillover.

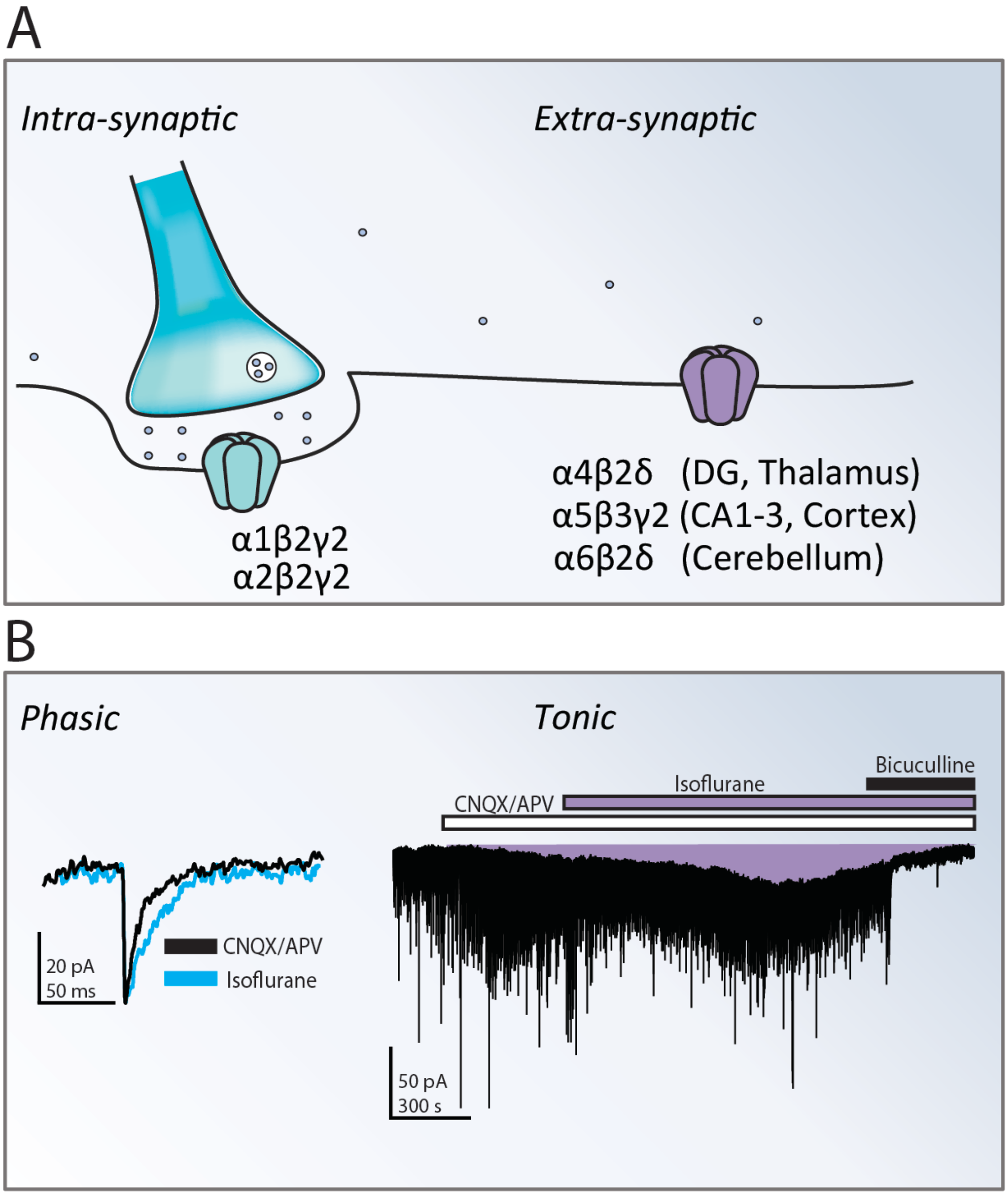

Figure 1.5 Intrasynaptic vs. extrasynaptic $GABA_A$ receptor currents.

Figure 1.5 Intrasynaptic vs. extrasynaptic $GABA_A$ receptor currents. $GABA_A$ receptors are distinguished anatomically by their distance to the synapse **(Panel A**). Due to both intrinsic properties based on subunit protein sequence as well as GABA exposure, intrasynaptic and extrasynaptic receptors generate two distinct forms of current, phasic and tonic current respectively (**Panel B**). Electrophysiological traces generated by Edyta Bichler and Iris Speigel

Subunit composition and sensitivity to anesthesia-related drugs

At clinically used doses, GABA-ergic anesthetics potentiate phasic currents by prolonging IPSC duration, and tonic currents by increasing the amplitude and charge transfer. Pharmacologic substances do not effect tonic and phasic conductances in the same way [83]. An enhanced sensitivity to GABA-ergic anesthetic drugs is a common feature of extrasynaptic receptors [84]. In hippocampal pyramidal neurons, low concentrations (25 μM) of isoflurane enhance the α_5 mediated tonic but not phasic current [75]. In the same experiments, 100 μM is the minimal dose to enhance IPSCs. Heterologously expressed $\alpha_5\beta_2\gamma_2$ receptors in HEK cells are potentiated by 25 μM isoflurane suggesting that anesthetic sensitivity is based on intrinsic channel properties [75]. These reactions to sub-anesthetic doses may explain why low doses of our anesthetics produce a sedation phenotype.

1.7 Neurophysiological consequences of specific $GABA_AR$ subunit compositions

Canonically, GABA-ergic signaling curtails neuronal activity. This effect occurs via either hyperpolarization or shunting, depending on the chloride driving force, the resting membrane potential, and the action potential threshold at the time the impulse arrives. GABA is depolarizing in the earliest developing neurons that have not yet expressed specific membrane transporters to establish the usual chloride gradient [85, 86]. Because the developing brain contains neurons at many different stages of development anesthetics potentiating GABA-mediated currents could be excitatory in some neurons [85].

Functionally, phasically mediated $GABA_AR$ currents decrease the probability of action potential firing. The temporal dynamics of phasic inhibition are important because synchronizing population activity into slow oscillatory waves requires precise timing of inhibitory input. In contrast, tonic currents cause a more persistent ongoing inhibition that is not temporally discrete. The importance of a tonic current may lie more specifically in creating a low-excitability cellular phenotype. For example, hippocampal dentate granule (DG) cells are described in an electrophysiologic study as reluctantly firing, owing partially to the strong tonic conductances mediated by $\alpha_4\beta_x\delta$ extrasynaptic receptors [87]. This feature is thought to be important for information processing because the DG is located at the entry of entorhinal excitatory projections into the hippocampus, and thought to have an important role in filtering the excitatory input into the dorsal subfields, which themselves are mostly excitatory neurons with more active firing profiles. A high firing threshold constrains inappropriate signal transfer into the hippocampus through "sparse" coding. Moreover, limiting excitation has an important protective feature for "gating" the hippocampal network, which is laden with recurrent connections and sensitive to epileptogenesis.

1.8 Specific $GABA_AR$ subtypes in neuroanatomical regions important to anesthesia

The receptor subtypes that underlie tonic and phasic currents are particular to brain region. Here we summarize receptor subtype distribution, and for each receptor population, it's hypothesized role in anesthesia. We focus on regions of the brain heavily involved in consciousness and memory.

The hippocampus. Traditionally associated with the formation of memories, the hippocampus and related structures have been studied for decades in order to understand anesthetic mechanisms in a convenient, standardized laboratory preparation (acute preparation of living *ex vivo* brain slices from the rodent). Intrasynaptic $GABA_A$Rs of the hippocampus CA1 subfield pyramidal neurons have been identified as being mostly $\alpha_1\beta_{2/3}\gamma_2$. Tonic current is mediated by extrasynaptic $\alpha_5\beta_3\gamma_2$ receptors [76, 88] in the same area. In the granular cell neurons of the dentate gyrus, phasic current is mediated by $\alpha_1\beta_{2/3}\gamma_2$ whereas tonic current is mediated by $\alpha_4\beta_x\delta$. The sensitivity of these receptors to alcohol is thought to be mediated by the δ subunit, and underlie amnestic effects of alcohol [89]. The difference between tonic current receptors in these subfields may be related to the neurophysiological differences between CA3/CA1 pyramidal cells and DG granule cells [87].

Plastic changes to tonic receptor distribution or expression within the hippocampal neuron plasma membrane can have profound behavioral effects. For example, $GABA_A$R α_5 subunit knockout mice are insensitive to the amnesic effects of anesthesia, thus hypothetically patients with depressed α_5 expression in the hippocampus may be vulnerable for anesthetic awareness. Experimental evidence suggests that α_5 expression is depressed in models of chronic alcohol and benzodiazepine abuse, or epilepsy.

The cortex. In most layers the extrasynaptic receptor is $\alpha_5\beta_3\gamma_2$, but in layer 2/3 extrasynaptics are $\alpha_4\beta_2\delta$[64]. These generalizations about cortical layers should be taken with consideration to the region, because the stratification of cortical layers can have a specific functional role within different processes. Cortical layers 2/3 receive information from other cortical areas.

Subcortical arousal centers. Wakefulness and somnolence are governed by a system of neuromodulatory projection neurons that originate in several subcortical nuclei that widely innervate the brain. Rationally, anesthetic action on these regions is a clear and direct mechanism for loss of consciousness. However, predicting the contribution of these subcortical arousal centers to anesthesia is complicated by the fundamental difference between the processes of falling asleep and anesthetic induction, as well as "redundancy" in arousal pathways. When $GABA_AR$ current sensitivity to propofol was tested in three arousal centers targeted by natural sleep pathways using the β_3 (N265M) transgenic mouse, the perifornicate and tuberomamillary nucleus (TMN) but not the locus coeruleus were affected [90], suggesting that the locus coeruleus has a paucity of β_3 receptors. The TMN is in the hypothalamus, and projects the arousal neurotransmitter histamine into cortex to generate wakefulness. In anesthesia, propofol enhancement of $GABA_ARs$ in TMN depresses histamine release into the cortex [91] . For a thorough review of subcortical areas involved in arousal and their influence on sleep and anesthesia see [10, 92]

1.9 $GABA_AR$ surface expression is controlled by intracellular trafficking

The strength of inhibitory currents, tonic or phasic, depends on the number of receptors expressed on the neuronal cell surface. This number is dynamically maintained, as $GABA_ARs$ undergo controlled rates of endocytosis, exocytosis, and degradation- in effect constantly recycling between the surface and the cytoplasm. These events are coordinated by a myriad of effecter and regulatory proteins, themselves controlled by second-messenger signaling events. Perturbations to all of these steps can potentially alter GABA-ergic signaling, e.g. an increase in surface expression and current can arise from increased rates of exocytosis, reduced endocytosis, or decreased degradation.

1.9.1 Receptor biosynthesis, exocytosis, and subcellular localization

$GABA_A$R subunits are synthesized in the endoplasmic reticulum [93]. Once made, correctly folded and oligomerized channels are transported to the Golgi apparatus for further post-translational processing and then sorted into vesicles for insertion into the plasma membrane. To exit the Golgi organelle, functional receptors need to undergo glycosylation and palmitoylation [93, 94]. Fully processed receptors are exported from the Golgi apparatus to the cell surface by the secretory pathway. Endosomes containing new receptors are actively transported along microtubules and actin filaments by molecular motors and inserted into the plasma membrane by exocytosis. Delivery to the cell surface is enabled by a number of receptor-associated proteins, including GABARAP, GRIF-1 PRIP-/21, Plic1, etc. [77].

Imaging and biochemical assays in cultured neurons suggest that receptor insertion occurs extrasynaptically [95], so intrasynaptic receptors undergo additional targeting to the postsynaptic density. Single-particle trafficking shows that newly inserted γ_2-containing receptors move into synapses by lateral diffusion [96]. This diffusion is consistent with the thermodynamics of Brownian motion, and rate measurements suggest that receptors transition between "motile" and "immotile" states when “trapped’ by protein binding. Pulse-chase labeling of newly inserted β_3 subunits suggest that movement into the synapse happens quickly, as the ratio of synaptic/extrasynaptic β_3 significantly increases by 15 minutes [95]. Synaptic confinement involves gephyrin [97], the cytoskeletal-bound post-synaptic scaffolding protein of inhibitory synapses. Gephyrin binding sites have been identified on α_1, α_2, α_3, β_2, and β_3 subunit large cytoplasmic loops [98, 99], which interact with a common $GABA_AR$ binding site on gephyrin [100]. At least for α_2, the association is robust enough that inserting the gephyrin binding sequence into other unrelated proteins (e.g.CD4, a T-helper cell glycoprotein) is sufficient for synaptic targeting [78].

Keeping extrasynaptic receptors in place is less understood. The $\alpha_5\beta_3\gamma_2$ receptors affixed to the cytoskeleton in extrasynaptic clusters by the scaffolding protein radixin. Their extrasynaptic confinement is not static, and dissociation from radixin and into synapses has been identified as a means of synaptic strengthening [101]. Within synapses, $\alpha_5\beta_3\gamma_2$ receptors mediate a slowly-decaying component of IPSCs [102]. Immunoprecipitation of adult rat brain lysate show that native gephyrin and α_5 bind *in vivo*, suggesting that these interactions are not an artifact of the use of primary neuron culture, development, or transgenic manipulation [102]. Receptor exchange between intrasynaptic and extrasynaptic sites is under active investigation as a potentially important mechanism of inhibitory plasticity. The extrasynaptic location of $\alpha_4\beta_2\delta$ receptors is attributed to the lack of an α_4-gephyrin interaction, as replacing the α_2-gephyrin domain in $\alpha_2\beta_x\gamma_2$ receptors with the homologous region in α_4 is sufficient to block α_2 synaptic clustering [102]. An extrasynaptic scaffolding protein for $\alpha_4\beta_2\delta$ analogous to the $\alpha_5\beta_3\gamma_2$-radixin interaction has not been identified. In general, structural and regulatory elements for extrasynaptic receptor densities have not been well identified, and their identities and organization may be important in understanding how extrasynaptic receptors are regulated or recycled. Exchange of surface receptors between extrasynaptic and synaptic domains has been demonstrated as a key determinant of synaptic plasticity in several major ion channels [103].

1.9.2 Endocytosis and post-endocytotic sorting: recycling vs. degradation

$GABA_A$Rs are removed from the cell surface via clathrin-mediated endocytosis. This process depends on the adaptor protein AP-2. Specifically, the μ2 subunit of AP-2 recognizes its binding site on the receptor, enabling recruitment of the AP-2 holoenzyme and creation of clathrin-coated pits. AP2 binds two different endocytic motifs that are conserved in the cytoplasmic loop of all three types of β subunits. The dileucine motif (L343L344) is involved in constitutive endocytosis in cortical neurons and heterologous expression systems e.g. HEK cells [104]. The other motif contains serine phosphorylation sites (S409 in β_1, S410 β_2, and S408/9 in β_3) that directly regulate endocytosis in another variety of contexts [105]. Phosphorylation at these sites by PKA ($\beta_{1,2}$), PKC($\beta_{1,2,3}$) or other kinases negatively regulates endocytosis by disrupting the capacity of AP-2 to bind the receptor, so dephosphorylation by a phosphatase unblocks or triggers endocytosis.

Another AP-2 binding motif on γ_2 (Y365/367) contains tyrosine residues that are targets for phosphorylation-based regulation by Fyn and Src kinases. Here, phosphorylation promotes endocytosis and phoshomimetic receptors show increased AP-2 affinity *in vitro*. Transgenic knock-in mice expressing γ_2 (Y265/7F) phosphomimetic mutant receptors show increased cell surface expression, larger inhibitory synapses, and impaired spatial memory [41]. Rate-measurements of intrasynaptic receptor constitutive endocytosis in hippocampal cultures gathered by biochemical assay suggest relatively rapid kinetics, with 25±3.5% of surface receptor β_3 subunits internalizing by 30 minutes in DIV 7 cultures, and 17±5% after 30 min in DIV 10-14 cultures [106]. Antibody-feeding based optical measurements in DIV 8 neurons also show significant changes in internalized γ_2 protein after 15 minutes [107].

Specific endocytotic mechanisms for the $\alpha_4\beta_2\delta$ receptors mediating tonic current are mediated through the δ subunit, which has its own μ_2-AP2 binding domain enabling $\alpha_4\beta_x\delta$ specific endocytosis [108]. Kinetically, constitutive or basal endocytosis of δ-containing receptors appears to occur more slowly than intrasynaptic receptors. The surface half-life of δ subunits is 103-171 minutes depending on the measurement method, immunostaining in culture or slice biotinylation in organotypic hippocampal slices respectively [107]. In contrast, evoked endocytosis of extrasynaptic receptors happens more quickly, as ethanol-evoked endocytosis of $\alpha_4\beta_x\delta$ can be measured within 15 minutes [108]. Protein kinase C phosphorylation regulates membrane insertion of $GABA_AR$ subtypes that mediate tonic inhibition [72].

Once internalized, $GABA_AR$ containing endosomes are sorted between recycling endosomes or late endosomes destined for lysosomal degradation. Endosomal sorting itself is controlled by protein regulators include the huntingtin-associated protein 1, which promotes rates of recycling over degradation to ultimately increase surface expression [106]. In principal, a sub-synaptic reservoir of receptor enables short and rapid synaptic plasticity because receptors are on-site for insertion. This is supported by evidence of a population of intracellular $GABA_ARs$ residing near gephyrin underneath the synapse [109]. Receptors can also be targeted for degradation within lysosomes, acidic organelles which enzymatically digest the proteins inside. Receptor targeting to lysosomes is mediated by the post-translational modification ubiquitinylation. Rate studies in cultured neurons suggest that 30% of neuronal $GABA_A$Rs become degraded over the course of 6 hours [106]. The balance of the rates of recycling versus degradation both influence surface expression. Huntingtin-associated protein-1 is involved in the $GABA_A$R endosomal sorting decision, by positively regulating recycling as well as synaptic targeting [106, 110].

1.9.3 Anesthetic effects on signal transduction pathways of trafficking regulation

Several networks of second messengers and signaling protein regulators control or influence the subcellular movement of $GABA_A$Rs. The interactions of these pathways with anesthetic agents are just being recognized, and remain an area of active investigation. Given that changes in surface expression can be observed *in vitro* on the time course of 15 – 30 minutes, it is conceivable that routine anesthesia care has major influence on the dynamics of membrane surface expression. Here I highlight some of the intracellular pathways affected by anesthetics.

Calcium and IP3R pathway. Intracellular calcium is one of the most important second messengers. Typically, inositol triphosphate (IP3) signaling operates as a signal transduction pathway when an extracellular stimulus triggers the cleavage of plasma membrane phospholipid PIP2 (phospholipid phosphatidylinositol 4,5-bisphosphate) into IP3. IP3 diffuses intracellularly to bind IP3 receptor (IP3R) calcium channels on the endoplasmic reticulum (ER), releasing stored calcium into the cytosol. Isoflurane itself will raise intracellular calcium by directly activating the IP3R channel [111]. This mechanism of disrupting of intracellular calcium homeostasis is heavily studied in anesthetic neurotoxicity, especially in developing neurons [112] (**Figure 1.6**). This phenomenon is also observed in mature and post-natal neuron preparations and adult brains, suggesting that this phenomenon is relevant *in vivo* [113]. Several different pathways affecting receptor surface expression are calcium-dependent, including PKC, which changes both extrasynaptic and intrasynaptics receptor surface expression by phosphorylation-based regulation of endocytosis.

PKC. Propofol itself can activate and allosterically enhance PKCε, a PKC isozyme that does not require calcium for activation**.** *In vitro* studies of the direct interaction between propofol and the regulatory domain of PKC show that propofol promotes PKC autophosphorylation at Ser729, a final step in initiating and maintaining enzyme activation. Propofol-mediated increases in catalytic activity can be seen in a canonical target of PKCε, the transcription factor CREB [114]. Interestingly, the initial study that demonstrated increased activity of an unidentified PKC in response to propofol shows a similar effect from halothane [115]. If the effect of halothane on PKCε extends to other volatile anesthetics, they may also disrupt $GABA_AR$ endocytosis through a similar mechanism.

Adaptive Response Pathways. Isoflurane can prevent hypoxic cell death in a number of organ systems, including CNS neurons, which has important implications for neuroprotection during stroke or ischemia. The predominantly studied mechanism is calcium mediated pre-conditioning, whereby isoflurane activation of various survival and anti-apoptotic signaling pathways prevents cell death. These studies have also yielded information about how isoflurane affects these pathways, including differential phosphorylation/activation of c-Jun, MAP kinases, etc. [116]. Both calcium-dependent and calcium-independent pathways were affected by isoflurane in the absence of hypoxia, suggesting some effects do not originate with IP3R activation. In some cases isoflurane paradoxically decreased activity of transcription factors targeted by regulatory proteins whose activity was increased by isoflurane. Clearly, isoflurane is complexly affecting intracellular signaling [116].

RhoA/ Kinase/ROCK signaling. Propofol has been shown to interfere with neuronal development by causing neurite retraction through the RhoA kinase /ROCK signaling pathway [117], itself activated by the effect of propofol on PKCε. How propofol directly interferes with RhoA/ROCK signaling may be important beyond development because this pathway regulates $\alpha_5\beta_3\gamma_2$ extrasynaptic localization by controlling α_5-radixin binding, which indirectly affects synaptic $\alpha_5\beta_3\gamma_2$ levels [101].

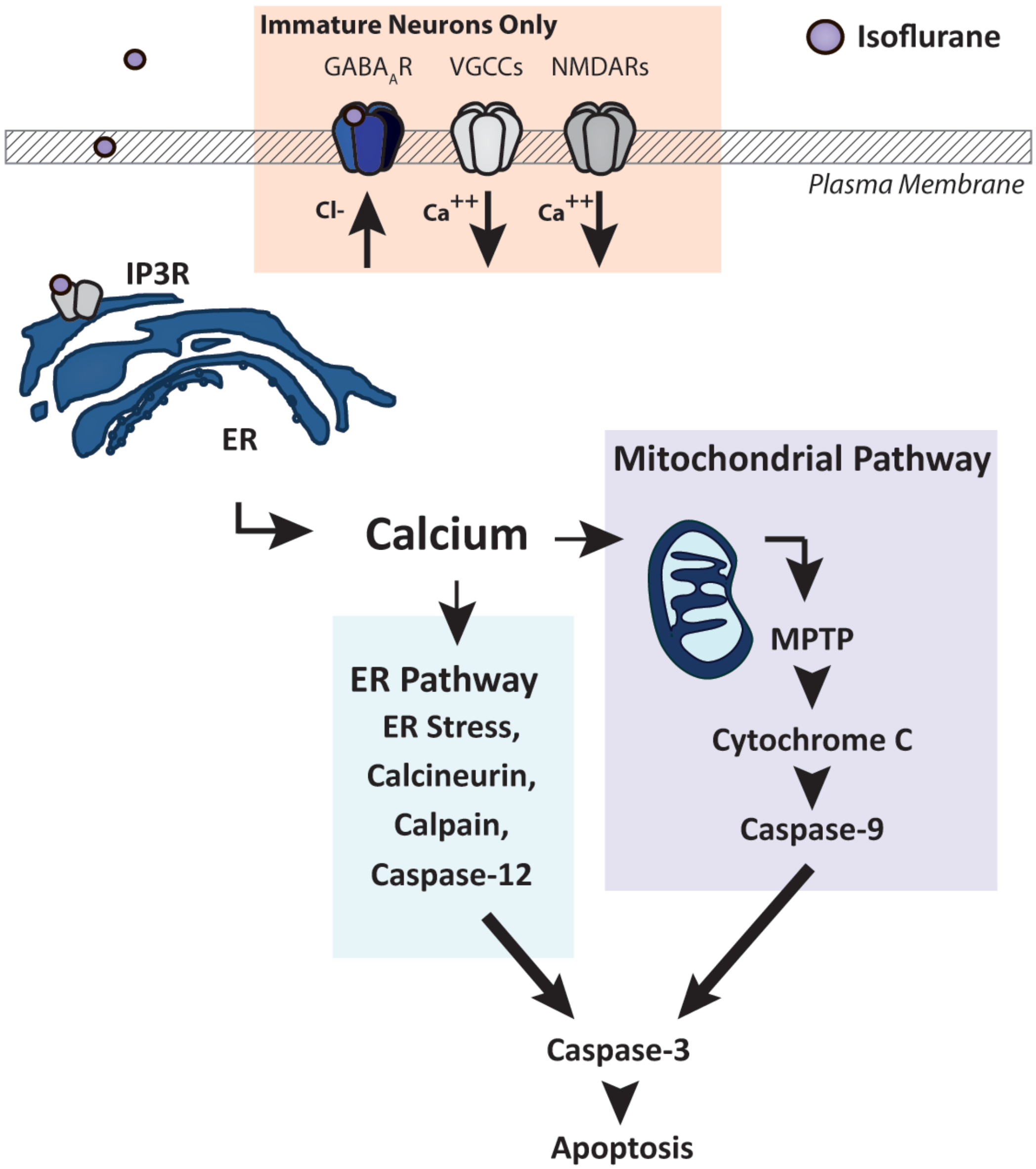

Figure 1.6 Intracellular mechanisms of isoflurane neurotoxicity.

Figure 1.6: Intracellular mechanisms of isoflurane neurotoxicity. The most thoroughly studied pathways for anesthetic-related neuron death are based on the activation of mitochondrial and ER-stress related processes. Additionally, within immature neurons, depolarizing conductances such as the voltage-gated calcium channels and NMDA receptors promote excitotoxicity (**peach**).

1.10 Effects of anesthetic agents on surface expression

Recent research has shown that anesthesia itself may cause changes to the surface expression of $GABA_A$Rs and other ion channels that control neurological function. At present, these changes appear to be mediated by the effect of anesthetics on the intracellular signaling pathways that control trafficking.

Propofol. Recently propofol has demonstrated an increase in β_3 subunit surface expression in hippocampal brain and primary cultures within 15, 30, and 60 minutes of exposure. A series of experiments strongly suggest that the underlying mechanism is PKC-mediated phosphorylation of β_3 at the AP-2 binding domain and inhibited endocytosis. Immunoprecipitation of β_3 from hippocampal lysates show a depressed association with AP-2 subunit β-adaptin, suggesting diminished recruitment of the entire AP-2 complex. Surface expression of GluR1, a subunit of AMPA receptors which are also trafficked using AP-2 and clathrin-mediated endocytosis, was not significantly affected, suggesting that propofol is not impairing general endocytotic mechanisms. Activated PKCε is increased at these timepoints. PKCε kinase activity on β_3 receptors measured with hippocampal lysate and recombinant PKC shows increased β_3 phosphorylation. The change in surface expression and decrease in AP-2 subunit binding are blocked with PKCε inhibitor [118]. Functionally, propofol causes an increase in evoked and miniature IPSC amplitude that can be partially reversed with PKCε inhibitor. Post-translational modification of channel kinetics by PKC and allosteric enhancement of channel function by propofol likely contribute to this effect, but the effect of the inhibitor suggests that ultimately propofol is creating a temporary sensitization of GABA-ergic transmission through PKCε-dependant mechanisms.

Etomidate. A temporary increase in α_5 surface expression has been associated with etomidate administration [119]. This increase appears to be in part responsible for post-anesthesia memory impairment. The expression levels return to normal in 2 weeks.

1.11 Anesthetics and inflammation

There are several lines of evidence that volatile anesthetic agents alter normal post-operative inflammatory signaling, and that neuroinflammation impacts cognitive outcome. Meta-studies of patient bloodwork show that peripheral inflammatory marker concentrations correlate with severity of cognitive symptoms [120, 121]. In animal models, isoflurane exposure mediated increases in inflammatory cytokines expression contribute to cognitive impairments [50, 122, 123].

In the setting of inflammation, increased surface expression of tonic $GABA_A$Rs can be observed. Application of the inflammatory cytokine IL1-β to hippocampal neurons increases $\alpha_5\beta_2\gamma_2$ surface expression, increasing both tonic current and its potentiation by anesthetics [124] [125]. Mice treated with lipopolysaccharide injections, which model sepsis by stimulating the innate immune system, show potentiated hypnosis and ataxia from isoflurane and etomidate [125]. Depressions in spatial memory, fear-based learning, and long-term potentiation seen in these animals also appear to be reversible with α_5 receptor antagonist or subunit deletion. The intracellular mechanisms that mediate this effect are not fully understood, although induction of MAPK signaling pathway by inflammation has been implicated.

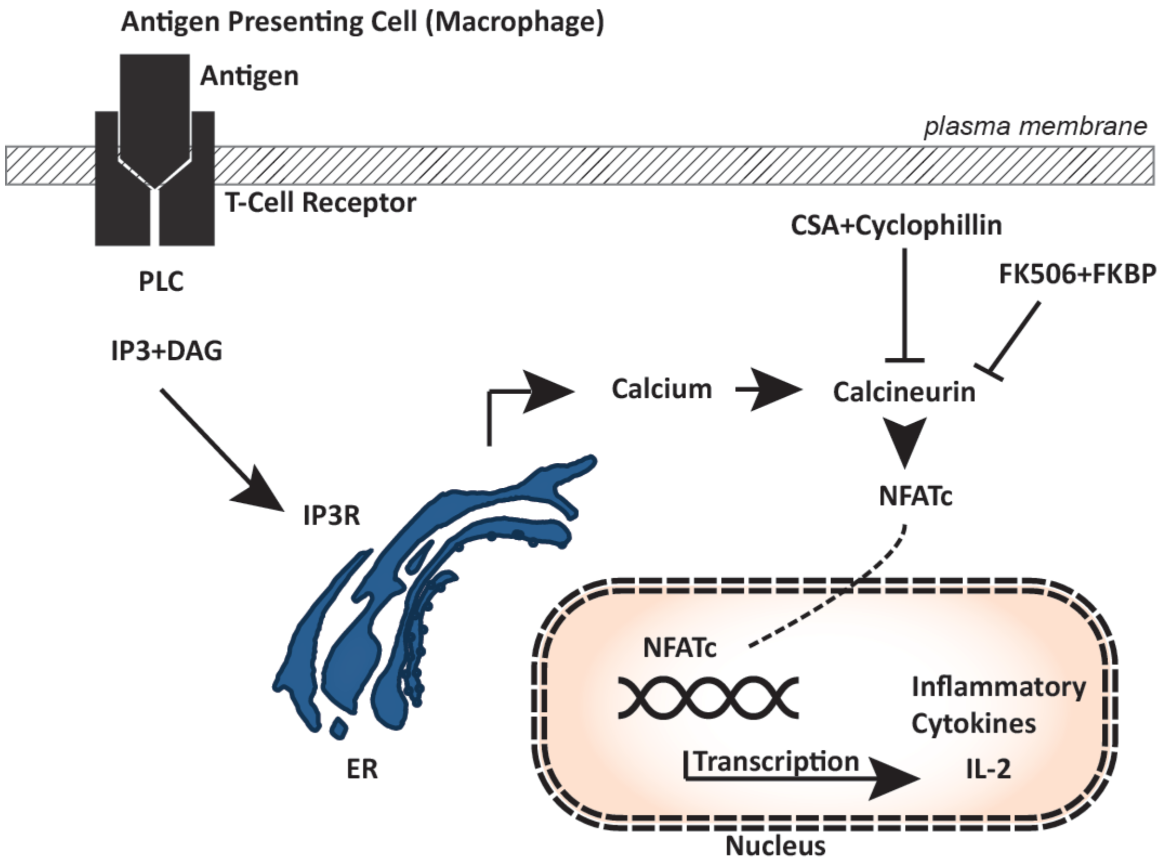

Figure 1.7 Calcineurin-mediated processes initiate the T-cell immune response.

Figure 1.7 Calcineurin-mediated processes initiate the T-cell immune response. T-cell lymphocytes are stimulated when T-cell receptors recognize and bind antigens presented on the macrophage surface. This extracellular event initiates an intracellular signaling cascade that activates calcineurin in a calcium-dependent manner. Once activated, calcineurin dephosphorylates and activates cytosolic nuclear factor of activated t-cells (NFATc) transcription factor, which then translocates to the nucleus and upregulates interleukin 2 (IL-2) expression, stimulating T-cell differentiation and eventually expression of other cytokines. Calcineurin inhibitors are the most common class of immunosuppressant drugs. Cyclosporine A (CSA) inhibits calcineurin through a protein complex formed with cyclophillin D, whereas FK506 (or Tacrolimus) inhibits calcineurin through a complex with FK506-binding protein (FKBP).

1.12 Summary of background information, and rationale of dissertation.

General anesthetics are invaluable and unique among medicines because of their capacity for controlled manipulation of consciousness. Although substantial work has been done to characterize the effect of anesthetic agents on biophysical function of $GABA_A$Rs and the resultant effect on global patterns of brain activity, much less is known about the long-term physiological consequences. The specific mechanisms by which anesthetics may be involved in the development or exacerbation of neurological dysfunction remain unresolved. Recent work suggests that increases in surface expression of the $\alpha_5\beta_3\gamma_2$ $GABA_A$R subtype contribute to impairments in memory and synaptic plasticity that persist up to two weeks following isoflurane anesthesia. Because immunomodulation can greatly affect the expression of post-anesthetic learning impairments, a link between neuroinflammation and inhibitory signaling is suspected. Several independent lines of work have shown that disabling various elements of the immune response can alter the expression of post-operative learning phenotypes.

The most commonly used immunosuppressant drugs are calcineurin inhibitors, the prototypic agent being Cyclosporin A. Calcineurin is a serine/threonine protein phosphatase that is ubiquitously expressed but also enriched in the central nervous system. Typically, calcineurin is activated by low (nm) levels of calcium via complex protein interactions wherein calcium binds the regulatory subunit and calmodulin binds the catalytic subunit in a calcium-dependent manner. Within the systemic immune system, calcineurin gates the t-cell response by controlling activated t-cell transcriptional upregulation of cytokines and subsequent proliferation (**Figure 1.7**).

The primary objective of this thesis project was to evaluate the possibility that these impairments from isoflurane are based on calcineurin-mediated aberrations in $GABA_AR$ trafficking and surface expression. Based on evidence that inflammation and neurodegenerative-like disease processes may be involved in animal models of post-operative memory impairments as well as altered receptor surface expression, we initially predicted that immunosuppression with Cyclosporine A would block the development of learning impairments and prevent upregulation of $\alpha_5\beta_3\gamma_2$ surface expression.

In Chapter 2, I present experiments that investigated the effects of isoflurane on $GABA_AR$ trafficking. The aim was to delineate the changes in $GABA_AR$ surface expression that occur in immediate response to isoflurane exposure, and determine a potential role for calcineurin. Although we were primarily interested in the immunomodulatory effects of calcineurin (CN) as a mechanism for anesthetic-related cognitive dysfunction, CN is well-characterized as a direct regulator of $GABA_AR$ trafficking and hippocampal inhibitory synaptic plasticity and we thus addressed the possibility of direct effects of isoflurane and CN inhibitors on surface expression. These experiments utilized *in vitro* approaches in primary hippocampal cultures, specifically cell-surface biotinylation and live-cell imaging.

In Chapter 3, a mouse model is used to investigate the effect of calcineurin inhibition on post-anesthetic changes in cognitive function. I used acute brain slice biotinylation and western immunoblot to measure total and cell-surface expression of key proteins associated with inhibitory neurotransmission, including the α_5 subunit.

In Chapter 4, I discuss these findings together. In particular, I discuss how these findings may cause us to reconsider the role of calcineurin in recovery of cognitive function following anesthesia.

Extended methods are described in Chapter 5. Whereas previous individual chapters include methods at a publication-appropriate length and level of detail, this chapter will provide design logic with appendix-style figures to fully explain the setups for experimenting with isoflurane.

Chapter 2: The effect of isoflurane on $GABA_AR$ surface expression

The effect of isoflurane on $GABA_AR$ surface expression

2.1 Introduction

$GABA_A$ receptor ($GABA_AR$) cell surface expression is fundamental to inhibitory neurotransmission because it controls the number and type of receptors available for GABA, endogenous modulators, and exogenously applied substances. Constant recycling of $GABA_ARs$ between the cell surface and the cytosol is actively regulated by intracellular signaling pathways. Several drugs that modulate $GABA_AR$ channel function (e.g. flumazenil [126], ethanol [73], and neurosteroids [127]) have been demonstrated to alter receptor trafficking. Many behavioral and clinical consequences result from alterations in receptor recycling, examples include: drug tolerance and habituation [128, 129], memory formation, anxiety-like behavior [130], and seizure threshold [131, 132]. Recent studies have demonstrated that the intravenous anesthetic agent propofol [118] can increase $GABA_AR$ surface expression in hippocampal neurons on the time scale of minutes/hours. Whether this property extends to isoflurane, one of the most commonly used anesthetic agent, is unknown.

Concerns over potential neurotoxic effects of isoflurane (and other GABA-ergic anesthetic agents) have emerged following demonstration of neuroapoptosis *in vitro* and memory deficits *in vivo* after isoflurane exposure [133]. One proposed mechanism of isoflurane-mediated adverse changes in neurological function is an influence on calcium homeostasis [112]. Intracellular calcium is a common mediator of numerous intracellular signaling pathways, with a particularly critical importance in activity-dependent processes like synaptic plasticity. Normally, sequestered calcium stores in the endoplasmic reticulum are controlled by inositol three phosphate (IP3), an intracellular second messenger that is generated when activated protein kinase C (PKC) translocates to the plasma membrane and hydrolyzes the phospholipid phosphatidylinositol 4,5-bisphosphate. Commensurate to IP3 synthesis and binding, IP3-gated calcium channel receptors on the endoplasmic reticulum (ER) permit calcium efflux into the cytosol, generating a signaling cascade that transduces PKC signaling into intracellular calcium levels. Isoflurane and structurally similar anesthetics (like sevoflurane and desflurane) can directly activate IP3 receptors and increase cytosolic calcium [111].

The isoflurane-mediated ectopic release of ER stored calcium into the cytosol has been established in several types of somatic cells, as well as in neural progenitor cells [134, 135] and mature hippocampal neurons [113]. This mechanism has been suggested to mediate anesthetic-induced changes in survival pathway signaling [136], and in progressive neurodegeneration [137]. However, the characterization of the full repertoire of calcium-sensitive processes and calcium-dependent proteins that are affected by clinically relevant exposures of isoflurane remains uncertain, especially the potential effects on calcium-dependent proteins that regulate synaptic function.

Isoflurane exposure has been shown to increase the activity of Calcineurin (CN), a calcium and calmodulin-dependent protein phosphatase that participates in $GABA_AR$ trafficking and surface expression [136, 138]. Within hippocampal circuits, CN activation regulates synaptic plasticity and memory formation by controlling the surface expression of several neurotransmitter receptors and ion channels. At inhibitory synapses, CN dephosphorylates the $GABA_AR$ γ_2 subunit at Serine327, which promotes dissociation from the post-synaptic density and subsequent endocytotic removal from the cell surface. However, Serine327 is also phosphorylated by PKC, which itself is also calcium-activated. Because the effect of isoflurane-mediated calcium release can activate both the phosphorylation and dephosphorylation of $GABA_A$Rs, predicting the outcome (if any) of this drug on $GABA_A$R surface expression is not straightforward.

The primary intent of this set of experiments was to evaluate the effects of isoflurane on $GABA_A$R receptor trafficking. We initially hypothesized that the net effect of isoflurane would be to augment CN-mediated dissociation and removal of $GABA_A$Rs from the cell surface, and that inhibition of CN with application of cyclosporine A (CSA) would result in an increase in the surface expression of $GABA_A$Rs. To evaluate this possibility, we conducted *in vitro* studies in mature primary hippocampal neuron cultures (DIV17-25), using cell-surface biotinylation and live-cell imaging.

2.2 Material and Methods

Primary Neuron Culture

Primary hippocampal neuron cultures were prepared based on previously published methods [139]. E17-E19 timed pregnant Sprague-Dawley rats (Charles River) were sacrificed by carbon dioxide asphyxiation, and pups removed by Caesarean section. The brain and hippocampi were isolated in sterile ice-cold Dissection HBSS (Calcium and Magnesium Free Hanks' Basic Salt Solution plus 10mM HEPES, both Invitrogen). Trypsinized tissue was then minced and transferred into a 15ml Falcon tube with 5ml Dissection-HBSS with 0.25% Trypsin (Invitrogen) and incubated at 37°C for 8 minutes. Tissue was washed three times in Plating Media (MEM (Invitrogen), 33 mM glucose (Sigma), 10 mM HEPES, 10% Horse serum (Atlanta Biologicals), 1% PenStrep

(Invitrogen), pH 7.3), and then triturated with fire-polished glass Pasteur pipettes. Viable cells were counted on a hemocytometer with a mixture of cell suspension and Trypan Blue. For biochemistry experiments, dissociated cells were plated onto 60mm plastic petri dishes at a density of 800,000-1 million per dish. For live cell imaging experiments, dissociated cells were plated onto 35mm glass-bottomed petri dishes (P35G-1.5-14-C, MatTek Corporation Ashland, MA) at a density of 350,000 per dish.

The day before dissection, all dishes and glass were pretreated with an overnight incubation of 0.1 mg/ml (plastic) or 1 mg/ml (glass) Poly-L-Lysine (Sigma) in Borate Buffer (in mM: 40 boric acid, 10 borax, pH 8.5). The next day, solution was aspirated and the dishes were washed three times in autoclaved Milli-Q deionized water and allowed to dry completely. Glass-bottomed dishes were pretreated as follows, per instructions from MatTek: 250 µl of 1M HCl was applied to the glass insert for 15 minutes then aspirated. Dishes were washed three times with sterile PBS (Invitrogen), two times with autoclaved Milli-Q water, and then allowed to dry completely.

On the day of dissection, coated dishes and plates were incubated with plating media for at least two hours before plating. All cells were maintained in a 5% CO_2 incubator at 37°C and left for 2 hours (glass) or overnight (plastic) after plating before changing the media to complete Neurobasal media (Neurobasal base medium, 1% glutamax, 2% B27, all Invitrogen). Two days after plating, 1 µM cytosine arabinoside (Sigma) was added to culture media to arrest glial proliferation. Four days after plating, media was exchanged with new complete Neurobasal media. Subsequently, a ~30% media change was made every three days.

Primary Neuron Culture Drug Application

Neurons were pretreated for one hour with CSA (20uM, 30024, Sigma) from stock solutions prepared in DMSO. Lorazepam and propofol , 2,6-diisopropylphenol (10µm, D126608, Sigma) exposures were similarly applied. For vehicle treatments, DMSO was added for an equivalent final concentration of 0.1%.

Vaporized Isoflurane Treatment of Cultured Neurons

Neurons were treated with vaporized isoflurane or sham gas using a setup modified from published methods [140]. Isoflurane was mixed into gas from content certified canisters containing 21 % oxygen, 5 % CO_2 and 75% nitrogen (NexAir, TN) using a calibrated isoflurane vaporizer (Ohio Medical products, Madison WI). For sham treatment, the vaporizer dial was set to zero, allowing gas to bypass the vaporizing chamber. Normal (sham) or isoflurane-containing gas was delivered into an airtight chamber (Posi-Seal mouse induction chamber, cat. no. AS-01-0532 Molecular Imaging Products, Bend OR) housed inside of a cell culture incubator (HeraCell 150i, Thermo Scientific) set to maintain a temperature of 37°C. The flow rate was 2L/min for the first 15 minutes of exposure, then 1L/min for the remainder of the treatment.

Culture plates were randomly placed inside the airtight chamber, on top of wet filter paper for humidity. Temperature within the chamber was monitored with a digital thermometer (VWR). Gas content was measured continuously throughout the experiment using a side-stream analysis circuit. Gas exiting the chamber was lead out of the incubator via tubing that bifurcated into an isoflurane air scavenger F/AIR filter canister

(Harvard Apparatus) and an anesthetic agent analyzer (Capnomac Ultima, Datex Ohmeda). Treatment terminated when the plates were removed from the chamber.

Cell surface biotinylation in primary neuron cultures

Cell surface biotinylation was performed immediately after terminating gas exposure. To limit endocytosis, 60 mm plates were packed into ice, all solutions were ice cold, and all washes (4ml/plate) and incubations were done on ice on an orbital rotator on a slow setting (120 rpm). Culture media is aspirated and washed once quickly with PBS supplemented with Calcium and Magnesium (Gibco life 10010-023, 1mM $CaCl_2$, 0.5mM $MgCl_2$, pH 7.4), followed by two washes at 5 minutes. Plates were then incubated with 1.5 ml of 1 mg/ml EZ-link Sulfo-NHS-biotin (Pierce, Thermo Scientific) in PBS/Ca^{++}/Mg^{++} for 20 minutes. The working biotin solution was made during the last wash from a single-use aliquot of 200mg/ml stock biotin in DMSO (stored at -80°C), and then used immediately. Plates were washed with two quick and two 5 minute incubations of TBS-Glycine (25 mM Tris, 140mM NaCl, 3mM KCl, pH 7.5, plus 100mM glycine). To harvest protein, neurons were scraped in ice-cold RIPA/PI (RIPA buffer with Halt Proteinase Inhibitor, both Pierce), flash frozen on dry ice, then stored at -80°C. Next, samples were thawed on ice and homogenized by sonication (3 pulses, 5 seconds, 25% on Fischer Scientific Dismembraner). Cellular lysates were clarified by centrifugation (4C°, 10,000g, 15 minutes) and supernatant was transferred to a new microcentrifuge tube. Protein concentration was measured by BCA assay (Bicinchoninic acid assay, Pierce). For each sample, an aliquot of clarified lysate was taken as “total” protein. Lysates were stored at -80°C until SDS-PAGE and Western Blot analysis.

Neutravidin Pulldown

Biotinylated proteins were purified with Neutravidin beads (Pierce), prepared as follows. For each sample, 250µl of bead slurry was aliquotted into microcentrifuge tubes. Beads were centrifuged (2 min, 4°C, 2,500 rcf) and supernatant was aspirated with a fine gel-loading pipette tip. Beads were resuspended and washed three times with TBS, and then twice with RIPA/PI, centrifuging and aspirating as described above each time. After the final wash, beads were resuspended in 250 µl RIPA/PI before adding 375 µg sample lysate that was diluted to 1µg/µl in RIPA/PI. Lysate was incubated with beads overnight for ~16-18 hours of end-over-end rotation at 4°C. Afterwards, microcentrifuge tubes were centrifuged (4°C, 2 minutes, 5,000 rcf) and supernatant removed. Beads were washed four times in 250 µl RIPA/PI, each with 20 minutes of end-over end rotation at 4°C. Neutravadin-bound protein was eluted with 60 µl of 2x Laemmli Buffer (Bio-Rad) with 5% (v/v) β-ME by boiling (95°C, 20 minutes) and centrifugation (10 minutes, 25°C, 13,500 rcf). Eluted samples were stored at -20 °C prior to SDS-PAGE and Western blot analysis.

Live Cell Imaging of γ_2 $GABA_AR$ subunit surface expression

Neurons were co-transfected at DIV 8-12 with cDNA for γ_2-SEP and tdTomato using the CalPhos Mammalian Transfection Kit (Clontech, Mountain View, CA) and previously published methods [141]. The γ_2-SEP plasmid was a gift from Tija Jacob & Stephen Moss (Addgene plasmid # 49170) [97]. Plasmid cDNA was prepared from transformed E.Coli, purified with a Maxiprep kit (Qiagen), and resuspended in Milli-Q deionized water at 1-2µg/µl. Neurons were imaged at DIV19-25 inside of a stage-top incubator (Model INUB-GSI-BP-F1, Tokai Hit) on an Olympus IX83-DSU Disk Scanning Unit confocal microscope. The incubator was humidified and set to maintain a lid temperature of 45°C and imaging solution temperature of 37°C. All imaging was done in HBS, 37°C, pH 7.4 unless otherwise stated. On the day of experimentation, HBS was supplemented with either 20 µM CSA/0.1% DMSO or 0.1% DMSO.

Aqueous solutions of 320 µM isoflurane were prepared inside of airtight 100ml saline intravenous drip bags based on previously published methods [35]. HBS (50ml) was agitated inside of a shaking incubator (32°C), and air bubbles removed through the injection port with a long 18g needle. For the isoflurane treatment solution, liquid isoflurane was injected with a 10µl HPLC/Gas Chromatography syringe (National Scientific), and mixed on a stir plate for 20-30 minutes. Sham HBS was prepared identically, sans isoflurane. Until use, bags sat inside of a cell culture incubator set to 37°C less than two hours. To prepare for imaging, individual MatTek dishes were pretreated with either DMSO or 20 µM CSA, and returned to the incubator for one hour. After pretreatment, neurons were washed twice with HBS, and the dish was set into the microscope stage-top incubator. Neurons were identified via tdTomato fluorescence to minimize GFP photobleaching. Baseline recordings were made in HBS. Isoflurane or sham HBS solution was perfused into the MatTek dish by gravity at a rate of 0.75ml/min through an intravenous flow rate controller and removed by vacuum aspiration. Washout HBS was applied as three 5 ml rinses of HBS, perfused into the dish through a syringe. At the start and end of the experiment, pH sensitivity was tested with a wash of imaging solution adjusted to pH 4. Any experiment where neurons presented signs of cell damage at any point (e.g. blebbing) was excluded from analysis.

Image Parameters and Analysis

Images were acquired with a 60x objective and an ImagEM X2 EM-CCD camera (model 9100-23B, Hammamatsu) using CellSens software (Olympus) as a Z-stack of 7-12 optical sections at a rate of one z-stack every two minutes. Image files were exported as .TIFF files. Intensity measurements were performed manually using the FIJI version of ImageJ (NIH). All images files were concatenated then pre-processed with the Stackreg macro to correct for minor (x,y) plane drift correction, and transformed into an inverted maximal Z projection. Images were generated in ImageJ from single frame maximal Z-projections with background and contrast adjusted. To analyze fluorescence values, mean intensity values were measured in every frame using ImageJ then exported to GraphPad for further analysis. Fluorescence was measured within regions of interest (dendrites expressing fluorescent clusters) hand drawn using the tdTomato image as a guide to the full dendritic arbor and somatic region of the analyzed neuron. Local background was measured as mean grey intensity and subtracted. Individual dendritic regions were combined by the XOR function, and fluorescence intensity of the frame was measured as the mean grey intensity. Time-course representations were made by plotting the mean intensity of a frame over time, and normalizing the single frame intensity (F) to the average intensity of the third five frames or 10 minutes of baseline (F_0). Single frame measurements were normalized to the average intensity of the third 10 minutes of baseline recording, and then normalized to the sham baseline.

SDS-PAGE/ Western Blotting

Protein samples were resolved in Criterion precast gel (Bio-Rad), then transferred to a PVDF membrane using a semidry system (Bio-Rad). All immunoblots were performed as follows. Membranes were blocked for one hour in 5% non-fat dry milk in TBST (25 mM Tris, 140mM NaCl, 3mM KCl, and 0.1% Tween-20), then probed overnight at 4°C with primary antibody diluted in 5% BSA in TBST. Membranes were washed, and then probed for one hour with horseradish peroxidase conjugated secondary antibody diluted in 5% milk TBST. Immunoreactive bands were detected with chemiluminescence using ECL substrate (ECL Prime, Abersham or West Pico, Pierce) on a Chemidoc imager (Bio-Rad), and quantified in ImageJ (NIH) using mean intensity measurements from regions of identical dimensions. To measure Neutravidin purified $GABA_AR$ subunits, membranes were cut for parallel blots of the subunit and transferrin receptor. Subunit intensity was normalized to the transferrin receptor. Total protein was normalized to β-Actin. To measure caspase-3 cleavage, intensity of the ~20kd region was first normalized to the intensity of full-length caspase, and then normalized to either GAPDH or β-actin.

The primary antibodies used were: $GABA_AR$ β_2 subunit, Abcam, Ab1560000; $GABA_AR$ γ_2, Abcam, Ab87328; GAD-67, Sigma, SAB4300642; GAPDH, Millipore, mab375; β-Actin, Sigma, A5441; Caspase-3, Cell Signaling, 96624; Transferrin Receptor, Life, 13-6800. Secondary antibodies were: mouse NA931, rabbit NA934, both Abersham, GE.

Statistical Analysis

All raw data was imported into Prism (Graphpad) for graphing and statistical analysis. The Kolmogorov-Smirnov test was used to assess Gaussian distribution, and one-way ANOVA and Student's t-tests were performed as described.

2.3 Results

Isoflurane (1h) has no significant effect on γ_2 or β_2 surface expression

To study the acute effect of isoflurane on $GABA_AR$ surface expression, we first used cell-surface biotinylation and affinity-purification with Neutravidin. Cultured hippocampal neurons (DIV17-23) were pretreated with vehicle or CSA (20 μM) for one hour, and then exposed to sham gas or vaporized isoflurane for one hour immediately prior to cell surface biotinylation. The γ_2 subunit was probed because it contains the known calcineurin regulatory sites [77, 142] within the large intracellular loop domain. When normalized to the control sample (receiving vehicle and sham gas), the ratio of γ_2 surface to total protein expression was not significantly affected by either isoflurane or CSA (isoflurane: 118%±18.3, n=5, p=0.9328; CSA: 110%±23.4, n=6, p=0.8966, isoflurane and CSA: 94.2%±11.3, n=6, p=0.8831; ANOVA with Dunnett's post-hoc test with comparison to vehicle/sham group) (**Figure 2.1**). The difference between the isoflurane treated group and the isoflurane and CSA co-treated group was also not significant (110±23.4 vs. 94.2±11.3, p=0.4612, ANOVA with Dunnett's post-hoc test).

Surface expression of β_2 was also analyzed because of its ubiquitous expression within most $GABA_AR$ subtypes, including the $\alpha_1\beta_2\gamma_2$ subtype, which is the most abundant in both the hippocampus and CNS in general. We found that β_2 subunit surface expression was also not significantly affected in any treatment group (**Figure 2.2**).

In contrast, identical biotinylation and affinity-purification protocols were performed on cultures exposed to 2,6-diisopropylphenol (propofol) showed a profound effect on β_2 subunit surface expression, as previous shown [118] (**Figure 2.3**). Compared to vehicle, 30 minutes of propofol significantly increased surface protein (219.2%± 47.4, p=0.0079, t-test) and the ratio of surface to total protein (236.8%±6.40, p=0.00418) but not total expression (93.19%±22.53, p=0.8309). Compared to vehicle, 60 minutes of propofol also increased surface protein (243.04%± 41.61, p=0.0559), the surface to total ratio significantly (p=0.0159), but not total protein (113.4%±36.16, p=0.734).

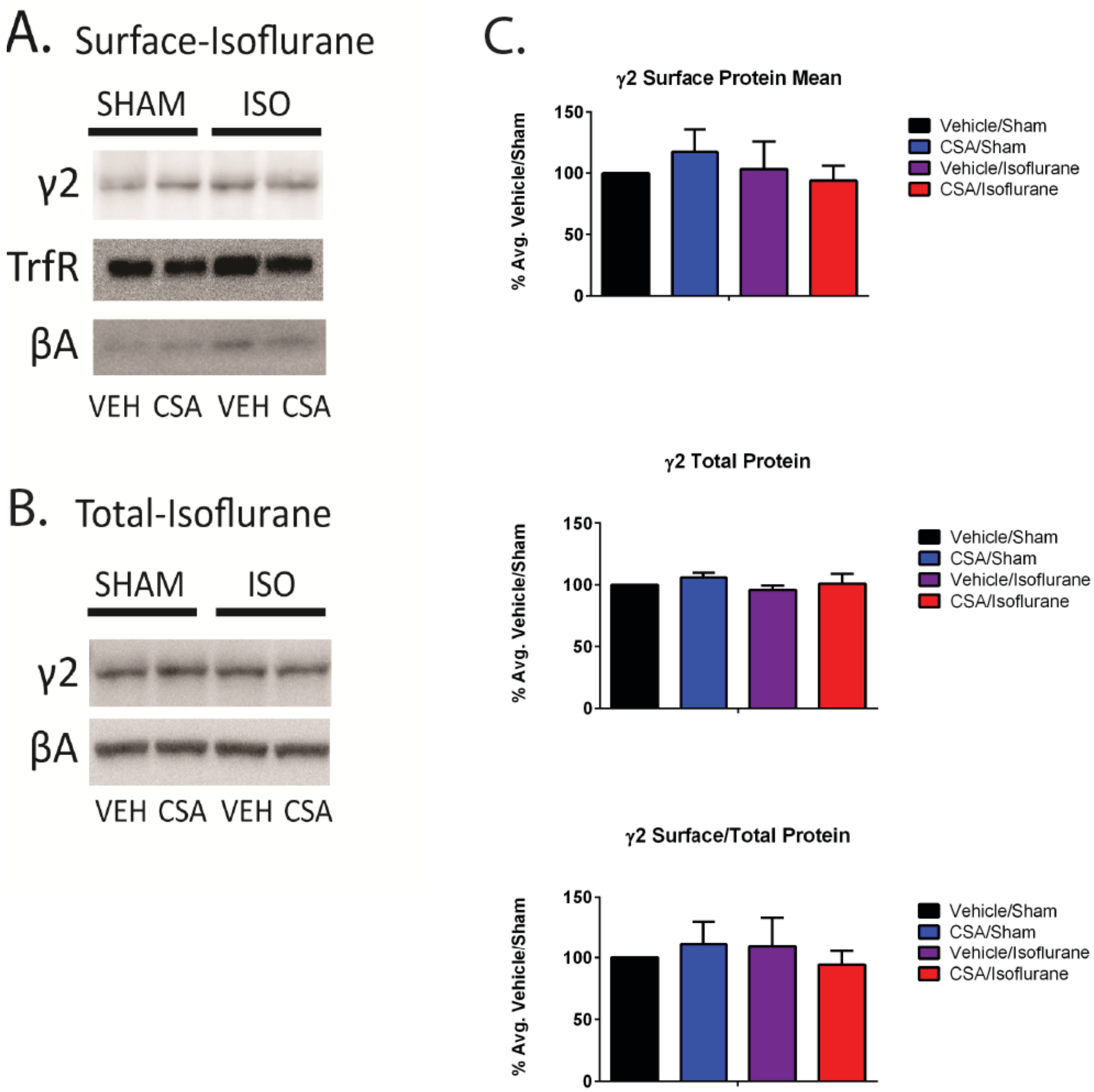

Figure 2.1 Effect of acute isoflurane exposure on γ_2 surface expression

Figure 2.1 Effect of acute isoflurane exposure on γ_2 surface expression. Western blot (A, B) of γ_2 subunit surface and total expression following isoflurane exposure. When quantified (C), no statistically significant changes were observed. Error bars are Mean± SEM.

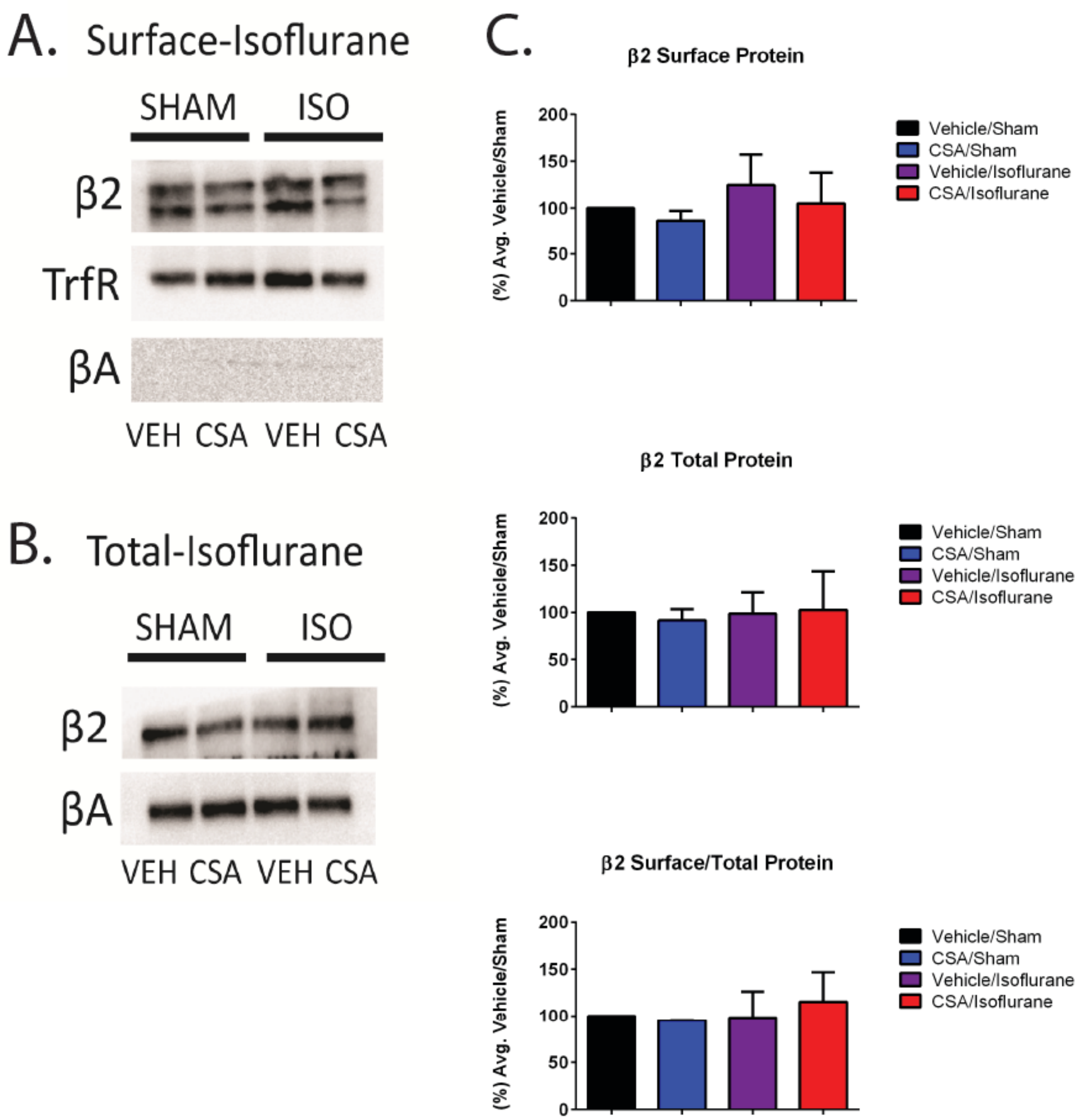

Figure 2.2 Effect of acute isoflurane exposure on β_2 surface expression

Figure 2.2 Effect of acute isoflurane exposure on β_2 surface expression. Western blot (A, B) of β_2 subunit surface and total expression following isoflurane exposure. When quantified (C), no statistically significant changes were observed. Error bars are Mean± SEM.

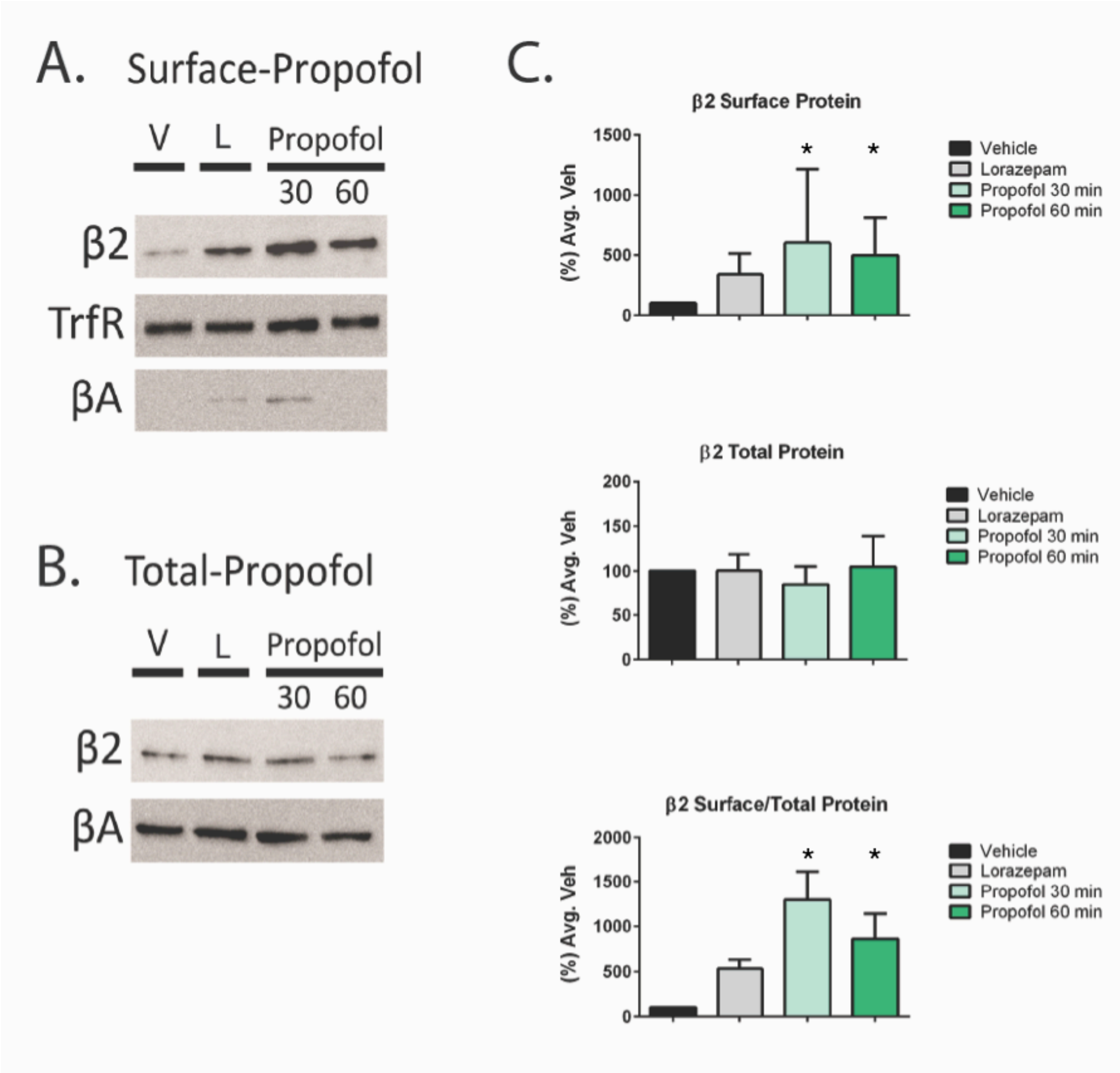

Figure 2.3 Effect of acute propofol exposure on β_2 surface expression

Figure 2.3 Effect of acute propofol exposure on β_2 surface expression. Western blot (A, B) and quantification (C) of β_2 subunit surface expression following propofol. Error bars are Mean± SEM.

Caspase-3 cleavage after isoflurane (1 hour) is unaltered by CSA

To address the possibility that the failure to measure an increase in surface expression of specific $GABA_AR$ by CSA was due to neurotoxic effects of CSA, isoflurane, or the combination, total lysate from biotinylated samples was probed for caspase-3 (**Figure 2.4**). Cleaved caspase-3 was not significantly changed in any group (Sham/Veh vs. Sham/CSA p=0.9198, Sham/Veh vs. Iso/Veh p=0.8898, Sham/Veh vs. Iso /CSA p=0.8800, Iso/Veh vs. Iso /CSA p=0.9382, all t-test). In contrast, an equal amount (25µg) of lysate from DIV 16 neurons treated with 6 hours isoflurane that was loaded onto the same immunoblot did show clear evidence of caspase-3 cleavage.

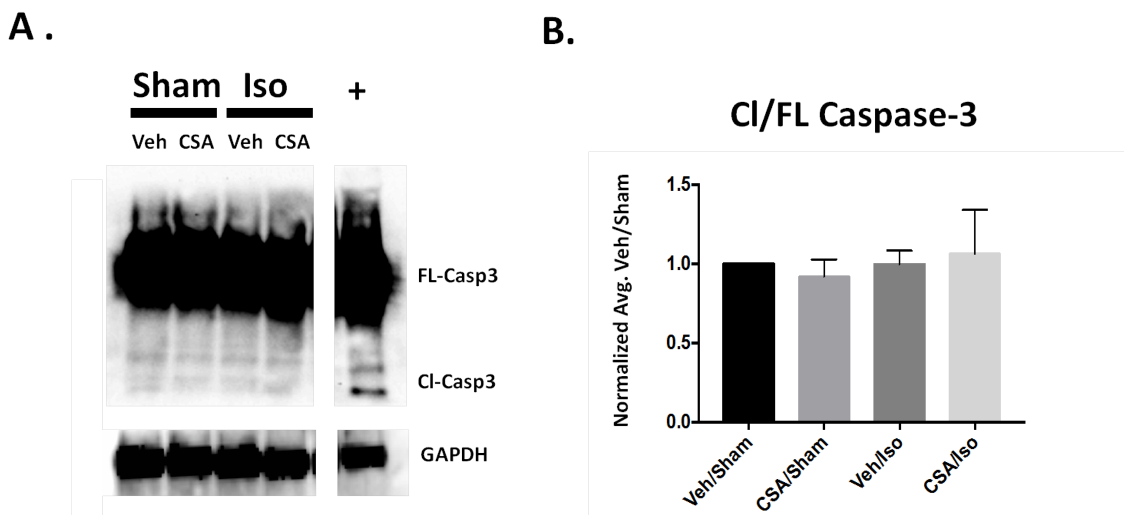

Figure 2.4. CSA does not alter caspase-3 cleavage after 1 hour isoflurane

Figure 2.4. CSA does not alter caspase-3 cleavage after 1 hour isoflurane. (A) Western blot: 25 μg lysate from DIV 20 neurons used in cell-surface biotinylation (left), and 25μg lysate from DIV 16 neurons treated with isoflurane for 6 hours (+, right). **(B)** Mean grey intensities of cleaved /full-length caspase-3 normalized to GAPDH. Error bars are Mean± SEM.

Live cell imaging

As demonstrated in **Figure 2.3**, a maximal increase in $GABA_AR$ subunit expression occurs within a half hour of propofol exposure. In order to monitor the dynamics of $GABA_AR$ trafficking throughout an isoflurane exposure on a time-course less than 1 hour, we performed live-cell imaging using hippocampal neurons expressing γ_2 subunits tagged with super-ecliptic pHluorin (γ_2-SEP), a pH-sensitive GFP variant that fluoresces when expressed on the cell surface. Fluorescence quenches upon endocytosis due to the acidity of internalized vesicles [143]. Expression of γ_2-SEP is shown in **Figure 2.5A**. The fluorescent signal presents as puncta found on the cell body and dendritic shaft that is lost upon exposure to acidified extracellular solution, confirming surface expression (**Figure 2.5A, right**). After pretreatment, neurons were imaged for thirty minutes of baseline recording in a HEPES-buffered saline (HBS), a fifty minute perfusion of HBS containing 320 μM (~ 1 MAC) isoflurane or a sham solution, and then a thirty-minute washout. To test the effect of calcineurin inhibition, 20 μm CSA was added in the media for pre-treatment and to the HBS perfusate. Surface expression was measured throughout the experiment as F/F_0, or the ratio of fluorescence in a given frame over the baseline fluorescence measurement, as presented in **Figure 2.5B** as a time-course representation. When F/F_0 values at 30 minutes after the onset of isoflurane perfusion was normalized to the sham F/F_0 (**Figure 2.5C**), isoflurane did not evoke a statistically significant increase F/F_0 (102.7%±1.10, p= 0.162, t-test). The increase was neither reversed by washout (p=0.8105, paired t-test), nor significantly different from sham treatment (104.0%±1.80, p=0.155, t-test). The addition of CSA to the isoflurane treatment also had no significant effect compared to sham (101.9%±0.31, p= 0.102, t-test). These results concur with surface biotinylation measures of native γ_2 receptors, which demonstrate that isoflurane treatment did not significantly increase surface expression. Collectively this data suggests that unlike propofol, short exposures isoflurane *in vitro* do not acutely affect $GABA_AR$ trafficking.

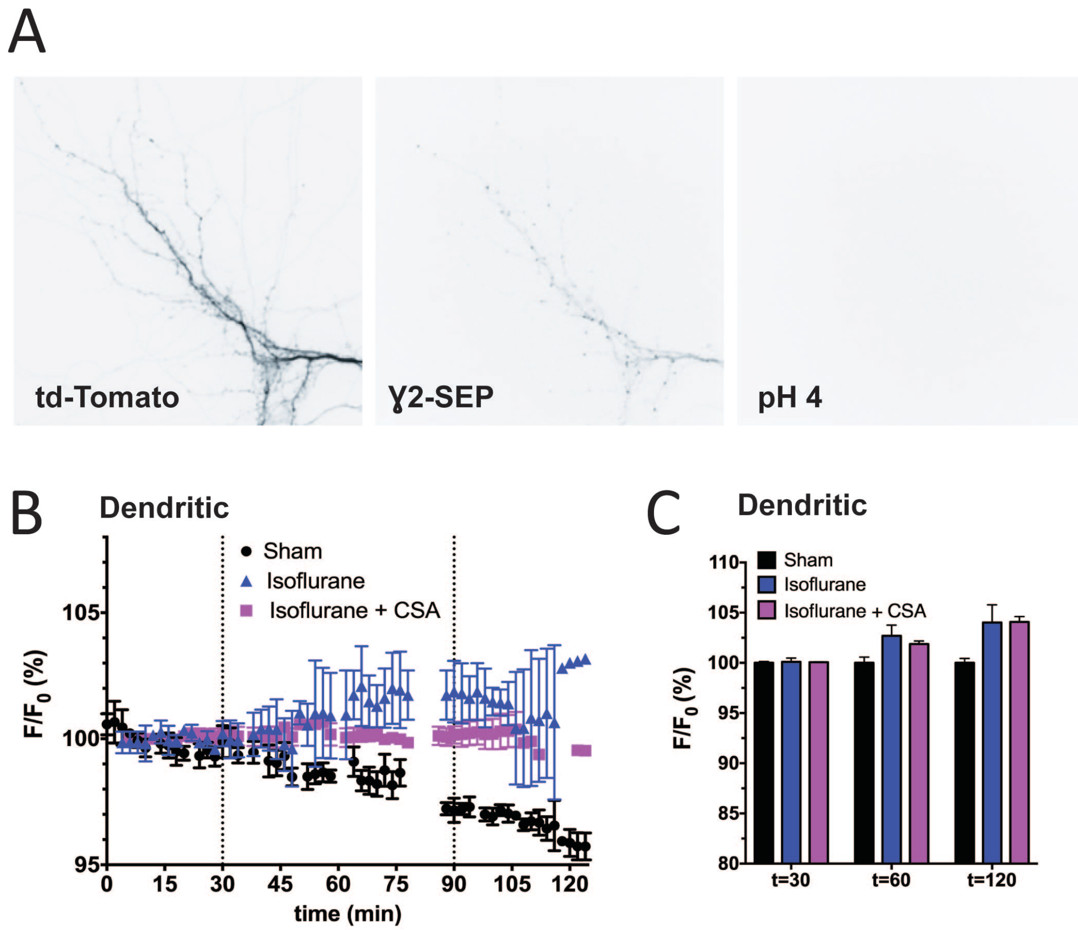

Figure 2.5 Live-Cell imaging of γ_2-SEP during an acute isoflurane exposure.

Figure 2.5 Live-Cell imaging of γ_2-SEP during an acute isoflurane exposure. Primary hippocampal neuron co-transfected with the cytosolic protein td-tomato and γ_2-superecliptic pHluorin (γ_2-SEP) subunit chimera **(A)**. γ_2-SEP fluorescence is quenched upon perfusion with an acidic extracellular solution **(A, Right)**. **(B)** Time-course of fluorescence throughout a perfusion of vehicle or 320 μM isoflurane (onset and offset marked by dotted lines), and then washout. For each frame, fluorescence (F) was baseline normalized to the average intensity of the last five frames (F_0) to generate F/F_0. **(C)** F/F_0 at t=30, 60, and 120 minutes from the start of recording, which correspond to the onset of isoflurane, the middle of isoflurane, and thirty minutes of washout respectively. F/F_0 values were normalized to the average sham treatment collected from the corresponding time-point. Error bars are Mean ±SEM

2.4 Discussion

$GABA_A$Rs constantly and dynamically transition between the cell surface and intracellular compartments through regular cycles of endocytosis and exocytosis. Several $GABA_A$R modulators (e.g. neurosteroids, ethanol) evoke changes in trafficking and surface expression that impact behavior and anesthetic sensitivity. Recent studies demonstrate that propofol and etomidate alter β_3 and α_5 subunit surface expression in hippocampal cultures [118, 119]. Calcineurin, a known regulator of $GABA_A$R trafficking, is activated following isoflurane exposure. These observations motivated us to test the hypothesis that isoflurane affects $GABA_A$R trafficking and surface expression through CN-mediated processes. Using biochemistry and imaging based experiments, we found that one hour of isoflurane did not have a significant effect on β_2 or γ_2 subunits surface expression levels. Similarly, we were unable to alter $GABA_A$R subunit surface expression with calcineurin inhibitors.

Cell Surface Biotinylation

Cell-surface biotinylation showed no significant effect of $GABA_A$R γ_2 and β_2 subunit surface expression following a one-hour exposure of isoflurane (**Figure 2.1-2.2**). Yet exposure to propofol did yield a significant effect on $GABA_A$R subunit expression (**Figure 2.3**), confirming results from other groups [118]. Our experiments were performed in slightly more mature neurons (DIV17-24) and enhance our collective knowledge of dynamic regulation of anesthetic $GABA_A$R subunit by anesthetics. Additionally, our demonstration of an increase of β_2 subunit surface expression is also novel as previously only β_3 subunits were known to increase in response to propofol exposure.

The mechanism by which propofol interferes with $GABA_AR$ trafficking is better characterized than the pluripotential effects of isoflurane. Propofol enhances PKCε, activity which normally regulates receptor endocytosis through phosphorylation sites on β subunits [114]. Specifically, $GABA_AR$ PKC sites (β_1-S409, β_2-S410, β_3-S408/9) are located within a protein-binding motif for the clathrin adaptor protein, and the phosphorylation state blocks the assembly of the protein complexes required for clathrin-mediated endocytosis [144]. Therefore, an increase in PKC leads to increased membrane expression. Because of its prolific use as an anesthetic induction agent, and increasingly as the main agent for total intravenous anesthesia, the ongoing characterization of intracellular targets and functional properties of propofol has a high clinical value. The physical interaction between propofol and PKC has been identified in the modulation of multiple other ion channels including the delayed rectifier potassium current in cortical neurons [145] and the vanilloid receptors within nociceptor sensory neurons [146]. Regardless, the effect of propofol on surface expression of the $GABA_AR$ subunits has not been associated with any behavioral effects or cognitive deficits.

By contrast, the manipulation of another $GABA_AR$ subunit, the α_5 subunit, has been associated with adverse memory testing in animal models [119, 124]. The GABA-ergic intravenous anesthetic, etomidate, has been shown to increase α_5 subunit surface expression in cultured hippocampal neurons after one hour of exposure [119]. However, that effect was contingent on specific culture technique using additional purified astrocyte layers. In the same study, etomidate had no effect on surface expression in neuron cultures prepared without this adaptation. It therefore remains possible that our culture conditions influenced our results - the presence of additional astrocytes may better resemble conditions in the brain, and is elaborated in the Discussion chapter. **Chapter 3** describes our investigation of the effects of isoflurane on the surface expression of the α_5 subunit with *in vivo* and *ex vivo* techniques.

We also used cell-surface biotinylation measures of surface expression to investigate neurotoxicity. The sulfo-NHS-biotin ligand used to covalently label or “biotinylate” receptors on the neuron cell surface is selective for external proteins because it is plasma membrane impermeant, but readily biotinylates intracellular proteins when the plasma membrane is compromised. Isoflurane has been implicated in two main pathways of neurotoxicity resulting from disrupted cytosolic calcium homeostasis [135]. The irregular activation of calcium-dependent regulatory proteins (including calcineurin) disturbs intracellular signaling cascades that maintain essential house-keeping functions [136], and there is evidence for resultant endoplasmic reticulum stress responses [147]. More directly, isoflurane can activate mitochondrial apoptosis pathways by inducing mitochondrial permeability transition pore (MPTP) opening, which collapses the mitochondrial electrochemical gradient and initiates a signaling cascade that culminates in caspase-3 activation and apoptosis. The calcineurin inhibitor used in this study, CSA, inhibits this process by blocking MPTP opening.

The reported kinetics of this phenomenon factored into our rationale for using an experimental model of a brief isoflurane exposure. The standard experimental paradigm for robust activation of the final apoptosis marker, cleaved caspase-3, in primary cultured neurons is a six-hour exposure of 2% isoflurane. After a shorter three-hour exposure, neurotoxicity pathway phosphorylated intermediates are increased compared to controls but not cleaved caspase-3 [147, 148], suggesting a longer time-course for the actual execution of cell death and plasma membrane degradation. Based on this, we reasoned that a one-hour isoflurane treatment would be sufficient to avoid the potential effect of apoptotic cell death on biotinylation [149]. In our study, we did find low levels of cleaved caspase-3 that were not differentially affected by either isoflurane and/or CSA pretreatment (**Figure 2.4**). Our interpretation is that this background apoptosis is derived from a minority of neurons undergoing necrosis or senescence within mature primary cultures, and is unrelated to isoflurane.

Live Cell Imaging

To increase the temporal resolution of surface receptor measurements, we performed live-cell imaging using γ_2 subunits tagged with super-ecliptic pHluorin (γ_2-SEP), a pH-sensitive GFP spectral variant. The premise is that when the receptor is expressed on the neuron cell surface, the N-terminal affixed SEP is exposed to neutral pH of the extracellular milieu and maximally fluorescent. When the receptor resides within intracellular compartments, many of which are acidified as a result of protein pumps, SEP fluorescence is quenched. We observed a progressive increase in fluorescence with the onset of an isoflurane perfusion (compared to sham perfusion) that did not reach statistical significance. This trend was also observed in the presence of the CN antagonist CSA, although there was a slight decrease compared to the isoflurane only group.

Altogether, these results suggest that one hour of isoflurane exposure is not sufficient to induce large changes in surface expression. As is, they do not exclude the possibility that longer isoflurane exposures may significantly alter surface expression, or that brief exposures have effects that require a longer time-course to manifest. In both techniques, isoflurane evoked a most increase in receptor expression that was not statistically significant. Further studies will be necessary to clarify whether these data indicate a real phenomenon with slower kinetics than propofol.

Strengths and Limitations

One limitation of this study is that biotinylation based affinity-purification of surface protein is a population measurement. A trade-off for quantitative sensitivity (~1 million cells assayed per sample) is the inability to resolve cellular subtype or intracellular sub-compartment differences. Primary dissociated neuron culture itself as a model system suffers from a loss of the natural patterns of neuronal connectivity and functional organization of the hippocampus because neurons are randomly redistributed upon plating. An organotypic or acute brain slice model would be superior in this aspect.

A limit of the live-imaging data is that dendritic rather than somatic γ_2 receptors were analyzed because of the high background and low resolution of somatic receptor clusters observed in our experiments. Somatic receptor clusters are more problematic to resolve with pHluorin-based imaging because the ER has a pH of 7.2, so fluorescence from inside this organelle is incompletely quenched [150, 151]. The distinction between dendritic and somatic receptors may be relevant to understanding the role of activated calcineurin in $GABA_AR$ trafficking because it was recently demonstrated that somatic but not dendritic α_2 containing receptor surface expression is increased through calcineurin dependent mechanism within a chemogenic epilepsy model [69]. If calcium-dependent processes are initiated from calcium released into the cytosol from the ER (e.g. by isoflurane) then it is reasonable to expect that the effects would invade the somatic or proximal dendrite regions before the distal dendrites.

One potential explanation of our data is that a one-hour of isoflurane exposure is insufficient to activate CN. However, the ability to exclude or more precisely delineate a potential role of CN in post-anesthetic receptor trafficking is limited by the absence of information about the temporal dynamics of calcineurin activation and its physical interaction (if any) with the $GABA_AR$ γ_2 subunit following isoflurane exposure. To date, the activation of CN following isoflurane exposure in mouse hippocampus immediately following a three-hour exposure has been demonstrated indirectly by immunoblot detection of downstream phosphatase targets and by immunodetection of a truncated (constitutively active) calcineurin form. Time-course studies relating anesthetic exposure to CN activity are currently lacking but will be necessary in order to resolve a potential role in expressing changes in neural function. Also, characterizations of the down-stream regulatory targets of isoflurane-activated CN could indicate which processes are vulnerable to anesthetic-mediated changes.

Finally, this study was limited in the scope of receptor subtypes assayed. We focused on γ_2 and β_2 subunits. However γ_2 also reports for the intrasynaptic $\alpha_1\beta\gamma_2$ assembly, which is the most abundantly expressed receptor subtype (reportedly 43%) in the CNS [61]. The $\alpha_5\beta_3\gamma_2$ assembly is of particular interest because of its unique role in the amnestic properties of anesthetics, and the future development of an α_5 subunit pHluorin probe would be experimentally valuable. Owing to its diffuse distribution and low expression within primary neuron cultures, much of the work describing $\alpha_5\beta_3\gamma_2$ surface dynamics has relied on biochemistry assays that leverage over-expression or immunoprecipitation, or advanced imaging techniques like quantum-dot labeling or immunostaining.

Significance

GABA$_A$Rs are drug targets of sedatives, hypnotics, and anti-convulsant agents, and surface expression governs sensitivity to powerful important clinical agents. In the context of anesthesia, these factors are directly relevant to understanding and predicting individual patient reaction to anesthetic agents and adjunct drugs. Moreover, GABA$_A$R surface expression changes are suspected in the development of adverse cognitive effects following anesthesia. Understanding the basic principles of how anesthetics and GABA$_A$R trafficking will be fundamental to elucidating the pathophysiology of these conditions. Further experiments using longer isoflurane incubation times are warranted, especially because multi-hour exposures are more appropriate models of the duration of surgery, but should be approached with caution because of the possible overlap of neurotoxicity and the potential impact on surface labeling results.

Chapter 3: Chronic Calcineurin Inhibition Impairs Visuospatial Memory After Isoflurane Anesthesia

Author experimental contributions

Christpher Ma collected behavioral data presented in figure 2.

Jonathan Fidler collected behavioral data presented in figures 3 and 4.

Jennifer Gooch prepared figure 6.

Edyta Bichler assisted in slice preparation for four animals in data presented in figures 6.

Iris Speigel prepared all figures, analyzed all data, and completed all biochemistry experiments.

This chapter has been slightly modified from the following manuscript. Speigel I, Fidler J, Ma C, Bichler E, Gooch JL, Garcia PS. Chronic Calcineurin Inhibition Impairs

Viuospatial Memory After Isoflurane Anesthesia (2017, in submission).

Chapter 3 Chronic Calcineurin Inhibition Impairs Visuospatial Learning After Isoflurane Anesthesia

3.1 Introduction

General anesthesia is suspected in the development of persistent deficits in wakefulness, attention, and memory, known loosely as post-operative cognitive dysfunction (POCD) [43-46]. Although still un-defined as a clinical entity [52], POCD has received intense focus in anesthesiology research because of pre-clinical data suggesting adverse effects of volatile anesthetics on learning and memory in animals [49-51].

Calcineurin (CN), a protein phosphatase activated by low levels of intracellular calcium, has been implicated in neurodegenerative diseases [152, 153], as well as isoflurane neurotoxicity [154]. CN activity increases after isoflurane anesthesia likely via activation of inositol triphosphate (IP3) receptors on the endoplasmic reticulum and subsequent calcium efflux [111]. CN is also involved in hippocampal synaptic plasticity, including regulating gene expression essential to synaptic function. CN also regulates the trafficking and surface expression of $GABA_A$ receptors ($GABA_ARs$) containing the γ_2 subunit [77]. Up-regulation of a particular γ_2-containing subtype, the extrasynaptic $\alpha_5\beta_3\gamma_2$ receptors, is associated with memory impairments following isoflurane and etomidate [119].

Our aim was to investigate the effect of chronic calcineurin inhibition on the recovery of cognitive functions (specifically memory) from a brief exposure to isoflurane. Cyclosporine A (CSA) reliably inhibits calcineurin in rodent models and can be orally administered for chronic exposure [155]. Initially, we hypothesized that CSA would protect against CN-mediated cognitive dysfunction induced by isoflurane in our mouse model.

3.2 Materials and Methods

Animals

All animal procedures were carried out according to the Atlanta VA Medical Center IACUC and adhered to the NIH guidelines for the care and use of laboratory animals. For all behavioral tests, eight- to ten-week old C57BL/6 male mice (Jackson Labs, Bar Harbor, Maine, USA) were purchased and allowed to acclimate one week before testing. Mice were individually housed in a climate- and humidity-controlled room on a 12-hour light:dark cycle with *ad libitum* food, water, and enrichment. All animals were assigned to one of four groups depending on whether they received chronic oral CSA vs. peanut oil vehicle (CSA vs. VEH) and whether they were exposed to isoflurane vs. sham anesthesia protocol (ISO vs. SHAM). Separate cohorts were subjected to motor coordination assays, memory testing, and tissue harvest for protein analysis. Treatment schedules are illustrated in **Figure 3.2A** and **Figure 3.3A**.

Oral administration of CSA:

Mice were treated with oral administration of 20mg/kg/day cyclosporine (Oral Solution, Teva Pharmaceuticals USA, Sellersville, PA) or peanut oil vehicle. CSA treatment was prepared by diluting the original solution (100mg/ml) into peanut oil for a final concentration of 0.8mg/ml. Individual food portions (20-25g) were supplemented with 500µl of peanut oil or 0.8mg/ml CSA solution. Dose was chosen based on minimal daily dosing for renal transplant recipients [156] adjusted for differences in metabolism and body surface area among mice and humans [157].

Wire-hang test:

Mice (n=10 per group) were challenged on experiment day 10 with the wire-hang test to grossly assess strength and coordination. Individual mice were placed into a clear cylindrical container sealed unilaterally with a metallic grate, and encouraged to grip through gentle shaking. The apparatus was inverted 180° and the latency to fall was timed. Three trials were performed per mouse at 10-minute intervals, and results were averaged across each mouse.

Anesthesia and emergence:

On Day 12 of pre-treatment, mice (n = 10 per group) were given a 30-minute treatment of isoflurane anesthesia or sham treatment (supplemental O_2). After a brief room acclimation, anesthesia was induced by placing mice into a pre-filled anesthetic chamber containing 2% isoflurane in pure oxygen (flow rate: 1.0 L/min). Body temperature was maintained with a ceramic heat lamp, and eyes coated with ophthalmologic ointment. After 30 minutes, mice were transferred to an "emergence" chamber, placed supine, and allowed to recover with atmospheric air. Three emergence metrics were scored: time to the first non-shivering forelimb movement, time to right (all four paws touching the ground), and time to the first grooming behavior. After emergence, mice were returned to home cages.

Vertical Movement data collection and analysis:

For experiment Day 11-14, mice (n=5 per group) were individually housed in cages outfitted with automated motion-sensing detectors based on an infrared beam grid system spanning horizontal and vertical axes (Oxymax, Columbus Ohio). The mice had continuous access to water, enrichment, and food, treated with vehicle or CSA as described, was replaced daily. To measure rearing activity, vertical axis beam-breaks were counted over the course of 24 hours of pre-anesthesia exposure, 0-24 hours post-anesthesia exposure, and 24-48 hours post-anesthesia exposure.

Water radial arm maze procedure and analysis:

Visuospatial learning was tested on experiment Days 15-26 (12 total, between 2:00 pm to 6:00 pm) via an 8-arm water radial arm maze (WRAM). The black maze, a chamber with 8 symmetrical arms numbered 1-8, was filled with water (18-21°C) dyed opaque black with non-toxic paint. Four black platforms were submerged (approximately 1/2 cm) at the far end of four different arms. Each wall surrounding the maze depicted a distinct visual cue. In each trial, a mouse was placed in the start arm. Each entry into an arm, until a platform was located, was recorded for each trial, up to 120 seconds per trial. If time expired, the mouse was gently guided to the nearest platform. Upon reaching a platform, the mouse was allowed to remain for 15 seconds for visual reference, and then returned to a heated cage for 30 seconds prior to starting the subsequent trial. The located platform was removed and the process repeated until the mouse had located all four platforms. On each day, platforms were consistently replaced in the same arm configuration for each mouse. The first day was a habituation day and omitted from analysis. Any entries into arms lacking platforms on a specific trial were counted as errors. Errors on a given day were summed per mouse and graphed on a sliding average. Error rates for each individual mouse was graphed over time as a percentage of baseline errors - calculated by: (# of errors for a given testing day)/(# of errors on testing Days 1-2). To minimize the effect of any one day on the shape of the learning curve (see Figure 1), a sliding average was used (ie. data from day 2 and day 3 were combined, as well as days 3 and 4, 5 and 6, etc). Error rates were also binned over the early (days 1 – 4), middle (5 – 8), and late (9 – 12) thirds of the testing paradigm.

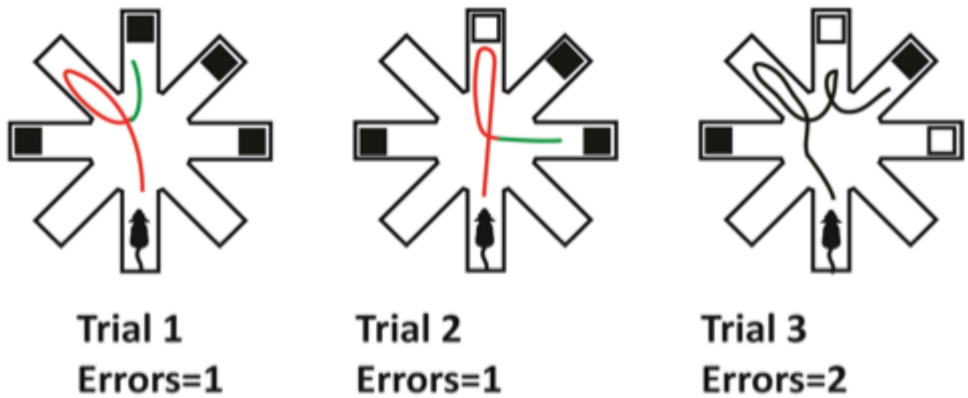

Figure 3.1 Water radial arm maze experimental paradigm.

Figure 3.1 Water radial arm maze experimental paradigm. The objective is to swim onto an escape platform by navigating into a correct arm (arm with black box). Subjects rely upon visuospatial memory to avoid the arms previously used for escape (arms with white boxes), as well as the arms that never contain escape platforms (arms with no box). Mice iteratively navigate the maze until all four platforms are found. Within each trial, errors accumulate (red path segment) until an escape platform is reached (green path segment).

Brain tissue preparation for protein measures

For sacrifice, mice (n=5 per group) were terminally anesthetized with 5% isoflurane and transcardially perfused with ice-cold phosphate-buffered saline. The frontal-temporal lobe was removed, then frozen and stored at -80°C. To extract protein, tissue was thawed and sonicated (Dismembranator, Fisher Scientific) in RIPA/PI (RIPA buffer and protease inhibitor, Pierce, Thermo). Lysate was then solubilized for 20 minutes of end-over-end rotation at 4°C and clarified with centrifugation (20 minutes, 4°C, 13,5000 rcf). Protein was measured for concentration by bicinchoninic acid (BCA) assay (Pierce, Thermo Scientific), diluted to 1 μg/μl with RIPA/PA, and then prepared in Laemmli buffer (Bio-Rad, Hercules California) with 5% (v/v) β-Mercaptoethanol for SDS-PAGE.

Brain slice surface biotinylation

Acute brain slice preparation

Mice (n =3 - 5 per group) were deeply anesthetized with isoflurane, and transcardially perfused with ice-cold sucrose-based artificial cerebrospinal fluid solution (in mM: 200 Sucrose, 2.5 KCl, 1.2 NaH2PO4, 25 NaHCO3, CaCl2, 7 MgCl2, 2.4 sodium pyruvite, 1.3 L-ascorbic acid, 20 dextrose) continuously gassed with carbogen (95% O_2/ 5% CO_2 mixture, Nexxair Corp). The brain was extracted, trimmed and cut in sucrose-ACSF on a Leica VT-1000S vibrating microtome into 350 μm horizontal slices. Slices were then transferred to carbogen gassed ACSF (in mM: 125 NaCl, 2.8 KCl, 1 NaH2PO4•2H20, 26 NaHCO3, 10 glucose, 2 CaCl2, 1.5 MgSO4; pH 7.2, mOsm

290-305), maintained at 32°C. From each animal, four slices containing the hippocampus were pooled for one sample.

Biotinylation

Slices were allowed to rest for 50-60 minutes before starting biotinylation, based on previously published methods [158]. Washes and incubations were done on ice, with gentle agitation. First, slices were rapidly chilled and washed with ice-cold, gassed ACSF. Then, slices were incubated for 20 minutes in 0.5mg/ml biotin-ACSF (EZ-link Sulfo-NHS-biotin, Pierce). To quench unreacted biotin, slices were washed and incubated in 100mM Glycine-ACSF. Slices were transferred to tubes, frozen in liquid nitrogen and stored at -80°C. To process, protein samples were sonicated in RIPA/PI, solubilized, and quantified as described above.

Neutravidin pulldown

Biotinylated proteins were purified with Neutravidin beads (Pierce, Thermo Scientific), prepared as follows. For each sample, 250µl of bead slurry was centrifuged (2 min, 4°C, 2,500 rcf) and supernatant was aspirated. Beads were resuspended and washed three times (as above) with TBS and twice with RIPA/PI. Sample lysate (375 µg) was incubated with beads overnight for ~16-18 hours of end-over-end rotation at 4°C. Afterwards, beads were centrifuged to remove supernatant, then washed four times in RIPA/PI, each with 20 minutes of end-over end rotation at 4°C. Neutravadin-bound protein was eluted with 2x Laemmli Buffer (5% βME) by boiling (95°C, 20 minutes) and centrifugation (10 minutes, 25°C, 13,500 rcf). Eluted samples were stored at -20 °C prior to Western blot analysis.

SDS-PAGE/ Western blotting

Protein samples were resolved in Criterion precast gel (Bio-Rad), then transferred to a PVDF membrane using a semidry system (Bio-Rad). All immunoblots were performed as follows. Membranes were blocked for one hour in 5% non-fat dry milk in TBST (25 mM Tris, 140mM NaCl, 3mM KCl, and 0.1% Tween-20), then probed overnight at 4°C with primary antibody diluted in 5% BSA in TBST. Membranes were washed, and then probed for one hour with horseradish peroxidase conjugated secondary antibody diluted in 5% milk TBST. Immunoreactive bands were detected with chemiluminescence using ECL substrate (ECL Prime, Abersham or West Pico, Pierce) on a Chemidoc imager (Bio-Rad), and quantified in ImageJ (NIH) using mean intensity measurements from ROIs of identical dimensions. To measure Neutravidin purified $GABA_AR$ subunits, membranes were cut for parallel blots of the subunit and transferrin receptor. Subunit intensity was normalized to the transferrin receptor. Total protein was normalized to β-Actin. To measure caspase-3 cleavage, intensity of the ~20kd region was first normalized to the intensity of full-length caspase, and then normalized to GAPDH.

The primary antibodies used were: $GABA_AR$ α_5 subunit, Abcam, Ab10098; $GABA_AR$ γ_2, Abcam, Ab87328; GAD-67, Sigma, SAB4300642; GAPDH, Millipore, mab375; β-Actin, Sigma, A5441; Caspase-3, Cell Signaling, 96624; Transferrin Receptor, Life, 13-6800. Secondary antibodies were: mouse NA931, rabbit NA934, both Abersham, GE.

Statistical analysis:

All raw data was imported into Prism (Graphpad™) for graphing and statistical analysis. All data for t-tests was checked for normality with Kolmogorov-Smirnoff testing. Comparisons among the four treatment groups were performed using ANOVA with post-hoc testing. Reported significant p-values and significance asterisks are for post-hoc testing unless otherwise specified in the text.

3.3 Results

CSA impairs visuospatial learning after isoflurane

To test the effect of CSA pre-treatment on the recovery of memory function from anesthesia, adult mice were subject to the treatment paradigm illustrated in **Figure 3.2A** and tested with the water radial arm maze (WRAM). All mice in all four groups completed the trials and demonstrated a decrease in the daily number of errors over time (**Figure 3.2B-D**). As expected, trial day had a significant effect on error rate (all groups, $p<0.0001$, RM 2-way ANOVA). However, neither CSA treatment in the absence of anesthesia, nor our brief isoflurane challenge in the absence of CSA resulted in delayed learning of the visuo-spatial task as compared to the control animals (**Figures 3.2B & 3.2C**, $p=0.055$ for VEH/SHAM vs. CSA/SHAM, $p=0.7234$ for VEH/SHAM vs. VEH/ISO). In contrast, the CSA/ISO group took longer to reduce their baseline error rate as compared to the other groups. Comparing this group to the VEH/ISO group reveals this trend **(Figure 3.2D)**, which did not quite reach statistical significance ($p=0.0712$). However, comparisons between the CSA/ISO group and the CSA/SHAM group (**Figure 3.2E**) revealed a more drastic effect on task performance ($p=0.0029$). Post-hoc analysis showed significant effects for individual trial days ($p=0.0107$; Tukey's post-hoc test). This decreased memory performance is most apparent in the middle third (days 5 – 8) of the 12 day task Figure 1F (2 way ANOVA, $p = 0.0196$, post-hoc significance for CSA/ISO group compared to: VEH/SHAM $p = 0.0007$, VEH/ISO $p = 0.0158$, CSA/SHAM $p = 0.0082$) (**Figure 3.3**).

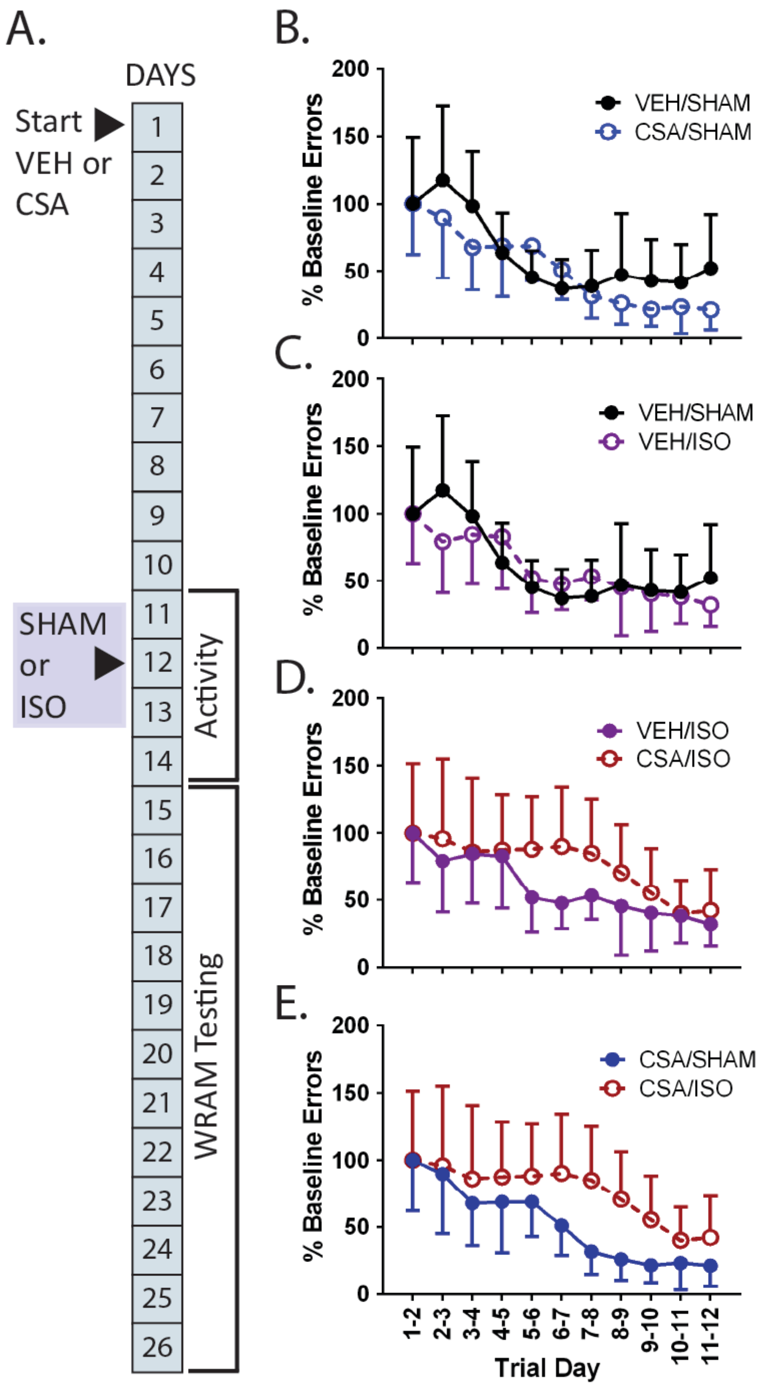

Figure 3.2 Behavioral measures of cognitive function following chronic CSA and isoflurane

Figure 3.2 Behavioral measures of cognitive function following chronic CSA and isoflurane (A) Treatment and testing paradigm **(B-E)** Water radial arm maze (WRAM) performance, graphed as percent change in errors normalized with a sliding average. Graphs compare (**B**) the effect of CSA on sham treatment isoflurane on vehicle treatment, (**C**) the effect of isoflurane on vehicle treatment, (**D**) CSA on isoflurane treatment, or (**E**) isoflurane on CSA treatment. Error bars are Mean±SD.

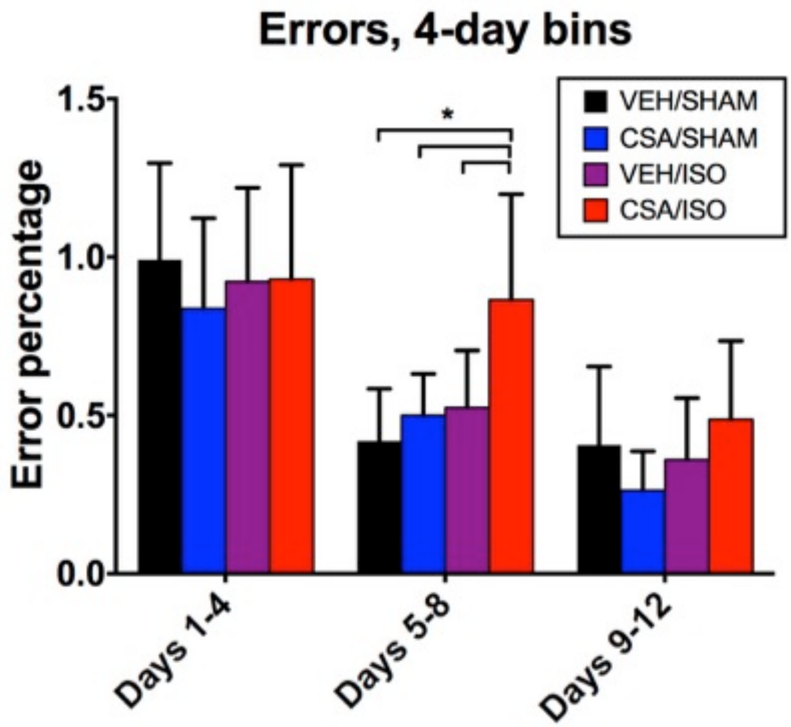

Figure 3.3 Water radial arm maze error rates

Figure 3.3 Water radial arm maze error rates binned over the early (days 1 – 4), middle (5 – 8), and late (9 – 12) thirds of the testing paradigm. Error bars are Mean±SD

Chronic CSA does not alter emergence or post-anesthesia measures of motor activity

Several observed behavioral endpoints were measured during anesthetic emergence (**Figure 3.4**). We observed no significant effect of our CSA regimen on latency to forelimb movement or return of righting reflex, nor in our proxy of more advanced anesthesia recovery, spontaneous grooming ($p=0.830$, $p=0.580$, $p=0.840$; $n=10$, t-test). Similarly, CSA did not change the time required to reach steady-state anesthesia ($p=0.650$, t-test), defined as the time from induction to loss of righting reflex. To further assess the effect of CSA on post-anesthetic activity, we measured vertical exploratory behavior (rearing) with a cage-mounted automated monitoring system. Rearing is an exploratory behavior correlated with cognitive activity [159]. Data was collected from one day of pre-exposure, and two days post-exposure (**Figure 3.5B**). No differences due to CSA administration were observed (pre-anesthesia, $p=0.202$, anesthesia day $p=0.863$, post-anesthesia $p=0.569$ respectively, t-test). In both groups, rearing behavior decreased on the day of isoflurane challenge (CSA: $p=0.0211$, VEH: $p=0.0086$; paired t-test). Prior to anesthesia challenge and memory testing (Day 10), we used the wire-hang test to grossly assess motor function. Compared to vehicle, CSA had no significant effect on performance ($p=0.2826$, t-test) (**Figure 3.6**).

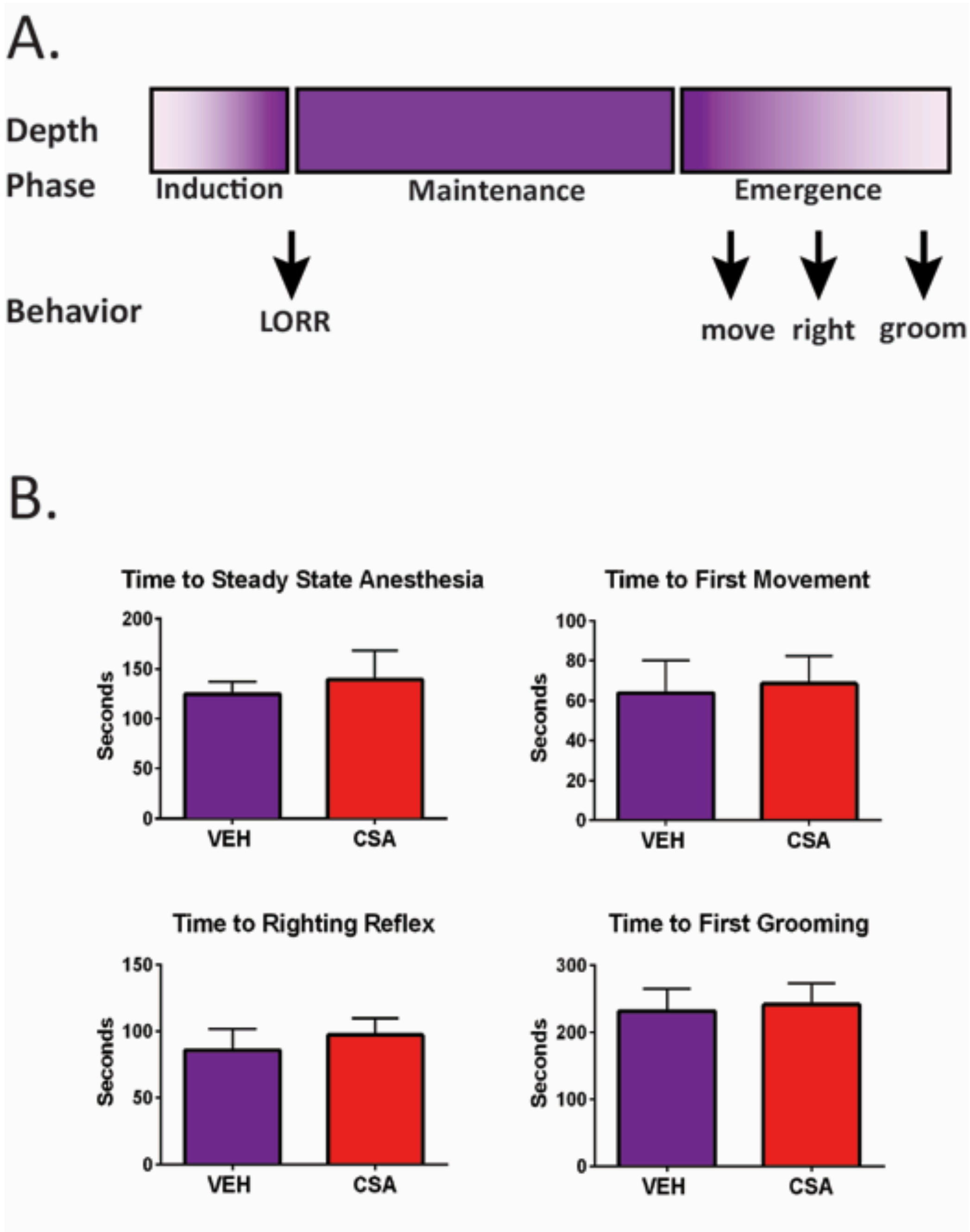

Figure 3.4 Paradigm and behavioral measures of induction and emergence.

Figure 3.4 Paradigm and behavioral measures of induction and emergence (A) Experimental paradigm for anesthetic induction, maintenance, emergence, and observation of canonical behavioral endpoints of anesthesia. Loss of righting reflex (LORR) is a proxy measure of hypnosis that is used with rodents. **(B)** Endpoints of induction (**upper-left**) and emergence. Error bars are Mean±SD.

A.

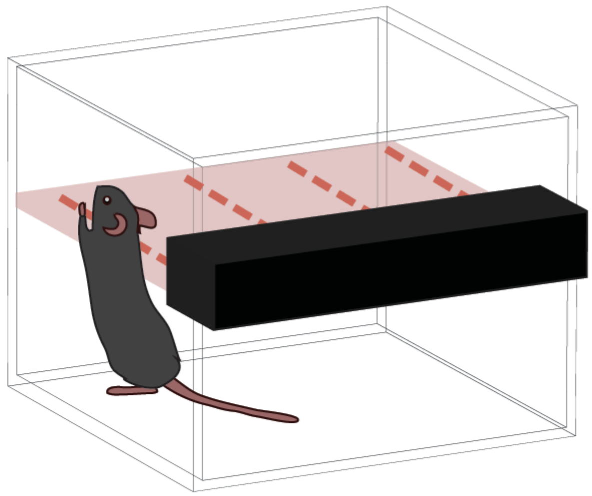

B.

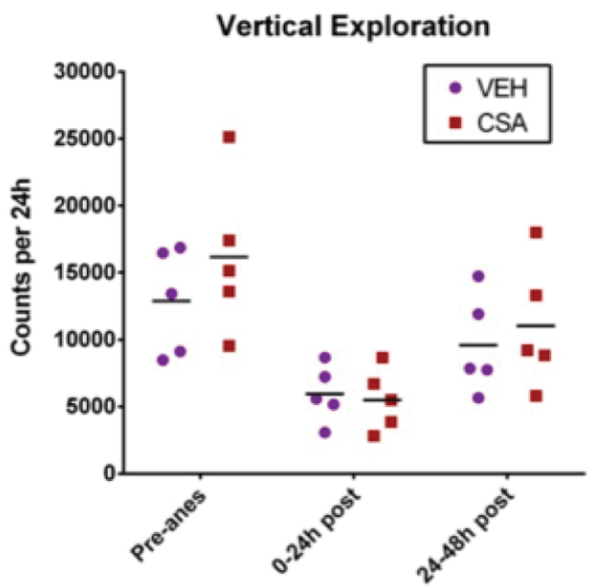

Figure 3.5 Paradigm and behavioral measures of vertical exploratory activity.

Figure 3.5 Paradigm and behavioral measures of vertical exploratory activity.

(A) Illustration of Oxymax infrared beam grid-based detection system for measuring vertical exploratory behavior as beam-breaks**. (B)** Vertical activity measured one day before, and one or two days post-anesthesia.

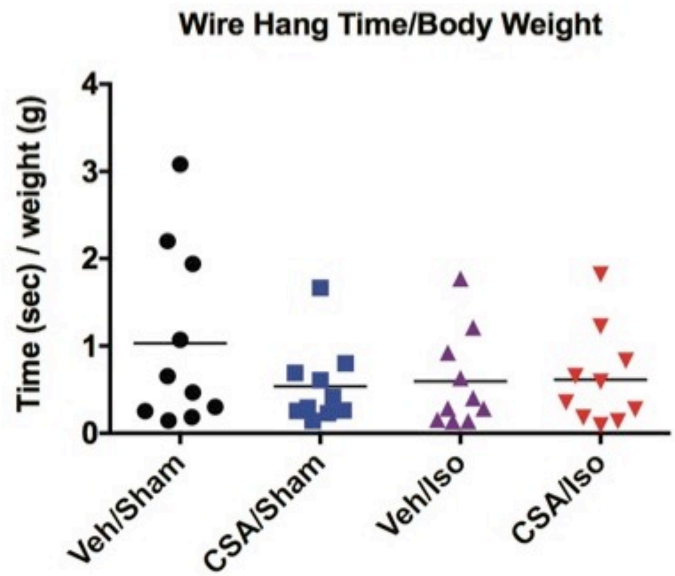

Figure 3.6 Wire-hang challenge motor assay. No significant differences in performance were detected in any group.

Expression of GAD-67 is decreased after isoflurane anesthesia.

Changes in protein expression associated with altered inhibitory network function were examined using lysate collected from the hippocampal and frontal-temporal lobe cortex three days after isoflurane exposure (**Figure 3.7A**). The GABA synthesis enzyme, GAD-67 was probed via Western blot. Compared to the control group, GAD-67 was significantly decreased by isoflurane exposure (VEH/SHAM vs. VEH/ISO p= 0.0192, all ANOVA with Tukey's post-hoc testing) (**Figure 3.7B, C**). The CSA/ISO group also demonstrated a decrease in GAD-67 compared to the VEH/SHAM group that did not quite reach statistical significance by post-hoc testing (p=0.0574). Comparison of isoflurane-treated groups revealed that chronic CSA exposure did not prevent the effects of isoflurane on GAD-67 expression (p=0.2554). Cortical samples also demonstrate an isoflurane-mediated decrease in GAD-67 expression (**Figure 3.7D**). The isoflurane-treated group showed a significant decrease compared to the control (p=0.0473, ANOVA with Tukey's post-hoc testing). In the CSA/ISO group GAD-67 was not significantly decreased from the VEH/SHAM group (p=0.4966), and not significantly difference from the VEH/ISO group (p=0.3506).

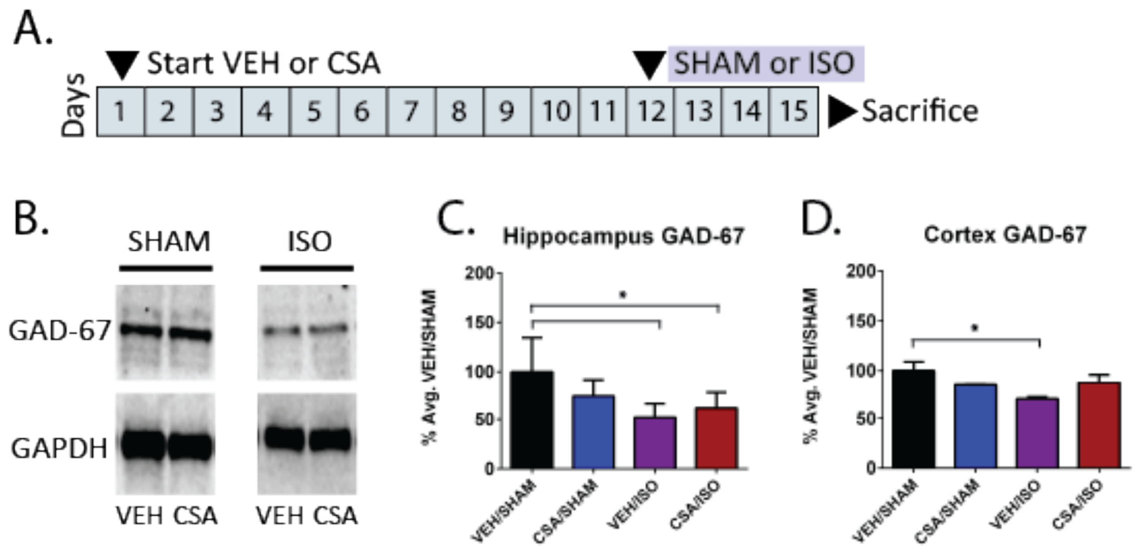

Figure 3.7 GAD-67 expression is decreased after isoflurane anesthesia

Figure 3.7 GAD-67 expression is decreased after isoflurane anesthesia

(A) Treatment paradigm for to protein expression analysis. **(B)** Western blot of GAD-67 in total protein collected from hippocampal brain slices three days after following isoflurane anesthesia. **(C)** Quantification of hippocampal GAD-67 showing a significant decrease by isoflurane. **(D)** Quantification of cortical GAD-67 levels after isoflurane anesthesia. Error bars are Mean±SEM.

Brain slice biotinylation: surface expression

We also examined $GABA_AR$ surface expression in the brains of mice subjected to the treatment paradigm as outlined in **Figure 3.7A** via biotinylation of acutely generated ex vivo brain slices containing the hippocampus (**Figure 3.8**). We probed for the α_5 and γ_2 subunits, constituents of the $\alpha_5\beta_3\gamma_2$ receptor. The combination of chronic CSA with 30-minute isoflurane challenge resulted in a decrease in total α_5 protein expression (VEH/SHAM vs. CSA/ISO p=0.0226; CSA/SHAM vs. CSA/ISO, p=0.0057). Isoflurane exposure increased α_5 subunit surface expression (VEH/SHAM vs. VEH/ISO, p=0.0192) but not total α_5 expression (p=0.7964) (**Figure 3.8A-D**). Although the CSA/ISO group did not exhibit a statistically significant increase in surface α_5 protein expression, the ratio of surface expression to total protein for α_5 surface protein was highest for this group (VEH/SHAM vs. VEH/ISO p=0.0320; VEH/SHAM vs. CSA/ISO, p=0.0063). This suggests that although isoflurane increases surface expression of α_5 subunits in both our experiments and those performed by others [119], chronic CSA treatment in combination with an isoflurane challenge can cause an abundance of surface localization in the setting of decreased protein expression. No significant changes in the surface expression, total, or normalized expression of the γ_2 subunit were found by any treatment (**Figure 3.8E-H**).

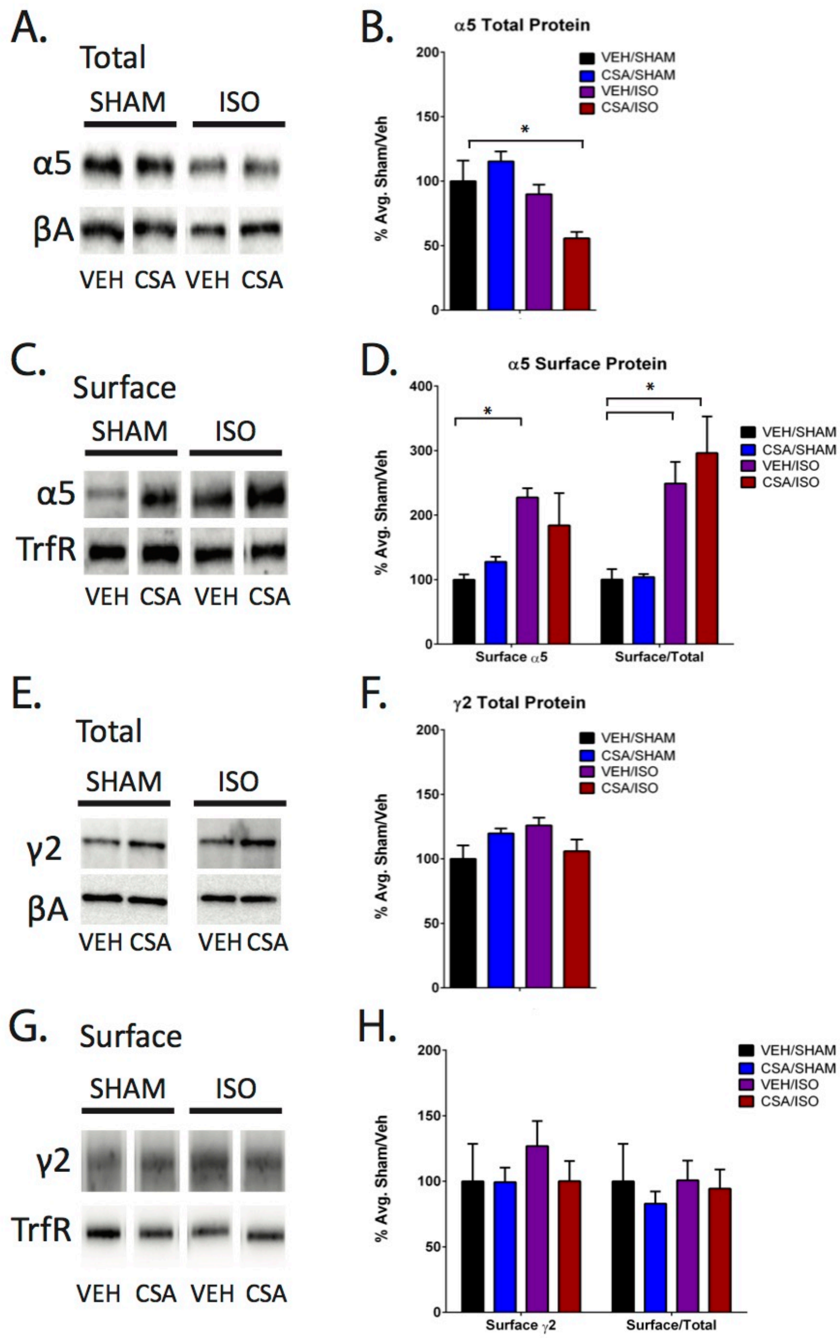

Figure 3.8 $GABA_AR$ α_5 and γ_2 subunit surface expression in hippocampal slices

Figure 3.8 GABA$_A$R α_5 and γ_2 subunit surface expression in hippocampal slices

Western blot and quantification of α_5 total **(A,B),** and surface expression **(C,D)**. Isoflurane alone increased surface but not total expression, whereas isoflurane with CSA did change total expression. Western blot and quantification of γ_2 total **(E, F)** and surface expression **(G, H)** reveals no significant changes. Error bars are Mean±SEM.

Cleaved Caspase-3 is not evident three days after isoflurane anesthesia

To test the possibility that neuroapoptosis underlies the behavioral memory deficits observed in the mice receiving an isoflurane challenge during chronic CSA therapy, we probed hippocampal protein for cleaved caspase-3. When enzymatically activated, this protein executes apoptotic signaling cascades. No differences were observed among any of the treatment groups (**Figure 3.9**).

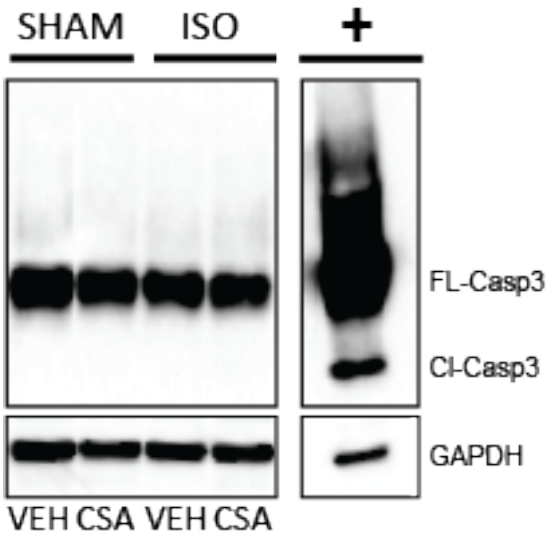

Figure 3.9 Caspase-3 expression following isoflurane exposure.

Figure 3.9 Caspase-3 expression following isoflurane exposure. Western blot of cleaved and full-length caspase-3 in total hippocampal protein collected three days after following isoflurane anesthesia. Lanes contain 25 μg of protein from sham treated animals (**left**) and isoflurane treated animals (**middle**). The positive control for caspase-3 cleavage (**right**) is lysate from cultured hippocampal neurons exposed to isoflurane for six hours, shown previously to activate caspase-3 pathways [154].

3.4 Discussion

Calcineurin (CN) mediated changes in synaptic protein regulation have been identified as pathophysiologic mechanisms in several neurological conditions [160-162]. Initially, we hypothesized that CN inhibition would rescue the dysfunctional changes to inhibitory networks observed in response to isoflurane anesthesia. Instead, we find that chronic CSA aggravates post-anesthetic learning impairments and does not reverse the effect of isoflurane on GAD-67 expression or α_5 surface expression, both potential contributors to memory problems associated with isoflurane exposure

CN is involved in many calcium-dependent intracellular processes throughout the body, but is particularly enriched in the central nervous system [152]. CN inhibitors, like CSA, suppress the immune system by preventing CN-mediated T-cell activation. Although anti-inflammatory agents have shown some promise in prevention of POCD in rodent models [138, 163], we have demonstrated that chronic immunosuppression via CSA administration may not be effective for minimizing adverse neurologic sequelae after surgery.

In our behavioral assays, we did not observe decreased performance in WRAM learning after isoflurane challenge unless combined with chronic CSA administration. We attribute this to our brief (30-minute) isoflurane exposure and cautiously interpret our findings in the setting of investigations focused on POCD using rodent models. Recently mitigation of isoflurane-induced cognitive impairment was observed after acute CSA administration in a rodent model [138]. Specifically, Ni et. al. administered a single CSA dose immediately before a 4 hour isoflurane (2%) challenge, and used a memory paradigm (Morris water maze), that places a larger emphasis on recalling memorized information than the WRAM. Memory recall is tested in the WRAM, but this test relies more heavily on working memory and attention [164] which are thought to be more typically affected in the cognitive dysfunction categorized as POCD or post-operative delirium [165].

Surprisingly, even the brief exposure of isoflurane used in our study increased the surface expression of α_5-containing $GABA_A$Rs, confirming the work of others which correlated learning impairments following etomidate or isoflurane anesthesia to an abundance of this particular subunit [119]. Here, we expand this work by also observing a decrease in total α_5 protein in the hippocampus, but not the cortex of mice treated with both CSA and isoflurane. Our interpretation is that chronic CSA treatment in combination with isoflurane can result in an abundance of surface localization in the setting of downregulation of receptor protein expression.

We also found that pre-synaptic network mechanisms can be affected by brief isoflurane exposure. The GABA synthesis enzyme, GAD-67, was decreased in both the hippocampus and frontal-temporal lobe of isoflurane-treated animals. Hippocampal GAD-67 expression is known to decrease in aged mice after isoflurane (2 hours) [166]. Our results confirm this effect of isoflurane on GAD-67 expression levels in young mice after only 30 minutes of exposure. While it remains possible that loss of GAD-67 expressing interneurons or GABA-ergic synapses by isoflurane-mediated toxicity would cause protein levels to decrease [167], we found no evidence of cleaved caspase-3 expression, suggesting that any cell death in this phenotype is not present three days post-anesthesia or is not readily detected using this method (e.g. occurring in a small subpopulation of neurons). These results suggest GAD-67 protein expression is transcriptionally downregulated after isoflurane, and that chronic CN inhibition via CSA administration does not rescue these off-target effects of isoflurane.

Basal CN activity regulates neuronal excitability via modulation of synapses, and CSA administration is associated with epileptiform activity in temporal lobe seizure models [168, 169] and in clinical practice [170]. We did not observe overt changes in activity or arousal levels due to the CSA regimen before or after isoflurane exposure. A limitation of this study is that we cannot examine all of the off-target cellular processes affected by CSA. In addition to CN inhibition, CSA is known to disrupt mitochondrial function like transition pore opening, which could impact behavior [154]. Likewise, we neglected the trafficking of other synaptic receptors or ion channels known to be regulated at least in part by CN, e.g. AMPA, mGluRs, or potassium channels [152]. Another limitation is the difficulty in reliably quantifying CN enzymatic activity as excessive isoflurane exposures have been shown to activate CN [136, 138]. It remains unclear if CN is activated with brief exposure to isoflurane.

In experimental models of Alzheimer's disease and brain injury, CN inhibition mitigates damage to synaptic circuits and learning processes by rescuing aberrant protein signaling [160, 171]. However, CN inhibition via chronic CSA administration was not able to reverse the effect of isoflurane on GAD-67 levels in the hippocampus. The immunosuppressant, CSA was also unable to reverse the effect of isoflurane on α_5 surface expression, despite evidence linking these receptors to inflammatory-mediated memory impairment [124]. Although there is strong evidence for a role of these pathways in POCD based on links between CN activity, anesthesia, inflammation and dysregulated protein function, the interactions are still unclear and warrant further investigation.

Additional research will inform anesthetic management of patients receiving CSA therapy chronically, and clarify the role of CN and general anesthetics in the pathophysiology of various neurodegenerative diseases and cognitive dysfunctional states.

Chapter 4 Discussion

Chapter 4 Discussion

4.1 General overview

Anesthesia is a complex pharmacological phenomenon, producing an altered state of consciousness that is generated by the modulatory effect of anesthetic agents on critical electrophysiological and protein functions in neurons. While influences of anesthetic drugs on proteins that modulate electrical activity among neurons has received a great deal of attention, the effects of anesthetic drugs on intracellular proteins has been less explored. Our work reveals that the influence of anesthetics on ion channels, mainly $GABA_A$ receptors, and the intracellular proteins that regulate their surface expression are mechanistically linked and must be considered in tandem. The augmented inhibition and resultant hyperpolarization observed in several key brain regions subsequently dissociates the neural processes that generate coherent consciousness and memory formation. This disruption of normal neurophysiological function by anesthesia was conventionally understood to be reversible upon clearance of anesthetic agents from the brain. However, the emergence of POCD as a potential clinical outcome has raised the possibility that the use of general anesthesia may have yet identified consequences for neurological function**.** Given that clinically relevant plasma concentrations of anesthetics appear to also exert profound effects on important regulatory proteins of the central nervous system, perhaps this should not be surprising.

In animal studies, single anesthetic exposures can be sufficient to induce subtle, but persistent memory impairments [172, 173]. One likely anatomical correlate is a persistent elevation in $\alpha_5\beta_3\gamma_2$ $GABA_AR$ surface expression and consequent increase in tonic inhibitory current, which suppresses neuronal excitability and synaptic plasticity.

As the mechanisms triggering and mediating this effect are still not known, we explored the potential role of calcineurin in isoflurane-mediated changes.

The primary aim of this project was to evaluate the effect of isoflurane on $GABA_AR$ receptor trafficking and surface expression in order to understand the mechanisms by which isoflurane generates $GABA_AR$-based memory impairments. Calcineurin was suspected to have a role in this phenomenon because not only is it involved in anesthetic neurotoxicity[136, 138] and the inflammatory response[174] but because it is also a calcium-dependent regulator of $GABA_ARs$. Trafficking of $\alpha_5\beta_3\gamma_2$ receptors has been shown to be sensitive to inflammation [124, 125], although the specific interplay between the immune system and anesthetics is complex we have contributed some knowledge to the interaction of this enzyme with $GABA_ARs$ and the anesthetic isoflurane.

In chapter 2, the acute effect of isoflurane on $GABA_AR$ surface expression was studied *in vitro* with primary hippocampal neurons. We tested the hypothesis that isoflurane affects $GABA_AR$ trafficking and surface expression through CN-mediated processes. Recent studies have demonstrated that the anesthetic agents interfere with intracellular signaling processes, including those that regulate $GABA_AR$ trafficking. In particular, another GABA-ergic anesthetic propofol induces aberrations in basal $GABA_AR$ endocytosis that results in a robust increase in surface expression. We found that unlike propofol, a one-hour exposure of isoflurane does not have a profound immediate effect on $GABA_AR$ surface expression *in vitro*. Unlike propofol, isoflurane can increase intracellular calcium levels [113, 116], resulting in activation/inactivation of cell processes that might mediate an activity dependent increase in $GABA_AR$ surface expression. Consequently, our results from live-cell imaging of synaptic receptors suggest that the effects of isoflurane may require a longer timescale to result in significant accumulation at the cell surface. These data exclude a decrease in excitation as a universal mechanism that leads to trafficking changes that increase tonic current, because both isoflurane and propofol are known to decrease firing yet only propofol increases expression of alpha5 receptors at time scales < 1 hour *in vitro*. Although the inhibition of calcineurin by cyclosporine did not confer an increase in α_5 expression by isoflurane challenge, the influence of isoflurane on other calcium-dependent processes cannot be ruled out as a possibility.

In **chapter 3**, the interplay of chronic CN inhibition and isoflurane on $GABA_AR$ surface expression was studied *in vivo* with a mouse model. These experiments also gave us insight into the behavioral results of manipulations of protein expression. We initially hypothesized that chronic administration of the calcineurin inhibitor CSA would protect against post-anesthetic cognitive impairments and related changes in inhibitory network function through a suppression of inflammation. Instead, we found that CSA had a negative impact on the recovery of working memory function following isoflurane anesthesia. Notably, behavioral observations of anesthetic threshold, emergence endpoints, and exploratory activity showed no difference. Biochemical analysis of inhibitory synapse markers revealed that isoflurane treatment was associated with a decrease in the expression GAD-67 and an increase in the surface expression of the α_5 subunit, both potential contributors to memory impairment.

4.2 Calcineurin

Calcineurin (CN) is a serine/threonine protein phosphatase that functions in critical regulation of immune and neurological functions. CN is canonically activated by low levels of calcium through complex interactions with both calcium itself and calcium-bound calmodulin. Once activated, CN targets proteins that are basally phosphorylated, ranging from ion channels / transporters to transcription factors. A calcium-insensitive mechanism for activation exists in a constitutively active and truncated calcineurin (ΔCN-48), which is a product of calpain-mediated proteolysis [175]. The appearance of this form of the protein has been implicated in several pathological processes notably including neurodegeneration, demonstrating the importance of controlling calcineurin activity [176, 177]. In addition to calcium and calmodulin, several endogenous binding proteins further regulate CN activity. The CABIN/CAIN (calcineurin binding/calcineurin inhibitor) proteins provide direct inhibition of CN activity, whereas the AKAP (A-kinase anchor) proteins serve as molecular scaffolds that affix CN to specific effector micro-domains within the cell, such as the dendritic post-synaptic density or mitochondria [178]. These pools of CN regulate a variety of intracellular processes in somatic and neuronal tissues. Specialized localization of differentially inducible CN pools and the potential for abnormal initiation of truncated calcineurin, may explain our results. At present, however, technological hurdles limit further elucidation, specifically, a lack of commercially available specific antibodies to the truncated form, or a pharmacological means for the isolation of the different CN pools.

In addition to lymphocytes and neurons, calcineurin has critical functions in the normal physiology of several other organ systems, particularly the kidney. In our model, blood urea nitrate tests indicated normal kidney function, excluding renal failure as an explanation for observed cognitive impairments.

4.3 Calcineurin in plasticity and learning

Calcineurin influences many different processes involved in several forms of plasticity and learning. Below, I review canonical (with respect to the hippocampus) mechanisms and sequences to better to contextualize and facilitate interpretation of the learning phenotype observed in our experiments. I will specifically compare our results to other studies where CN is inhibited by CSA. Briefly, we found no effect of CSA alone on learning, and an impairing effect when combined with isoflurane; this conflicts with the findings of other studies showing that CSA does affect learning, in a positive way.

CN participates in many forms of synaptic plasticity, including long-term potentiation of Schaeffer collateral/CA1 excitatory synapses. In this model, activity-dependent increases in excitatory synaptic strength are accompanied by activity-dependent decreases in inhibitory synaptic strength, or inhibitory long-term depression. This latter mechanism is mediated by NMDA-receptor dependent increases in intracellular Calcium resulting in activation of CN. It follows that activated CN dephosphorylates the γ2 subunit on $GABA_A$Rs promoting their endocytosis, which further increases their excitability. Conversely, CN also mediates excitatory synapse long-term depression by promoting AMPA receptor dephosphorylation and endocytosis. This apparent contradiction is best conceptualized in the Lisman model of bi-directional control of synaptic strength based on local gradients of calcium[178]. Within dendritic spines, modest depolarizing stimuli and small increases in calcium preferentially activate calcineurin, whereas stronger stimuli that generate larger NMDA-mediated calcium influx allow kinases to outcompete calcineurin-mediated phosphatase activity and receptor removal. Remote from dendritic spines, $GABA_ARs$ are now exposed to increased calcium and local calcineurin is activated. The subsequent removal of $GABA_ARs$ from the inhibitory synapse increases excitability in the post-synaptic neuron [179]. In epilepsy models, calcineurin participates in exaggerated $GABA_AR$ endocytosis, which promotes a feed-forward decline in $GABA_AR$ surface expression that progressively increases hyper-excitability [69].

Given the diverse roles, as expected, CN is highly expressed throughout the hippocampus, and enriched within the dendrites and spines of excitatory principal cells [178]. This intracellular localization may explain why isoflurane-mediated rises in cytosolic calcium failed to engage CN-mediated $GABA_AR$ endocytosis (see below). In our studies of receptor trafficking (**Chapter 2**), we found that a one-hour exposure of isoflurane failed to produce significant effects on surface expression. The original motivation for these experiments was to test the possibility that isoflurane could directly evoke calcineurin-mediated $GABA_AR$ endocytosis via ER-released calcium, but this hypothesis was not supported by our observations. One explanation for this result could be that a brief exposure of isoflurane cannot sufficiently increase calcium in the vicinity of the inhibitory post-synaptic density. Activity-dependent and NMDAR- mediated calcium differs from ER-released calcium in spatial expression within the neuron, the former entering via ion channels located on dendritic spines and the latter initiating from the cell body. Although some intracellular pools of CN can be activated by isoflurane exposure, the CN that is affixed to the inhibitory post-synaptic density may not be.

Different experiments (e.g. synaptosomal or synaptic-protein affinity based biochemistry or imaging) would be necessary to determine whether the spatiotemporal dynamics of isoflurane-mediated increases in intracellular calcium suit it to influence dendritic processes.

However, the outcome may be completely different for pathological conditions where intracellular calcium homeostasis is dysregulated [112]. Additionally, as explored in **Chapter 2,** these results describe only a one-hour isoflurane exposure. The rationale behind a short isoflurane treatment was twofold: to avoid confounding surface labeling with isoflurane-mediated neurotoxicity, and to allow a direct comparison with the known trafficking effects of other anesthetic agents. However, by surgical standards this is a brief exposure. It remains to be seen whether isoflurane has a biological effect on surface expression resulting from longer exposures for significant accumulation.

The putative role of CN in learning and memory is complex, and the behavioral outcomes of CN blockade vary by method, with notable differences between pharmacological and transgenic approaches. Several investigations demonstrate improvements in hippocampal memory-dependent tasks with CSA pretreatment, suggesting that CN normally constrains learning [152]. For example direct injections of CSA into the hippocampus improve both spatial learning and spatial reversal learning when administered immediately before testing, suggesting an augmentation of both acquisition and possibly active extinction of prior memories [180]. These effects are also seen when CN is inhibited by antisense oligonucleotide delivered prior to the learning task. In contrast, our data (**Chapter 3**) showed chronic CSA had no effect on learning by itself, and conferred a learning impairment when combined with an isoflurane challenge.

While our results are consistent with two prior studies showing no effect of chronic CSA on an avoidance-based memory task [181, 182], it should be noted that the effect of chronic CSA on cognitive function is understudied in relation to its clinical relevance.

Transgenic studies have become progressively more illuminating in demonstrating specific consequences of CN inactivity. Several types of hippocampus-specific genetic knockdowns show variously enhanced learning phenotypes, whereas global CN knockout mice are deficient in tasks that rely on reference memory, such context-specific fear conditioning and the Morris Water Maze [152, 183]. Forebrain-specific CN knockout mice have intact Schaeffer collateral / CA1 long-term potentiation and normal reference memory. Instead, performance was impaired in paradigms that utilize spatial working memory, including the delayed-matching-to- place task and the 8-arm radial maze [184].

In our study, mice treated chronically with CSA alone show no significant impairment in the water radial arm maze, which also relies heavily on working memory. This task differs only slightly from the 8-arm radial maze, primarily in the motivational factors. Both paradigms rely on largely identical arenas that radiate maze arms containing rewards (removal from water and food respectively), the principal being that rewards are iteratively removed during each trial and working memory is engaged to remember the previously entered arms.

Given the plethora of roles that CN has in various aspects of synaptic plasticity, in both excitatory and inhibitory neurotransmission, the absence of a significant phenotype with CSA alone may be the result of a mixture of effects. In our experiments, CSA was delivered as a chronic treatment; therefore, the development of compensatory mechanisms may also explain how our results differ from those obtained with acute injections or treatments. Additionally, our results do not exclude other types of learning impairments, and a larger battery of behavioral tests would be necessary to further characterize this cognitive phenotype. In summary, given that CN is engaged in numerous complex molecular functions, it should be unsurprising that characterizations of the consequences of calcineurin inhibition have accordingly complex outcomes.

4.3 Role of α_5 receptors in the hippocampus, and functional implication of protein expression changes following anesthesia

Previous studies have demonstrated that elevated $\alpha_5\beta_3\gamma_2$ receptor surface expression contributes to memory impairments generated by isoflurane and etomidate. Investigating the relationship between these receptors and cognition is of high value, as α_5-targeting drugs are being investigated for cognitive enhancement and for treating various neuropsychiatric disorders [185, 186]. In this section, I will review $\alpha_5\beta_3\gamma_2$ associated functions, and then interpret our results within that context.

Within the central nervous system, $\alpha_5\beta_3\gamma_2$ receptors are primarily expressed on the dendrites of hippocampal CA1 and CA3 subfield pyramidal neurons [187-189], comprising 20-25% of regional $GABA_A$ receptors [187, 188]. These receptors are highly sensitive to low concentrations of GABA present in the extracellular space and when activated generate a persistent inhibitory conductance that modulates excitability. Within learning and memory, this serves to constrain or dampen plasticity. Pharmacological and genetic studies consistently demonstrate that α_5 inhibition and deletion will improve performance in several types of hippocampal-dependent learning, including trace fear conditioning [190] and spatial navigation learning [191, 192]. Reports do vary as to the degree to which measures of synaptic plasticity and LTP induction are impaired, supporting a role as an inhibitory conductance that modulates the threshold for plasticity rather than inhibiting it *per se*. This constraint on excitability also provides resilience against unmitigated excitation, a relevant concern for potentially self-strengthening or dynamically plastic networks such as the CA subfields of the hippocampus. Genetic deletion of α_5 is associated with network hyperexcitability [193] and decreased α_5 protein expression within CA1 and CA3 is observed in pilocarpine models of temporal lobe epilepsy [194, 195].

Our interest in measuring expression of α_5 receptors is based on the experiments by Zurek *et al*. demonstrating that elevated surface levels and hippocampal learning impairments develop after anesthesia. Specifically, this study found that hypnotic doses of two GABA-ergic anesthetics, etomidate and isoflurane, both produced impairments in Schaeffer collateral / CA1 plasticity and a significantly elevated tonic current that was reversible with an α_5 inverse agonist. While no changes were observed in the surface or total protein expression of the δ subunit, which defines the other tonic current-mediating receptor assembly ($\alpha_4\beta_x\delta$) in the hippocampus, there was a significant increase in α_5 receptor surface but not total protein expression first observed 24 hours after anesthesia and persisting between one to two weeks after anesthesia. Memory deficits were shown at 24 hours, one day, and three days following etomidate anesthesia, using the novel object recognition assay. While we also showed that α_5 increased with isoflurane exposure, we failed to detect a more persistent impairment on working memory following exposure to isoflurane. Assuming that the surface α_5 elevation corresponds with impairment in memory, which was not directly tested with isoflurane, one explanation for the difference may be dosage. Zurek *et al*. used a one-hour exposure whereas we used a 30-minute isoflurane exposure. Alternately, there is the possibility that isoflurane impairs novel-object recognition but not WRAM-sensitive working or spatial memory. While these are possible, we suggest that these subtle differences are not likely to explain the discrepancy among our work and that of Zurek. The other possibility is that increases in surface expression of α_5 do not mediate the behavioral effects, but rather that the behavioral effects are mediated by the ability of the animal to compensate or dynamically adjust their surface expression, and the combination of CN inhibition and isoflurane exposure decreases the animal's dynamic resilience.

Our results suggest that a straightforward explanation for post-anesthetic working impairments based solely on increased α_5 receptor expression cannot be entirely supported. CSA/isoflurane co-treated animals displayed worse working memory performance compared to every other group groups despite a decrease in α_5 total protein expression. Notably, surface α_5 is highest in the CSA/isoflurane group when normalized to total protein expression. We found no evidence for ongoing neurotoxicity at the time of protein harvest three days post-anesthesia, but (as elaborated in the next section) at present we cannot exclude acute neurotoxicity as a possible mechanism for loss of α_5 protein. Electrophysiological examination would be necessary to establish the actual effect of the CSA/isoflurane phenotype on tonic current amplitude and net charge transfer. Regardless, in our study 30 minutes of isoflurane was sufficient to recapitulate the previous demonstrated elevation in α_5 surface expression, although only generating working significant memory impairments during chronic calcineurin inhibition. However complicated, our results suggest that α_5 surface levels alone do not predict post-anesthetic memory function.

Whether other neurophysiological changes develop alongside increased α_5 surface expression following anesthesia was initially unclear. The reversal of memory impairment with an acute pre-test administration of the α_5 inverse agonist L655,708, as well as the absence of a memory impairment within α_5 knockout mice both strongly suggest a primarily α_5-mediated mechanism. However, as described earlier, both manipulations generally improve cognition and memory in untreated wild-type animals. What is apparent, however, is that other neurophysiological changes develop in response to increased α_5 surface expression. By one week after anesthesia, Zurek *et al.* found that recognition memory performance had fully recovered whereas elevated α_5 receptor-mediated tonic current persisted. This supports a model whereby even a brief exposure to isoflurane can instigate a number of long-term neurophysiological changes, even if it is insufficient as a single exposure to elicit profound memory impairment. Arguably, this is consistent with human presentation of POCD, which is often subtle and cumulative, resulting from multiple exposures, especially in young healthy patients.

4.5 Implications of depressed GAD-67 protein expression:

In considering how learning can recover prior to the restoration of normal α_5-mediated tonic current [119], and how isoflurane-treated animals in our study can show elevated α_5 receptor surface expression in the absence of a significant learning impairment, we investigated potential markers that could indicate compensatory changes in inhibitory network function.

GAD-67 is one of two isoforms of the enzyme glutamic acid decarboxylase (GAD), which synthesizes GABA from glutamic acid and therefore rate-controls GABA production. Multiple studies have shown GAD-67 protein expression to be dynamically regulated to normalize network activity and function [196, 197]. We used immunoblot to measure hippocampal GAD-67 protein levels, hypothesizing that an isoflurane-mediated elevation in α_5 receptor surface expression is concomitant with a depression in GAD-67 protein. In principal, an increase in inhibitory tonic current should elicit a decrease in GABA synthesis to restore inhibition. The failure to develop such an adaptive response could potentially explain differences in memory performance between anesthetized animals given vehicle versus CSA.

Within the isoflurane treated animals there was a depression of GAD-67 in total hippocampal protein was significantly different than vehicle. This GAD-67 depression is coincident with α_5 expression in isoflurane treated animals, as protein was measured from the same tissue collected three days post-anesthesia, as the α_5 experiments. However, within the isoflurane treated animals GAD-67 did not differ significantly between vehicle and CSA treatment and thus would not fully explain the observed learning impairments specific to CSA/isoflurane treated animals. Whether GAD-67 down-regulation underlies the recovery of memory function observed by Zurek *et al*. a week following anesthesia remains to be tested.

Describing the exact impact that the combined aberrations in GAD-67 and surface α_5 expression have on inhibitory network function and excitability can be approached with electrophysiology experiments, especially because other compensatory mechanisms (e.g. alterations in chloride transporter or potassium channel expression) may be present.

Specifically, predicting the outcome of GAD-67 on GABA production and on synaptic release is problematic because the exact contributions of the two GAD isoforms to GABA production are debated. GAD-65 is thought to be the isoform that resides in synapses and synthesizes most of the GABA packaged into vesicles for synaptic transmission. In contrast, GAD-67 is abundantly expressed in the cytosol. However, there is evidence that both enzymes critically contribute to vesicular GABA content, and paradoxically GAD-67 transcriptional control appears to be more dynamically affected by changes in neuronal activity.

Another possibility is that this decrease in GAD-67 protein does not represent transcriptional down-regulation, but rather loss of protein by interneuron death. GABA-ergic interneuron death and depressed GAD-67 protein is a feature of many neurological (and possibly neuropsychiatric) conditions including aging [198]. Both cell/synapse loss itself and the resulting compensatory response mechanisms have been speculated as the basis for changes in inhibitory signaling.

4.6 Calcineurin in anesthetic dysregulation of neuronal function and toxicity

CN has been implicated in post-anesthetic cognitive dysfunction mainly by dysregulating proteins that act as transcription factors, including some involved in cell survival signaling pathways. Recent studies have demonstrated activation of hippocampal CN by isoflurane exposure via immunodetection of the dephosphorylated forms of CN targets STAT3 and NFATc4 [136, 138], as well as immunodetection of the constitutively active truncated ΔCN-48, but the exact time-course of activity in relation to exposure is unknown. The STAT3 down regulation effect promotes neurotoxicity by subsequent suppression of anti-apoptotic factors survivin and bcl, whereas CN-mediated NFATc4 activation and nuclear import has been related to aberrant synaptic plasticity in animal models of neurodegeneration. In terms of outcome, the straightforward prediction of these studies would have been that CSA should have improved post-anesthetic cognition; both demonstrated reversal of adverse cognitive effects with CN inhibitor pretreatment. Instead, in our experiments we found that CSA conferred vulnerability to an otherwise safe isoflurane exposure.

If we consider instead the possibility that the protein targets of isoflurane-activated CN contributes to cognitive resiliency from adverse effects from anesthesia rather than cognitive dysfunction, a myriad of options emerge. Transcription factor targets of CN with demonstrated effects on synaptic function include CREB, MEF-2, NF-κB [183] etc. In addition to regulating gene transcription, several lines of work have demonstrated CN-mediated homeostatic plasticity and restoration of neuronal activity following insult and excitatory perturbation, through alterations in AMPA receptor and potassium channel trafficking [152, 199, 200].

While we did not assay for acute neurotoxicity by measuring apoptosis during anesthesia exposure, we found no evidence for protracted isoflurane or CSA-related neurotoxicity based on caspase-3 cleavage measures three days following anesthesia. Acute neurotoxicity was not initially predicted to result from our anesthesia exposure model; POCD is rare in young healthy patients and would be especially unlikely in a brief thirty-minute anesthesia. Initially these experiments were designed to address the possibility of CSA neurotoxicity, a collection of neurological complications well known as a danger for transplant patients associated with chronic CSA treatment. Symptoms range from tremor, headache and neuralgias and can progress to hallucinations and seizure[174]. Cerebrovascular and ischemic mechanisms have been proposed as principal causes, and white-matter lesions (ostensibly degenerated axons) are a reliable diagnostic feature, although the sequence of events relating these symptoms has not been delineated. In short, our caspase-3 cleavage results preclude this type of protracted neurological reaction but do not preclude less catastrophic forms of neurotoxicity that are restricted to shortly after or during isoflurane exposure. Another caveat to our interpretation of caspase-3 protein levels from brain substructure lysate is that they are essentially population measurements. This approach is limited in detecting neurotoxicity within important subpopulations; to this end future, studies using immunohistochemistry and cell-type specific markers would be ideal.

Is GAD-67 depression a reflection of toxicity? The possibility that hippocampal GABA-ergic interneurons are selectively sensitive to isoflurane neurotoxicity has been actively explored in the developing nervous system. Co-labeling studies in the cortex of neonate models of isoflurane exposure identify a high incidence of caspase-3 activation within GAD-67 expressing cells at six hours post-exposure [167]. We did not observe significant caspase-3 cleavage; however we only looked at caspase-3 three days following exposure. Although toxicity can persist up to 72 hours following isoflurane exposure, measurements taken closer to or during exposure may yield higher sensitivity that would allow us to directly compare whether interneuron sensitivity is a feature of mature nervous system as well.

Regardless of apoptotic measurements, evidence currently suggests that GAD-67 neuron loss does not underlie the behavioral phenotype observed in CSA/ISO treated mice. Firstly, we observed decreased GAD-67 in both isoflurane-treated groups, including the vehicle group, which did not display a learning impairment. Moreover, CN is largely absent from GABA-ergic interneurons [201], which may explain why calcium-dependent plasticity fails to occur at the post-synaptic domain of synapses onto these neurons. If interneurons are indeed susceptible to CN-mediated isoflurane neurotoxicity, then it is not through apoptotic mechanisms that occur purely within the cell (e.g. through CN-mediated dysregulation of apoptotic pathway control) but rather extrinsically as a consequence of a neuron population phenomenon (e.g. network hyperexcitability that then promotes excitotoxic cell death).

Another potential theory for persistent learning impairments following anesthesia is the suppression of adult neurogenesis [133]. In humans and rodents the dentate gyrus generates new granule cells, which are excitatory principal cells that project onto CA3, from precursor cells residing in the subventricular zone. Anesthetics are suspected in impairing this process through activity-dependent [202] as well as activity-independent mechanisms [133], with precursor cell developmental stage and duration of anesthesia exposure being key determinants of outcome. Basal CN/NFATc4 signaling has also been identified as a regulatory mechanism for neurogenesis [203]. Hypothetically, a connection would be a two-hit model whereby anesthetics impair neurogenesis in a subset of nascent cells and then chronic CSA prevents the CN-mediated replenishment. As is, our data do not provide evidence for or against this, but it remains a possibility.

4.7 The study of working memory outcomes following anesthesia: interpreting animal models within the context of clinical knowledge

Roughly, about 10% of elderly patients develop some persistent adverse cognitive effects post-operatively [45, 204]. These problems are primarily with executive function: disorientation, memory lapses, difficulty in focus and attention, confusion etc. By comparison, animal models of POCD have been largely typified by working memory impairments. The identification of specific biochemical makers with significant predictive value remains elusive. Even without such diagnostics, research focusing on risk factors for POCD or POCD-like syndromes will be necessary to identify vulnerable populations.

Another caveat to the interpretation of animal models is age. In general, understanding the role of age in vulnerability to adverse outcomes following anesthesia has been a serious challenge in anesthesia research. Adverse effects are clearest at the extremes of age, and why young-adult or middle-aged animals and humans seem to have resilience is unclear. Because of the profound differences in GABA-ergic signaling between developing and mature neurons, experiments using mature neurons should be emphasized, despite the increased technical challenges of working with older neurons *in vitro*. Future research strategies include studies using combined living cell microscopy and photolabeling that can help detect important changes in expression levels on relevant time scales.

Although our interest in evaluating learning and memory outcomes following anesthesia is partially motivated by POCD, our animal model here is by no means a POCD animal model. We demonstrate anesthetic-related impairments in young-adult, healthy mice whereas POCD is rare in young-adult, healthy humans. Instead, what we present is a vulnerability to POCD-like behavioral phenotypes stemming from chronic CSA treatment, and a possibility that dynamic alterations in CN activity has a protective role in cognitive recovery.

One potential contribution of our experiments to understanding the pathophysiology of anesthetic-related cognitive impairments, at least in rodent models, is the description of a timeframe during which CSA-mediated cognitive effects develop. The absence of a profound CN-dependent effect of isoflurane on surface expression during exposure itself, as measured from *in vitro* experiments, tentatively suggests that the window for this role may be post-operative rather than intra-operative.

What hypothetical mechanisms could potentially explain the development of this phenotype in our animal model? Clearly, isoflurane exposure increased surface expression of extrasynaptic $GABA_A$Rs, specifically α_5 containing receptors. However, only the chronic CSA treatment group appeared to suffer learning impairments after this very brief isoflurane exposure. This was also the only group to demonstrate a decrease in total α_5 protein. If chronic CSA itself alone decreased total α_5 expression levels, we would have seen that in the CSA only group. Therefore, we need to consider mechanistic explanations for our data that accounts for an interaction between calcineurin and isoflurane.

First, we must consider that our *in vitro* data showed no effect of acute CSA or acute isoflurane on expression levels. And we must consider a potential major role of PKC in regulating $GABA_A$R surface expression basally or in response to anesthesia in dynamic opposition to CN. If we were to imagine the regulation of surface expression of

$GABA_A$Rs γ_2 existing more or less in balance between CN and PKC activity, as a dynamic competition between a calcium-dependent phosphatase and kinase we might be able to explain our *in vitro* findings: isoflurane activates both CN and PKC resulting in no change in expression levels, whereas propofol only activates PKC leading to an increase in surface expression. Perhaps the temporary CN inhibition caused by acute application of CSA is easily compensated for by a corresponding decrease of PKC activity – resulting in our observed non-effect of acute CSA application on trafficking. Or, perhaps a temporary CN inhibition is a non-issue for surface expression during brief isoflurane exposures because the actions of PKC predominate regardless, resulting in our observed increase in surface expression and non-effect of additional CSA. Repeating these experiments with manipulations of the PKC pathway could provide some indirect insight into the plausibility of this mechanism.

Other explanations are possible. It is known that after ethanol intoxication, aberrant $\alpha_4\,\beta_x\gamma_2$ $GABA_A$Rs are trafficked to the surface in specific brain regions that naturally contain $\alpha_4\,\beta_x\delta$ (e.g. hippocampus dentate gyrus). It is possible that a similar effect is seen after acute isoflurane exposure. Perhaps in the setting of chronic calcineurin inhibition, these aberrant $GABA_A$Rs are not removed from the surface as readily as the naturally occurring $\alpha_5\beta_3\gamma_2$. The expression of this phenomenon in dentate gyrus may lead to the slower learning we observed in our animals. Experimentally addressing this potential mechanism would involve either surface-specific immunohistochemistry or biotinylation of specific thalamic nuclei or the dentate gyrus. Additionally, pharmacologic manipulations with α_4 specific compounds could be helpful.

Finally, we speculate that a host of neurophysiological events occur in response to isoflurane anesthesia alone, including both deleterious and adaptive responses. These adaptive changes may include altered expression and trafficking of ion channels and neurotransmitter synthesis enzymes (including, but not limited to, α_5 subunits and GAD-67) that serve to accommodate changes in excitability or synaptic function, and probably extend to many different neurotransmitter systems. Chronic CSA may provide protection against some isoflurane related cellular stress or toxicity by preventing mitochondrial cell death pathways, but in the long term serves to undermine cognitive recovery by blocking or perturbing the expression of at least some adaptive changes in gene expression that normalize memory function. This paradigm could be tested by withholding the start of chronic CSA until the peri- and post-isoflurane period, or by rescuing CN activity post-isoflurane e.g. with delivery of overexpression oligonucleotides. Molecular approaches to suppress CN activity could provide more precise blockade than pharmacological inhibition, and thus elucidate region and pathway-specific interactions, such as the VIVIT peptide, which specifically inhibits calcineurin/NFATc interactions and could be directly injected into the hippocampus [205]. Cell-type specific manipulations (e.g. using specific promoter sequences) could also serve to elucidate the role of CN in neurons versus glia, such as astrocytes, which express CN in response to inflammation [171].

4.8 Pharmacology of Cyclosporine A and implications for anesthetic management

The immunosuppressant effects of Cyclosporine A revolutionized organ transplant medicine, and remains one of the most important immunosuppressant drugs available. Over 25,000 organ transplants are performed every year, and chronic administration of CSA is a standard of care treatment to prevent transplant rejection [174]. The danger of chronic CSA treatment has largely focused on kidney cell and organ toxicity because of the high incidence of eventual renal stress and failure, but following problems related to kidney function, neurological dysfunctions are probably the most serious side effect of CSA.

CSA inhibits CN through an intermediary protein complex formed by CSA and cyclophilin D. The CSA-cyclophilin complex does affect molecular targets within the cell besides CN, including the mitochondrial transition pore (which cyclophilin modulates) and inhibits pore opening. This pharmacological promiscuity does provide difficulty in explaining the behavioral effects of CSA/ISO mice purely through mechanisms of neuronal plasticity. Ultimately, the off-target effects on mitochondrial function (previously demonstrated to be neuroprotective) do not explain the expression of post-anesthetic learning impairments seen during a chronic CSA treatment.

4.9 Conclusion: Summary and perspectives

We initially hypothesized that calcineurin contributes to negative changes in cognitive function induced by isoflurane anesthesia, and that inhibition of CN could improve cognitive outcomes. Instead, our studies showed that CN inhibition impaired working memory outcomes and failed to prevent isoflurane-induced dysfunctional changes in inhibitory transmission. These results suggest that CN has a role in the neurological recovery of the learning and memory circuits following isoflurane anesthesia, or at least that inhibition or suppression of CN activity confers vulnerability to the development of impairments following isoflurane anesthesia.

Although anti-inflammatory agents have shown promise in prevention of POCD in rodent models, we demonstrate that chronic immunosuppression via CSA may not be effective for minimizing adverse neurologic outcomes after surgery. Instead, our data suggests that CSA confers a vulnerability to memory impairments following isoflurane exposure. Given that *in vitro* studies of the effect of isoflurane on $GABA_AR$ trafficking show that a short exposure does not dramatically alter surface expression, we speculate that the effects of isoflurane on surface expression and memory *in vivo* develop during recovery.

Clearly, complex neurophysiological changes occur during and after anesthesia. Both acute and persistent changes in $GABA_AR$ surface expression manifest in response to the use of various anesthetic agents, suggesting dysfunction in the intracellular signaling pathways that control receptor trafficking. Despite specific knowledge regarding individual $GABA_AR$ subunit composition, subcellular localization, regional anatomy, and pharmacological attributes, it is unclear how these features generate intra- and post-operative consequences. Off-target effects of anesthetic agents on receptor trafficking or subtype expression can impart neurophysiologic differences that likely influence the heterogeneity of individual patient recovery of cognitive function.

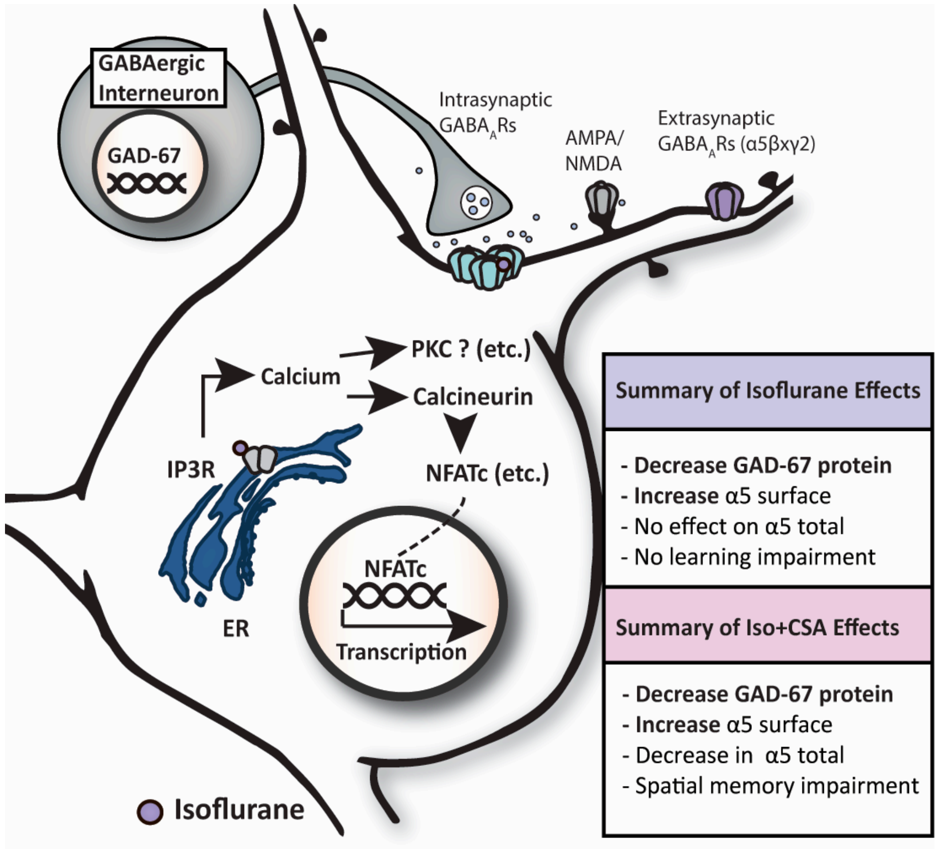

Figure 4.1 Summary of experimental results

Figure 4.1 Summary of experimental results The “classical” targets of anesthetics, the intrasynaptic and extrasynaptic subpopulations of $GABA_A$Rs, are driven by synaptic and tonic GABA arising from GABAergic interneurons. In addition, “off-target” effects of anesthetics include the release of intracellular calcium through IP3Rs and activation of calcineurin. Potential downstream effects include aberrant NFATc-mediated gene transcription, although other potential transcriptional changes resulting from altered activity or other disturbed intracellular signaling pathways are also plausible. In our mouse model of anesthesia, isoflurane exposure is associated with decreased GAD-67 protein, suggesting transcriptional down-regulation. Isoflurane is also associated with aberrations in the production and surface expression of the α5 extrasynaptic $GABA_A$R subunit. Given that our exposure was insufficient to generate a behavioral learning impairment, additional compensatory changes likely also occur after anesthesia to normalize or maintain hippocampal-based learning function, suggesting the existence of natural resilience or recovery mechanisms.

Because CSA did not have a significant effect on GAD-67, the post-anesthetic downregulation is likely CN-independent. The increase in surface α5 is also likely CN independent because the inhibitor failed to reverse upregulation. Alternately, perhaps isoflurane that is unmasking the effects of CSA by altering pathways that normally compensate for its chronic use.

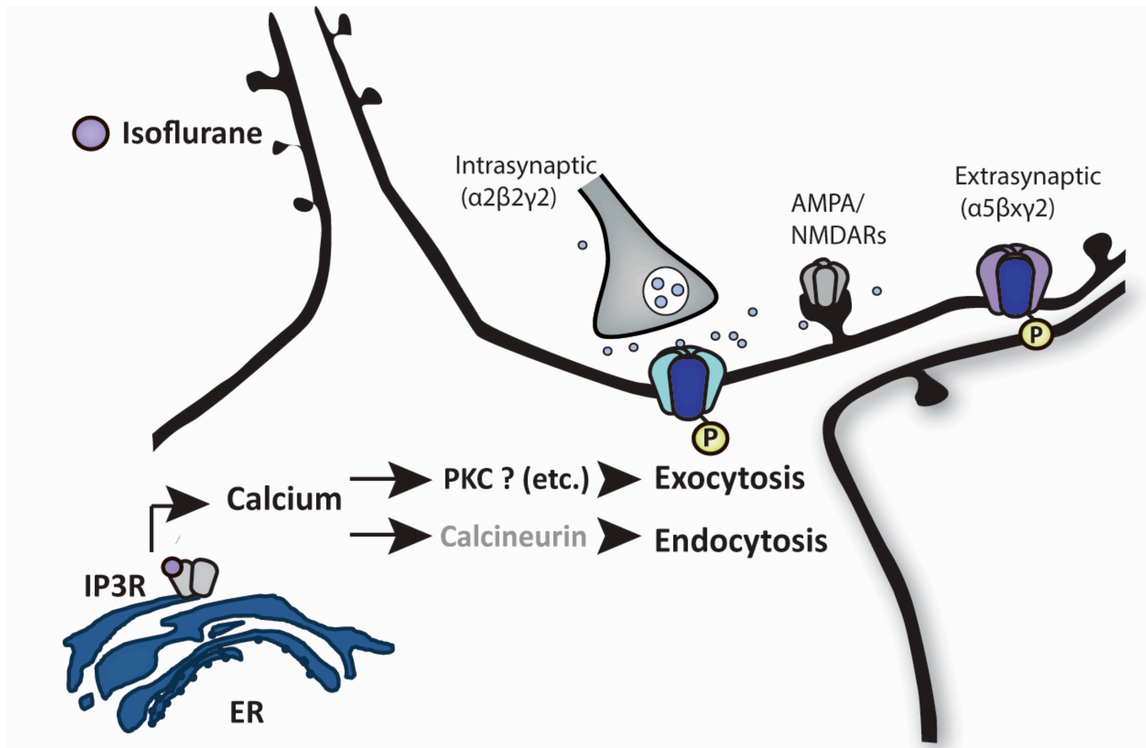

Figure 4.2 Summary of experimental results, specific to intracellular trafficking

Figure 4.2 Summary of experimental results, specific to intracellular trafficking. To investigate whether isoflurane anesthesia alters $GABA_AR$ surface expression by interfering with receptor trafficking, we conducted *in vitro* experiments to monitor surface levels during an acute isoflurane exposure. Initially, we hypothesized that the calcineurin activated by isoflurane via IP3R-mediate calcium efflux directly acting on its $GABA_AR$ $\gamma2$ regulatory site would promote exocytosis. Instead, we found a small increase in surface expression following isoflurane exposure, with no significant additional effect of CSA. This result suggests that following isoflurane exposure, the kinase activity of PKC (or another regulatory protein) predominates over calcineurin phosphatase activity at $\gamma2$, which leads to a gross effect of a small increase in surface expression that is not reversible by calcineurin inhibition. However, direct experimentation with a PKC inhibitor would be necessary to test this hypothesis. More generally, the totality of changes in protein function induced by isoflurane is probably best investigated using a proteomics approach. Collectively, these experiments support a largely gene transcription-related phenomenon underlying learning impairments expressed by CSA/ISO treated mice.

Chapter 5: Extended Methods for isoflurane exposure *in vitro*, *in vivo*, and *ex vivo* techniques

Chapter 5: Extended Methods for isoflurane exposure *in vitro*, *in vivo*, and *ex vivo* techniques

This chapter is a discussion of the experimental approaches used within this thesis to study the effects of anesthetics on reduced and intact animal nervous systems. Here, I describe fundamental design principles of anesthetic delivery, explain their relevance for experimentation, and detail the technical specifics of the setups used in this thesis. The first part will address considerations for *in vitro* systems (**Chapter 2** experiments), and then second will address *in vivo* mouse anesthesia (**Chapter 3** experiments).

5.1 Anesthetic delivery for *in vitro* systems

The delivery of anesthesia in a reduced system can pose problems to researchers interested in anesthetic mechanisms. The most common drugs are inhaled which become absorbed in our blood stream and quickly diffuse into brain tissues. Although we monitor and describe these concentrations clinically as fractions of inspired gas, these are not easily translatable to cell culture or brain tissue systems. Common admisistration problems are typically related to the preference for these drugs to exist in the gaseous phase. In contrast, most intravenous anesthetic agents like propofol can be treated similarly to most nonpolar soluble drugs and need only to be diluted in vehicle, ex. DMSO.

Administering clinically relevant concentrations of inhalational or volatile anesthetics, like isoflurane, with accuracy and precision in cell culture is less straightforward. For our experiments, the target concentrations were designed to be equivalent to 1 MAC, which is a comprehensive unit of general anesthetic potency. The

MAC or minimal alveolar concentration of an anesthetic vapor is the steady-state concentration (usually expressed in % atm or % vol) at which 50% of normal adult subjects will not move in response to surgical stimulation, not unlike an EC50 value for immobility. Likewise, 1.5 MAC will typically block response in 95% of patients. The accepted molar concentration that corresponds from inhaling 1 MAC of isoflurane is 320 μM [206]. For animal studies, gas volume doses from 1.5 to 2% are typically used for producing adequate anesthesia for surgical intervention.

Whether using gaseous or liquid delivery, temperature is critical determinant for accurate isoflurane dosing *in vitro*. Firstly, temperature affects how much vapor anesthetic can be solubilized into the bodily organ tissues or into aqueous solutions because the gas partition-coefficient of isoflurane and other volatile agents is temperature-sensitive. Secondly, the potentiation of $GABA_AR$ channel function by volatile agents is also sensitive to temperature [207], with temperature being inversely proportional to anesthetic potency for a given molar concentration. In general, the best strategy to replicate physiological MAC is to conduct experimental anesthesia exposure at bodily temperature (37°). Conveniently, cultured hippocampal neurons are typically maintained at 37°. Within mammalian systems, MAC values are very consistent between species [206]. So, while the relationship between temperature, agent delivery, and agent effect is a critical issue that continues to complicate the interpretation of many *in vitro* studies of anesthetic mechanisms, our experiments largely avoid these problems because they are performed at normal bodily temperature.

The choice between aqueous or gaseous isoflurane delivery comes down to practicality. With aqueous solutions, the main problem is maintaining actual concentrations. Isoflurane vapor preferentially partitions into the gas phase over the aqueous phase, so solvated isoflurane will spontaneously dissipate as the solution is exposed to air. In electrophysiological experiments, the common practice is to create a solution in an air-tight container, and then for exposure constantly and rapidly perfuse this solution without recycling. With aqueous delivery of volatile anesthetics, it is important to ensure that effective concentrations are reaching the cells of interest, as the lack of a response could be due to air bubbles in the system or absorbance of drug from tubing or connectors. Actual quantifiable measures for anesthetic concentrations can be obtained via chromatography or normalized physiologic response measures. With gaseous delivery of isoflurane, which is superior for longer exposures where constant liquid perfusion is not realistic, the main difficulty is constructing the gas circuit. However, clinical infrared gas analyzers can be used to measure fractional components of volatile concentrations in a side-stream sample from the expiratory (outflow) limb of the gas circuit. Below, I will first describe the technicalities of our gaseous system used for cell-surface biotinylation of cultured hippocampal neurons, and then the protocol for the aqueous solution application used for live-cell imaging.

Vaporized Isoflurane Exposure System for Cultured Cells

To measure the acute effect of isoflurane on $GABA_AR$ surface expression in hippocampal neurons using cell-surface biotinylation, we designed a system for stable delivery and real-time measurement of gaseous isoflurane based on an anesthetic gas circuit housed inside of a cell-culture incubator. A diagram of the gas circuit and pictures of the setup are shown in **Figure 5.1** and **Figure 5.2** respectively.

Isoflurane (2%) was mixed into gas from content certified canisters containing 21 % oxygen, 5 % CO2 and 75% Nitrogen (NexAir, TN) using a calibrated isoflurane vaporizer (Ohio Medical products, Madison WI). For non-isoflurane conditions, the vaporizer dial was set to 0, allowing gas to bypass the isoflurane vaporizer.

The cell culture incubator includes a silicon plug with a port for lead insertion, which was modified to accept a trimmed 1ml syringe. The trimmed side was fitted by friction to tubing carrying gas from vaporizer, and the male Luer slip end faced inside the incubator. At flow rates controlled by a regulator, normal or isoflurane-containing gas was delivered into an airtight chamber (Posi-Seal mouse induction chamber, cat. no. AS-01-0532 Molecular Imaging Products, Bend OR) housed inside of a water-jacketed cell culture incubator (HeraCell 150i, Thermo Scientific). Gas was delivered into the chamber via 1.975m of tubing wrapped around a weighted 50ml conical tube submerged in 1L of water, designed to heat incoming gas.

In general, tubing should be airtight, and conductive rubber should be avoided because it has been demonstrated to both absorb and leak volatile gases into the outside environment [208]. Most medical-grade intravenous tubing is made of plastic polymer (e.g. polyvinyl chloride, polypropylene, or polyethylene) that is acceptable for these setups. Compared to other options, polyvinyl chloride will absorb some volatile gases but not leak it into the environment. This loss is negligible if the anesthetic gas content is measured at the end of the air circuit and maintained accordingly.

Temperature within the chamber was monitored with a digital thermometer (P/N 4047CC, VWR) placed inside. Gas exiting the chamber was lead out of the incubator via tubing passed through a silicone plug installed in the incubator door. This exiting line bifurcated into an isoflurane air scavenger F/AIR filter canister (Harvard Apparatus, cat. no. 600979) and an anesthetic agent analyzer (Capnomac Ultima, Datex Ohmeda) for side-stream analysis of gases exiting the chamber. Every 5 minutes during the experiment, the gas concentrations of oxygen, carbon dioxide, and isoflurane were recorded from the agent analyzer. Temperature inside the chamber was simultaneously observed as recorded (**Figure 5.2**).

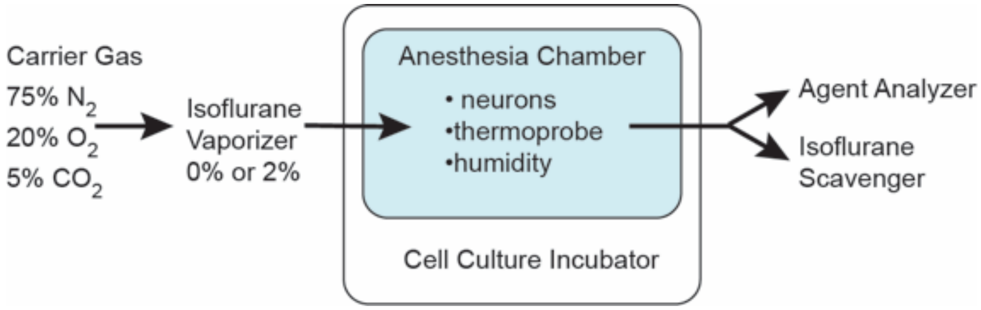

Figure 5.1 Diagram of isoflurane exposure system

Figure 5.1 Diagram of isoflurane exposure system

The set-up employed is a non-recirculating circuit driven by positive pressure. Pressurized carrier gas mixture is released by a regulator into an isoflurane vaporizer, which adds isoflurane to fresh gas flow at a set final concentration. When the vaporizer dial is set to 0%, all incoming carrier gas enters the bypass pathway, allowing pure carrier gas to flow through. This gas exits the vaporizer and then continuously fills the anesthesia chamber, housed within a cell culture incubator for thermal regulation. Expelled gas from this chamber exits the cell-culture incubator into an isoflurane scavenger. A minute amount is diverted into a side-stream analyzer that measures gas content.

Figure 5.2. Vaporized isoflurane circuit for cultured neuron exposure.

Figure 5.2 Vaporized isoflurane circuit for cultured neuron exposure. Views from the outside (top) and the inside (bottom) of the cell culture incubator. The outer water-jacketed door is typically closed to maintain temperature. The top view better depicts the second half of the circuit as it exits the incubator and feeds into the anesthetic scavenger and side-stream agent analyzer. The bottom view better shows the gas circuit entry into the incubator and then into the anesthesia chamber. Neuron plates are placed inside the green box.

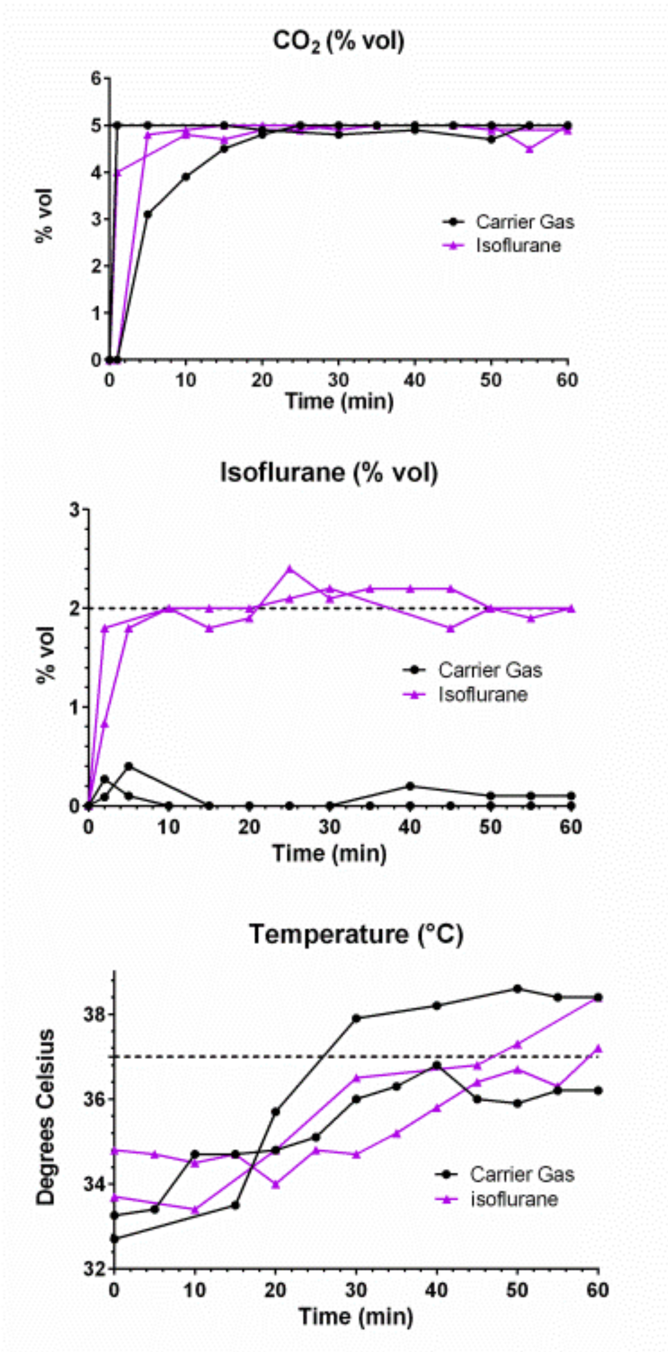

Figure 5.3 Isoflurane chamber results.

Figure 5.3 Isoflurane chamber results. Gas content (% volume) and temperature readings from two isoflurane and two sham (carrier gas) experiments.

Aqueous isoflurane solutions

The following protocol for preparing aqueous isoflurane solution has been found to give reproducible effects, as tested with electrophysiological measures of $GABA_AR$ current potentiation used by our research group in prior experiments [35]. Solutions were prepared fresh immediately before experimentation inside of 100ml intravenous drip bags with small stir magnets inside. Each bag was filled with 50ml of room temperature buffer, set on a stir plate for 15 minutes, agitated inside of an incubator shaker set at 32°C, and air bubbles thoroughly removed through the injection port with a long 18g needle. To make the isoflurane treatment solution, 5µl of liquid isoflurane from stock was injected with an insulin syringe or 10µl HPLC/Gas Chromatography syringe (National Scientific), and mixed on a stir plate for 20-30 minutes. Control treatment solution is prepared identically, sans isoflurane. Imaging buffer was supplemented with DMSO or CSA before preparation in bags.

Until use, bags sat inside of a cell culture incubator set to 37°C no longer than thirty minutes. Although the isoflurane gas-phase partition is very sensitive (inversely correlated) to temperature, the aqueous-phase partition coefficient is relatively constant with temperature, so once mixed the concentration is stable. The bag is air-tight, precluding the entry of atmospheric gases which would alter pH. Isoflurane or control recording solution was perfused into the Mat-tek dish by gravity at a rate of 0.75ml/min through an Intravenous flow rate control line (**Figure 5.4**), and then removed by vacuum aspiration. The Mat-Tek dish was housed inside of a stage-top incubator which maintained dish solution temperature at 37.3°, as measured with a submerged thermocouple.

Figure 5.4 Aqueous isoflurane solution perfusion lines for live-cell imaging (or electrophysiology). Sham or isoflurane-containing solution is prepared inside of a used saline intravenous fluid bag (upper right). Once prepared, it is gravity fed through a flow-rate controller (blue/white) into a glass-bottom dish containing hippocampal neurons, which is housed inside a stage-top incubator (left).

5. 2 Anesthetic delivery for *in vivo* systems

For experiments in chapter 3, adult mice were anesthetized with isoflurane and then assessed for behavioral measures of anesthetic induction and emergence. Here I describe in depth the procedures for anesthetic induction, maintenance, and emergence with isoflurane.

Prior to anesthesia challenge, (individually housed) mice were in their home cages were brought into the room to acclimate 10-15 minutes Anesthesia was induced by placing each mouse in an air-tight plexiglass anesthesia chamber, which was pre-charged and continuously maintained with 2% isoflurane with an anesthetic vaporizer at a flow-rate of 1.25 L/min. The carrier and sham gas was pure oxygen. In general, mice are sensitive to hypoxia if not ventilated owing to depressed autonomic reflexes and small tidal volume and small blood oxygen reserves, so 100% is used. As an alternative, 30% oxygen could be used in combination with a pulse oximeter to detect hypoxia. Clinically, inspired O_2 concentrations vary dramatically between 30-95%. Temperature was maintained with a ceramic heat lamp and a heating pad. Once steady-state anesthesia is reached, ophthalmalogic ointment is applied to lubricate the eyes, as the blink reflex is impaired with anesthesia.

For an anesthetic induction (and indirectly, sensitivity) measure, loss of righting reflex is the standard proxy for hypnosis or unconsciousness in a rodent model. In our protocol, time to loss of righting reflex is scored as the latency from placement into the induction chamber until the mouse fails to right itself after being gently turned onto its back. Once this occurs, mice are replaced supine to aid observation of respiratory patterns. After a pre-set time (thirty minutes) of anesthesia, mice are removed from the anesthesia chamber and placed into an emergence chambers for observation.

Emergence endpoints serve not only to suggest anesthetic sensitivity, but also to potentially suggest the presence of delayed emergence. We measured three emergence endpoints: time to movement, time to return of righting reflex, and time to grooming. Time to movement reflects the return of autonomic and motor reflexes, which are blunted by anesthesia. Return of righting is when the animal is first observed to make a deliberate movement to an upright stance resulting in all four paws touching the floor of the chamber. Time to grooming is a basic proxy measure of recovery of cognitive function. The principal is that sedation (incomplete emergence) and delirium-like confusion are both marked by inattentiveness, so a large latency to resume normal grooming behavior and awareness (e.g. of ophthalmologic ointment) can indicate that higher cognitive function took may have taken longer to fully recover.

References

1. Weiser, T.G., et al., *An estimation of the global volume of surgery: a modelling strategy based on available data.* Lancet, 2008. **372**(9633): p. 139-44.
2. Brown, E.N., R. Lydic, and N.D. Schiff, *General anesthesia, sleep, and coma.* N Engl J Med, 2010. **363**(27): p. 2638-50.
3. Hudson, A.E., et al., *Recovery of consciousness is mediated by a network of discrete metastable activity states.* Proc Natl Acad Sci U S A, 2014. **111**(25): p. 9283-8.
4. Dennett, D.C., *Consciousness explained*. 1st ed. 1991, Boston: Little, Brown and Co. xiii, 511 p.
5. Cohen, M.A. and D.C. Dennett, *Consciousness cannot be separated from function.* Trends Cogn Sci, 2011. **15**(8): p. 358-64.
6. Koch, C., et al., *Neural correlates of consciousness: progress and problems.* Nat Rev Neurosci, 2016. **17**(5): p. 307-21.
7. Tsuchiya, N., et al., *No-Report Paradigms: Extracting the True Neural Correlates of Consciousness.* Trends Cogn Sci, 2015. **19**(12): p. 757-70.
8. Alkire, M.T. and J. Miller, *General anesthesia and the neural correlates of consciousness.* Prog Brain Res, 2005. **150**: p. 229-44.
9. Laureys, S., *The neural correlate of (un)awareness: lessons from the vegetative state.* Trends Cogn Sci, 2005. **9**(12): p. 556-9.
10. Brown, E.N., P.L. Purdon, and C.J. Van Dort, *General anesthesia and altered states of arousal: a systems neuroscience analysis.* Annu Rev Neurosci, 2011. **34**: p. 601-28.
11. Edelman, G.M., J.A. Gally, and B.J. Baars, *Biology of consciousness.* Front Psychol, 2011. **2**: p. 4.
12. Tononi, G., et al., *Integrated information theory: from consciousness to its physical substrate.* Nat Rev Neurosci, 2016. **17**(7): p. 450-61.
13. Llinas, R.R. and M. Steriade, *Bursting of thalamic neurons and states of vigilance.* J Neurophysiol, 2006. **95**(6): p. 3297-308.
14. Imas, O.A., et al., *Volatile anesthetics disrupt frontal-posterior recurrent information transfer at gamma frequencies in rat.* Neurosci Lett, 2005. **387**(3): p. 145-50.
15. Hudetz, A.G. and G.A. Mashour, *Disconnecting Consciousness: Is There a Common Anesthetic End Point?* Anesth Analg, 2016.
16. Dagnino, J., *Coca leaf and local anesthesia.* Anesthesiology, 2004. **100**(5): p. 1322; author reply 1323.
17. Izuo, M., *Medical history: Seishu Hanaoka and his success in breast cancer surgery under general anesthesia two hundred years ago.* Breast Cancer, 2004. **11**(4): p. 319-24.
18. Hemmings, H.C., Jr. and T.D. Egan, *Pharmacology and Physiology for Anesthesia*. 2013, Philadelphia, PA: Elsevier.
19. Anaya-Prado, R. and D. Schadegg-Pena, *Crawford Williamson Long: The True Pioneer of Surgical Anesthesia.* J Invest Surg, 2015. **28**(4): p. 181-7.

20. Smith, G.B. and N.P. Hirsch, *Gardner Quincy Colton: pioneer of nitrous oxide anesthesia.* Anesth Analg, 1991. **72**(3): p. 382-91.
21. Burns, W.B. and E.I. Eger, 2nd, *Ross C. Terrell, PhD, an anesthetic pioneer.* Anesth Analg, 2011. **113**(2): p. 387-9.
22. Weiser, B.P., et al., *Mechanisms revealed through general anesthetic photolabeling.* Curr Anesthesiol Rep, 2014. **4**(1): p. 57-66.
23. McKinstry-Wu, A.R., et al., *Discovery of a novel general anesthetic chemotype using high-throughput screening.* Anesthesiology, 2015. **122**(2): p. 325-33.
24. Mashour, G.A., *Consciousness, Awareness, and Anesthesia*. 2010.
25. Avidan, M.S., et al., *Anesthesia awareness and the bispectral index.* N Engl J Med, 2008. **358**(11): p. 1097-108.
26. Franks, N.P., *Molecular targets underlying general anaesthesia.* Br J Pharmacol, 2006. **147 Suppl 1**: p. S72-81.
27. Franks, N.P. and W.R. Lieb, *Do general anaesthetics act by competitive binding to specific receptors?* Nature, 1984. **310**(5978): p. 599-601.
28. Belelli, D., et al., *The interaction of the general anesthetic etomidate with the gamma-aminobutyric acid type A receptor is influenced by a single amino acid.* Proc Natl Acad Sci U S A, 1997. **94**(20): p. 11031-6.
29. Mihic, S.J., et al., *Sites of alcohol and volatile anaesthetic action on GABA(A) and glycine receptors.* Nature, 1997. **389**(6649): p. 385-9.
30. Jurd, R., et al., *General anesthetic actions in vivo strongly attenuated by a point mutation in the GABA(A) receptor beta3 subunit.* FASEB J, 2003. **17**(2): p. 250-2.
31. Franks, N.P., *General anaesthesia: from molecular targets to neuronal pathways of sleep and arousal.* Nat Rev Neurosci, 2008. **9**(5): p. 370-86.
32. Alkire, M.T., *Probing the mind: anesthesia and neuroimaging.* Clin Pharmacol Ther, 2008. **84**(1): p. 149-52.
33. Alkire, M.T., A.G. Hudetz, and G. Tononi, *Consciousness and anesthesia.* Science, 2008. **322**(5903): p. 876-80.
34. Antognini, J.F. and K. Schwartz, *Exaggerated anesthetic requirements in the preferentially anesthetized brain.* Anesthesiology, 1993. **79**(6): p. 1244-9.
35. Safavynia, S.A., et al., *Effects of gamma-Aminobutyric Acid Type A Receptor Modulation by Flumazenil on Emergence from General Anesthesia.* Anesthesiology, 2016. **125**(1): p. 147-58.
36. Solt, K., et al., *Methylphenidate actively induces emergence from general anesthesia.* Anesthesiology, 2011. **115**(4): p. 791-803.
37. Hudetz, A.G., J.D. Wood, and J.P. Kampine, *Cholinergic reversal of isoflurane anesthesia in rats as measured by cross-approximate entropy of the electroencephalogram.* Anesthesiology, 2003. **99**(5): p. 1125-31.
38. Chander, D., et al., *Electroencephalographic variation during end maintenance and emergence from surgical anesthesia.* PLoS One, 2014. **9**(9): p. e106291.
39. Mashour, G.A. and M.S. Avidan, *Intraoperative awareness: controversies and non-controversies.* Br J Anaesth, 2015. **115 Suppl 1**: p. i20-i26.
40. Crosby, G., *General anesthesia--minding the mind during surgery.* N Engl J Med, 2011. **365**(7): p. 660-1.

41. Kretschmannova, K., et al., *Enhanced tonic inhibition influences the hypnotic and amnestic actions of the intravenous anesthetics etomidate and propofol.* J Neurosci, 2013. **33**(17): p. 7264-73.
42. Bliss, T.V. and T. Lomo, *Long-lasting potentiation of synaptic transmission in the dentate area of the anaesthetized rabbit following stimulation of the perforant path.* J Physiol, 1973. **232**(2): p. 331-56.
43. Newman, M.F., et al., *Longitudinal assessment of neurocognitive function after coronary-artery bypass surgery.* N Engl J Med, 2001. **344**(6): p. 395-402.
44. McDonagh, D.L., et al., *Cognitive function after major noncardiac surgery, apolipoprotein E4 genotype, and biomarkers of brain injury.* Anesthesiology, 2010. **112**(4): p. 852-9.
45. Moller, J.T., et al., *Long-term postoperative cognitive dysfunction in the elderly ISPOCD1 study. ISPOCD investigators. International Study of Post-Operative Cognitive Dysfunction.* Lancet, 1998. **351**(9106): p. 857-61.
46. Monk, T.G., et al., *Predictors of cognitive dysfunction after major noncardiac surgery.* Anesthesiology, 2008. **108**(1): p. 18-30.
47. Price, C.C., C.W. Garvan, and T.G. Monk, *Type and severity of cognitive decline in older adults after noncardiac surgery.* Anesthesiology, 2008. **108**(1): p. 8-17.
48. Chan, M.T., et al., *BIS-guided anesthesia decreases postoperative delirium and cognitive decline.* J Neurosurg Anesthesiol, 2013. **25**(1): p. 33-42.
49. Bianchi, S.L., et al., *Brain and behavior changes in 12-month-old Tg2576 and nontransgenic mice exposed to anesthetics.* Neurobiol Aging, 2008. **29**(7): p. 1002-10.
50. Cao, L., et al., *Isoflurane induces learning impairment that is mediated by interleukin 1beta in rodents.* PLoS One, 2012. **7**(12): p. e51431.
51. Jevtovic-Todorovic, V. and L.B. Carter, *The anesthetics nitrous oxide and ketamine are more neurotoxic to old than to young rat brain.* Neurobiol Aging, 2005. **26**(6): p. 947-56.
52. Rudolph, J.L., et al., *Measurement of post-operative cognitive dysfunction after cardiac surgery: a systematic review.* Acta Anaesthesiol Scand, 2010. **54**(6): p. 663-77.
53. Rudolph, U. and B. Antkowiak, *Molecular and neuronal substrates for general anaesthetics.* Nat Rev Neurosci, 2004. **5**(9): p. 709-20.
54. Garcia, P.S., S.E. Kolesky, and A. Jenkins, *General anesthetic actions on GABA(A) receptors.* Curr Neuropharmacol, 2010. **8**(1): p. 2-9.
55. Hemmings, H.C., Jr., et al., *Emerging molecular mechanisms of general anesthetic action.* Trends Pharmacol Sci, 2005. **26**(10): p. 503-10.
56. Pan, J.Z., et al., *Inhaled anesthetics elicit region-specific changes in protein expression in mammalian brain.* Proteomics, 2008. **8**(14): p. 2983-92.
57. Correia, A.C., P.C. Silva, and B.A. da Silva, *Malignant hyperthermia: clinical and molecular aspects.* Rev Bras Anestesiol, 2012. **62**(6): p. 820-37.
58. Xie, Z. and Z. Xu, *General anesthetics and beta-amyloid protein.* Prog Neuropsychopharmacol Biol Psychiatry, 2013. **47**: p. 140-6.
59. Miller, P.S. and A.R. Aricescu, *Crystal structure of a human GABAA receptor.* Nature, 2014. **512**(7514): p. 270-5.

60. Nury, H., et al., *X-ray structures of general anaesthetics bound to a pentameric ligand-gated ion channel.* Nature, 2011. **469**(7330): p. 428-31.
61. McKernan, R.M. and P.J. Whiting, *Which GABAA-receptor subtypes really occur in the brain?* Trends Neurosci, 1996. **19**(4): p. 139-43.
62. Olsen, R.W. and W. Sieghart, *International Union of Pharmacology. LXX. Subtypes of gamma-aminobutyric acid(A) receptors: classification on the basis of subunit composition, pharmacology, and function. Update.* Pharmacol Rev, 2008. **60**(3): p. 243-60.
63. Wisden, W. and P.H. Seeburg, *GABAA receptor channels: from subunits to functional entities.* Curr Opin Neurobiol, 1992. **2**(3): p. 263-9.
64. Farrant, M. and Z. Nusser, *Variations on an inhibitory theme: phasic and tonic activation of GABA(A) receptors.* Nat Rev Neurosci, 2005. **6**(3): p. 215-29.
65. Mody, I. and R.A. Pearce, *Diversity of inhibitory neurotransmission through GABA(A) receptors.* Trends Neurosci, 2004. **27**(9): p. 569-75.
66. Jia, F., et al., *An extrasynaptic GABAA receptor mediates tonic inhibition in thalamic VB neurons.* J Neurophysiol, 2005. **94**(6): p. 4491-501.
67. Jenkins, A., et al., *Evidence for a common binding cavity for three general anesthetics within the GABAA receptor.* J Neurosci, 2001. **21**(6): p. RC136.
68. Yip, G.M., et al., *A propofol binding site on mammalian GABAA receptors identified by photolabeling.* Nat Chem Biol, 2013. **9**(11): p. 715-20.
69. Eckel, R., et al., *Activation of calcineurin underlies altered trafficking of alpha2 subunit containing GABAA receptors during prolonged epileptiform activity.* Neuropharmacology, 2015. **88**: p. 82-90.
70. Maguire, J. and I. Mody, *Neurosteroid synthesis-mediated regulation of GABA(A) receptors: relevance to the ovarian cycle and stress.* J Neurosci, 2007. **27**(9): p. 2155-62.
71. Belelli, D. and J.J. Lambert, *Neurosteroids: endogenous regulators of the GABA(A) receptor.* Nat Rev Neurosci, 2005. **6**(7): p. 565-75.
72. Abramian, A.M., et al., *Protein kinase C phosphorylation regulates membrane insertion of GABAA receptor subtypes that mediate tonic inhibition.* J Biol Chem, 2010. **285**(53): p. 41795-805.
73. Liang, J., et al., *Mechanisms of reversible GABAA receptor plasticity after ethanol intoxication.* J Neurosci, 2007. **27**(45): p. 12367-77.
74. Sun, C., W. Sieghart, and J. Kapur, *Distribution of alpha1, alpha4, gamma2, and delta subunits of GABAA receptors in hippocampal granule cells.* Brain Res, 2004. **1029**(2): p. 207-16.
75. Caraiscos, V.B., et al., *Selective enhancement of tonic GABAergic inhibition in murine hippocampal neurons by low concentrations of the volatile anesthetic isoflurane.* J Neurosci, 2004. **24**(39): p. 8454-8.
76. Caraiscos, V.B., et al., *Tonic inhibition in mouse hippocampal CA1 pyramidal neurons is mediated by alpha5 subunit-containing gamma-aminobutyric acid type A receptors.* Proc Natl Acad Sci U S A, 2004. **101**(10): p. 3662-7.
77. Luscher, B., T. Fuchs, and C.L. Kilpatrick, *GABAA receptor trafficking-mediated plasticity of inhibitory synapses.* Neuron, 2011. **70**(3): p. 385-409.

78. Tretter, V., et al., *The clustering of GABA(A) receptor subtypes at inhibitory synapses is facilitated via the direct binding of receptor alpha 2 subunits to gephyrin.* J Neurosci, 2008. **28**(6): p. 1356-65.
79. Stell, B.M. and I. Mody, *Receptors with different affinities mediate phasic and tonic GABA(A) conductances in hippocampal neurons.* J Neurosci, 2002. **22**(10): p. RC223.
80. Lerma, J., et al., *In vivo determination of extracellular concentration of amino acids in the rat hippocampus. A method based on brain dialysis and computerized analysis.* Brain Res, 1986. **384**(1): p. 145-55.
81. Tossman, U., G. Jonsson, and U. Ungerstedt, *Regional distribution and extracellular levels of amino acids in rat central nervous system.* Acta Physiol Scand, 1986. **127**(4): p. 533-45.
82. de Groote, L. and A.C. Linthorst, *Exposure to novelty and forced swimming evoke stressor-dependent changes in extracellular GABA in the rat hippocampus.* Neuroscience, 2007. **148**(3): p. 794-805.
83. Bieda, M.C., H. Su, and M.B. Maciver, *Anesthetics discriminate between tonic and phasic gamma-aminobutyric acid receptors on hippocampal CA1 neurons.* Anesth Analg, 2009. **108**(2): p. 484-90.
84. Bonin, R.P. and B.A. Orser, *GABA(A) receptor subtypes underlying general anesthesia.* Pharmacol Biochem Behav, 2008. **90**(1): p. 105-12.
85. Ben-Ari, Y., *Commentary: GABA depolarizes immature neurons and inhibits network activity in the neonatal neocortex in vivo.* Front Cell Neurosci, 2015. **9**: p. 478.
86. Ganguly, K., et al., *GABA itself promotes the developmental switch of neuronal GABAergic responses from excitation to inhibition.* Cell, 2001. **105**(4): p. 521-32.
87. Coulter, D.A. and G.C. Carlson, *Functional regulation of the dentate gyrus by GABA-mediated inhibition.* Prog Brain Res, 2007. **163**: p. 235-43.
88. Sperk, G., et al., *GABA(A) receptor subunits in the rat hippocampus I: immunocytochemical distribution of 13 subunits.* Neuroscience, 1997. **80**(4): p. 987-1000.
89. Glykys, J., et al., *A new naturally occurring GABA(A) receptor subunit partnership with high sensitivity to ethanol.* Nat Neurosci, 2007. **10**(1): p. 40-8.
90. Zecharia, A.Y., et al., *The involvement of hypothalamic sleep pathways in general anesthesia: testing the hypothesis using the GABAA receptor beta3N265M knock-in mouse.* J Neurosci, 2009. **29**(7): p. 2177-87.
91. Zecharia, A.Y. and N.P. Franks, *General anesthesia and ascending arousal pathways.* Anesthesiology, 2009. **111**(4): p. 695-6.
92. Silber, M.H. and D.B. Rye, *Solving the mysteries of narcolepsy: the hypocretin story.* Neurology, 2001. **56**(12): p. 1616-8.
93. Kittler, J.T., K. McAinsh, and S.J. Moss, *Mechanisms of GABAA receptor assembly and trafficking: implications for the modulation of inhibitory neurotransmission.* Mol Neurobiol, 2002. **26**(2-3): p. 251-68.
94. Lo, W.Y., et al., *Glycosylation of {beta}2 subunits regulates GABAA receptor biogenesis and channel gating.* J Biol Chem, 2010. **285**(41): p. 31348-61.

95. Bogdanov, Y., et al., *Synaptic GABAA receptors are directly recruited from their extrasynaptic counterparts.* EMBO J, 2006. **25**(18): p. 4381-9.
96. Bannai, H., et al., *Activity-dependent tuning of inhibitory neurotransmission based on GABAAR diffusion dynamics.* Neuron, 2009. **62**(5): p. 670-82.
97. Jacob, T.C., et al., *Gephyrin regulates the cell surface dynamics of synaptic GABAA receptors.* J Neurosci, 2005. **25**(45): p. 10469-78.
98. Kowalczyk, S., et al., *Direct binding of GABAA receptor beta2 and beta3 subunits to gephyrin.* Eur J Neurosci, 2013. **37**(4): p. 544-54.
99. Tretter, V., et al., *Gephyrin, the enigmatic organizer at GABAergic synapses.* Front Cell Neurosci, 2012. **6**: p. 23.
100. Maric, H.M., et al., *Gephyrin-mediated gamma-aminobutyric acid type A and glycine receptor clustering relies on a common binding site.* J Biol Chem, 2011. **286**(49): p. 42105-14.
101. Hausrat, T.J., et al., *Radixin regulates synaptic GABAA receptor density and is essential for reversal learning and short-term memory.* Nat Commun, 2015. **6**: p. 6872.
102. Brady, M.L. and T.C. Jacob, *Synaptic localization of alpha5 GABA (A) receptors via gephyrin interaction regulates dendritic outgrowth and spine maturation.* Dev Neurobiol, 2015. **75**(11): p. 1241-51.
103. Triller, A. and D. Choquet, *Surface trafficking of receptors between synaptic and extrasynaptic membranes: and yet they do move!* Trends Neurosci, 2005. **28**(3): p. 133-9.
104. Kittler, J.T., et al., *Constitutive endocytosis of GABAA receptors by an association with the adaptin AP2 complex modulates inhibitory synaptic currents in hippocampal neurons.* J Neurosci, 2000. **20**(21): p. 7972-7.
105. Moss, S.J., C.A. Doherty, and R.L. Huganir, *Identification of the cAMP-dependent protein kinase and protein kinase C phosphorylation sites within the major intracellular domains of the beta 1, gamma 2S, and gamma 2L subunits of the gamma-aminobutyric acid type A receptor.* J Biol Chem, 1992. **267**(20): p. 14470-6.
106. Kittler, J.T., et al., *Huntingtin-associated protein 1 regulates inhibitory synaptic transmission by modulating gamma-aminobutyric acid type A receptor membrane trafficking.* Proc Natl Acad Sci U S A, 2004. **101**(34): p. 12736-41.
107. Joshi, S. and J. Kapur, *Slow intracellular accumulation of GABA(A) receptor delta subunit is modulated by brain-derived neurotrophic factor.* Neuroscience, 2009. **164**(2): p. 507-19.
108. Gonzalez, C., S.J. Moss, and R.W. Olsen, *Ethanol promotes clathrin adaptor-mediated endocytosis via the intracellular domain of delta-containing GABAA receptors.* J Neurosci, 2012. **32**(49): p. 17874-81.
109. van Rijnsoever, C., C. Sidler, and J.M. Fritschy, *Internalized GABA-receptor subunits are transferred to an intracellular pool associated with the postsynaptic density.* Eur J Neurosci, 2005. **21**(2): p. 327-38.
110. Twelvetrees, A.E., et al., *Delivery of GABAARs to synapses is mediated by HAP1-KIF5 and disrupted by mutant huntingtin.* Neuron, 2010. **65**(1): p. 53-65.

111. Joseph, J.D., et al., *General anesthetic isoflurane modulates inositol 1,4,5-trisphosphate receptor calcium channel opening.* Anesthesiology, 2014. **121**(3): p. 528-37.
112. Wei, H. and Z. Xie, *Anesthesia, calcium homeostasis and Alzheimer's disease.* Curr Alzheimer Res, 2009. **6**(1): p. 30-5.
113. Kindler, C.H., et al., *Volatile anesthetics increase intracellular calcium in cerebrocortical and hippocampal neurons.* Anesthesiology, 1999. **90**(4): p. 1137-45.
114. Wickley, P.J., et al., *Propofol activates and allosterically modulates recombinant protein kinase C epsilon.* Anesthesiology, 2009. **111**(1): p. 36-43.
115. Hemmings, H.C., Jr. and A.I. Adamo, *Effects of halothane and propofol on purified brain protein kinase C activation.* Anesthesiology, 1994. **81**(1): p. 147-55.
116. Bickler, P.E. and C.S. Fahlman, *The inhaled anesthetic, isoflurane, enhances Ca2+-dependent survival signaling in cortical neurons and modulates MAP kinases, apoptosis proteins and transcription factors during hypoxia.* Anesth Analg, 2006. **103**(2): p. 419-29, table of contents.
117. Bjornstrom, K., et al., *Orexin A inhibits propofol-induced neurite retraction by a phospholipase D/protein kinase Cepsilon-dependent mechanism in neurons.* PLoS One, 2014. **9**(5): p. e97129.
118. Li, Y., et al., *Propofol Regulates the Surface Expression of GABAA Receptors: Implications in Synaptic Inhibition.* Anesth Analg, 2015. **121**(5): p. 1176-83.
119. Zurek, A.A., et al., *Sustained increase in alpha5GABAA receptor function impairs memory after anesthesia.* J Clin Invest, 2014. **124**(12): p. 5437-41.
120. Peng, L., L. Xu, and W. Ouyang, *Role of peripheral inflammatory markers in postoperative cognitive dysfunction (POCD): a meta-analysis.* PLoS One, 2013. **8**(11): p. e79624.
121. Buvanendran, A., et al., *Upregulation of prostaglandin E2 and interleukins in the central nervous system and peripheral tissue during and after surgery in humans.* Anesthesiology, 2006. **104**(3): p. 403-10.
122. Fidalgo, A.R., et al., *Systemic inflammation enhances surgery-induced cognitive dysfunction in mice.* Neurosci Lett, 2011. **498**(1): p. 63-6.
123. Cibelli, M., et al., *Role of interleukin-1beta in postoperative cognitive dysfunction.* Ann Neurol, 2010. **68**(3): p. 360-8.
124. Wang, D.S., et al., *Memory deficits induced by inflammation are regulated by alpha5-subunit-containing GABAA receptors.* Cell Rep, 2012. **2**(3): p. 488-96.
125. Avramescu, S., et al., *Inflammation Increases Neuronal Sensitivity to General Anesthetics.* Anesthesiology, 2016. **124**(2): p. 417-27.
126. Kuver, A. and S.S. Smith, *Flumazenil decreases surface expression of alpha4beta2delta GABAA receptors by increasing the rate of receptor internalization.* Brain Res Bull, 2016. **120**: p. 131-43.
127. Abramian, A.M., et al., *Neurosteroids promote phosphorylation and membrane insertion of extrasynaptic GABAA receptors.* Proc Natl Acad Sci U S A, 2014. **111**(19): p. 7132-7.

128. Vinkers, C.H. and B. Olivier, *Mechanisms Underlying Tolerance after Long-Term Benzodiazepine Use: A Future for Subtype-Selective GABA(A) Receptor Modulators?* Adv Pharmacol Sci, 2012. **2012**: p. 416864.
129. Pietrzykowski, A.Z. and S.N. Treistman, *The molecular basis of tolerance.* Alcohol Res Health, 2008. **31**(4): p. 298-309.
130. Almeida-Suhett, C.P., et al., *Reduced GABAergic inhibition in the basolateral amygdala and the development of anxiety-like behaviors after mild traumatic brain injury.* PLoS One, 2014. **9**(7): p. e102627.
131. Zhang, N., et al., *Altered localization of GABA(A) receptor subunits on dentate granule cell dendrites influences tonic and phasic inhibition in a mouse model of epilepsy.* J Neurosci, 2007. **27**(28): p. 7520-31.
132. Peng, Z., et al., *Altered expression of the delta subunit of the GABAA receptor in a mouse model of temporal lobe epilepsy.* J Neurosci, 2004. **24**(39): p. 8629-39.
133. Vutskits, L. and Z. Xie, *Lasting impact of general anaesthesia on the brain: mechanisms and relevance.* Nat Rev Neurosci, 2016. **17**(11): p. 705-717.
134. Zhao, X., et al., *Dual effects of isoflurane on proliferation, differentiation, and survival in human neuroprogenitor cells.* Anesthesiology, 2013. **118**(3): p. 537-49.
135. Zhang, Y., et al., *Different effects of anesthetic isoflurane on caspase-3 activation and cytosol cytochrome c levels between mice neural progenitor cells and neurons.* Front Cell Neurosci, 2014. **8**: p. 14.
136. Yang, Y., et al., *STAT3 degradation mediated by calcineurin involved in the neurotoxicity of isoflurane.* Neuroreport, 2016. **27**(2): p. 124-30.
137. Wang, Q., et al., *The common inhaled anesthetic isoflurane increases aggregation of huntingtin and alters calcium homeostasis in a cell model of Huntington's disease.* Toxicol Appl Pharmacol, 2011. **250**(3): p. 291-8.
138. Ni, C., et al., *Isoflurane induced cognitive impairment in aged rats through hippocampal calcineurin/NFAT signaling.* Biochem Biophys Res Commun, 2015. **460**(4): p. 889-95.
139. Kaech, S. and G. Banker, *Culturing hippocampal neurons.* Nat Protoc, 2006. **1**(5): p. 2406-15.
140. Culley, D.J., et al., *Isoflurane decreases self-renewal capacity of rat cultured neural stem cells.* Anesthesiology, 2011. **115**(4): p. 754-63.
141. Jiang, M. and G. Chen, *High Ca2+-phosphate transfection efficiency in low-density neuronal cultures.* Nat Protoc, 2006. **1**(2): p. 695-700.
142. Wang, J., et al., *Interaction of calcineurin and type-A GABA receptor gamma 2 subunits produces long-term depression at CA1 inhibitory synapses.* J Neurosci, 2003. **23**(3): p. 826-36.
143. Miesenbock, G., D.A. De Angelis, and J.E. Rothman, *Visualizing secretion and synaptic transmission with pH-sensitive green fluorescent proteins.* Nature, 1998. **394**(6689): p. 192-5.
144. Terunuma, M., et al., *Deficits in phosphorylation of GABA(A) receptors by intimately associated protein kinase C activity underlie compromised synaptic inhibition during status epilepticus.* J Neurosci, 2008. **28**(2): p. 376-84.

145. Song, C.Y., et al., *Propofol inhibited the delayed rectifier potassium current (I(k)) via activation of protein kinase C epsilon in rat parietal cortical neurons.* Eur J Pharmacol, 2011. **653**(1-3): p. 16-20.
146. Wickley, P.J., et al., *Propofol modulates agonist-induced transient receptor potential vanilloid subtype-1 receptor desensitization via a protein kinase Cepsilon-dependent pathway in mouse dorsal root ganglion sensory neurons.* Anesthesiology, 2010. **113**(4): p. 833-44.
147. Wang, H., et al., *Isoflurane induces endoplasmic reticulum stress and caspase activation through ryanodine receptors.* Br J Anaesth, 2014. **113**(4): p. 695-707.
148. Zhang, Y., et al., *Propofol and magnesium attenuate isoflurane-induced caspase-3 activation via inhibiting mitochondrial permeability transition pore.* Med Gas Res, 2012. **2**(1): p. 20.
149. Wei, H., et al., *Isoflurane and sevoflurane affect cell survival and BCL-2/BAX ratio differently.* Brain Res, 2005. **1037**(1-2): p. 139-47.
150. Asokan, A. and M.J. Cho, *Exploitation of intracellular pH gradients in the cellular delivery of macromolecules.* J Pharm Sci, 2002. **91**(4): p. 903-13.
151. Lin, D.T., et al., *Regulation of AMPA receptor extrasynaptic insertion by 4.1N, phosphorylation and palmitoylation.* Nat Neurosci, 2009. **12**(7): p. 879-87.
152. Baumgartel, K. and I.M. Mansuy, *Neural functions of calcineurin in synaptic plasticity and memory.* Learn Mem, 2012. **19**(9): p. 375-84.
153. Reese, L.C. and G. Taglialatela, *A role for calcineurin in Alzheimer's disease.* Curr Neuropharmacol, 2011. **9**(4): p. 685-92.
154. Zhang, Y., et al., *Anesthetics isoflurane and desflurane differently affect mitochondrial function, learning, and memory.* Ann Neurol, 2012. **71**(5): p. 687-98.
155. Liu, J., et al., *Calcineurin is a common target of cyclophilin-cyclosporin A and FKBP-FK506 complexes.* Cell, 1991. **66**(4): p. 807-15.
156. Klintmalm, G., et al., *Cyclosporine plasma levels in renal transplant patients. Association with renal toxicity and allograft rejection.* Transplantation, 1985. **39**(2): p. 132-7.
157. Reagan-Shaw, S., M. Nihal, and N. Ahmad, *Dose translation from animal to human studies revisited.* FASEB J, 2008. **22**(3): p. 659-61.
158. Gross, C., et al., *Fragile X mental retardation protein regulates protein expression and mRNA translation of the potassium channel Kv4.2.* J Neurosci, 2011. **31**(15): p. 5693-8.
159. Parker, J.G., et al., *Attenuating GABA(A) receptor signaling in dopamine neurons selectively enhances reward learning and alters risk preference in mice.* J Neurosci, 2011. **31**(47): p. 17103-12.
160. Yin, Y., et al., *Tau accumulation induces synaptic impairment and memory deficit by calcineurin-mediated inactivation of nuclear CaMKIV/CREB signaling.* Proc Natl Acad Sci U S A, 2016. **113**(26): p. E3773-81.
161. Supnet, C. and I. Bezprozvanny, *Neuronal calcium signaling, mitochondrial dysfunction, and Alzheimer's disease.* J Alzheimers Dis, 2010. **20 Suppl 2**: p. S487-98.

162. Mukherjee, A. and C. Soto, *Role of calcineurin in neurodegeneration produced by misfolded proteins and endoplasmic reticulum stress.* Curr Opin Cell Biol, 2011. **23**(2): p. 223-30.
163. Lin, D., et al., *Lidocaine attenuates cognitive impairment after isoflurane anesthesia in old rats.* Behav Brain Res, 2012. **228**(2): p. 319-27.
164. Jarrard, L.E., et al., *On the role of hippocampal connections in the performance of place and cue tasks: comparisons with damage to hippocampus.* Behav Neurosci, 1984. **98**(6): p. 946-54.
165. Deiner, S. and J.H. Silverstein, *Postoperative delirium and cognitive dysfunction.* Br J Anaesth, 2009. **103 Suppl 1**: p. i41-46.
166. Li, X.M., et al., *Disruption of hippocampal neuregulin 1-ErbB4 signaling contributes to the hippocampus-dependent cognitive impairment induced by isoflurane in aged mice.* Anesthesiology, 2014. **121**(1): p. 79-88.
167. Istaphanous, G.K., et al., *Characterization and quantification of isoflurane-induced developmental apoptotic cell death in mouse cerebral cortex.* Anesth Analg, 2013. **116**(4): p. 845-54.
168. Wong, M. and K.A. Yamada, *Cyclosporine induces epileptiform activity in an in vitro seizure model.* Epilepsia, 2000. **41**(3): p. 271-6.
169. Racusen, L.C., et al., *Cyclosporine lowers seizure threshold in an experimental model of electroshock-induced seizures in Munich-Wistar rats.* Life Sci, 1990. **46**(14): p. 1021-6.
170. Garcia-Escrig, M., et al., *Severe central nervous system toxicity after chronic treatment with cyclosporine.* Clin Neuropharmacol, 1994. **17**(3): p. 298-302.
171. Furman, J.L., et al., *Blockade of Astrocytic Calcineurin/NFAT Signaling Helps to Normalize Hippocampal Synaptic Function and Plasticity in a Rat Model of Traumatic Brain Injury.* J Neurosci, 2016. **36**(5): p. 1502-15.
172. Culley, D.J., et al., *Impaired acquisition of spatial memory 2 weeks after isoflurane and isoflurane-nitrous oxide anesthesia in aged rats.* Anesth Analg, 2004. **99**(5): p. 1393-7; table of contents.
173. Culley, D.J., et al., *The memory effects of general anesthesia persist for weeks in young and aged rats.* Anesth Analg, 2003. **96**(4): p. 1004-9, table of contents.
174. Williams, C.R. and J.L. Gooch, *Calcineurin inhibitors and immunosuppression - a tale of two isoforms.* Expert Rev Mol Med, 2012. **14**: p. e14.
175. Wu, H.Y., et al., *Amyloid beta induces the morphological neurodegenerative triad of spine loss, dendritic simplification, and neuritic dystrophies through calcineurin activation.* J Neurosci, 2010. **30**(7): p. 2636-49.
176. Norris, C.M., et al., *Calcineurin triggers reactive/inflammatory processes in astrocytes and is upregulated in aging and Alzheimer's models.* J Neurosci, 2005. **25**(18): p. 4649-58.
177. Mohmmad Abdul, H., et al., *Proteolysis of calcineurin is increased in human hippocampus during mild cognitive impairment and is stimulated by oligomeric Abeta in primary cell culture.* Aging Cell, 2011. **10**(1): p. 103-13.
178. Winder, D.G. and J.D. Sweatt, *Roles of serine/threonine phosphatases in hippocampal synaptic plasticity.* Nat Rev Neurosci, 2001. **2**(7): p. 461-74.

179. Lu, Y.M., et al., *Calcineurin-mediated LTD of GABAergic inhibition underlies the increased excitability of CA1 neurons associated with LTP.* Neuron, 2000. **26**(1): p. 197-205.
180. Shaw, J.A., et al., *Role of calcineurin in inhibiting disadvantageous associations.* Neuroscience, 2012. **203**: p. 144-52.
181. Borlongan, C.V., T. Fujisaki, and S. Watanabe, *Chronic cyclosporine-A injection in rats with damaged blood-brain barrier does not impair retention of passive avoidance.* Neurosci Res, 1998. **32**(3): p. 195-200.
182. Borlongan, C.V., T. Fujisaki, and S. Watanabe, *Chronic administration of cyclosporine A does not impair memory retention in rats.* Neuroreport, 1997. **8**(3): p. 673-6.
183. Groth, R.D., R.L. Dunbar, and P.G. Mermelstein, *Calcineurin regulation of neuronal plasticity.* Biochem Biophys Res Commun, 2003. **311**(4): p. 1159-71.
184. Zeng, H., et al., *Forebrain-specific calcineurin knockout selectively impairs bidirectional synaptic plasticity and working/episodic-like memory.* Cell, 2001. **107**(5): p. 617-29.
185. Chambers, M.S., et al., *An orally bioavailable, functionally selective inverse agonist at the benzodiazepine site of GABAA alpha5 receptors with cognition enhancing properties.* J Med Chem, 2004. **47**(24): p. 5829-32.
186. Rudolph, U. and H. Mohler, *GABAA receptor subtypes: Therapeutic potential in Down syndrome, affective disorders, schizophrenia, and autism.* Annu Rev Pharmacol Toxicol, 2014. **54**: p. 483-507.
187. Sur, C., et al., *Autoradiographic localization of alpha5 subunit-containing GABAA receptors in rat brain.* Brain Res, 1999. **822**(1-2): p. 265-70.
188. Pirker, S., et al., *GABA(A) receptors: immunocytochemical distribution of 13 subunits in the adult rat brain.* Neuroscience, 2000. **101**(4): p. 815-50.
189. Ali, A.B. and A.M. Thomson, *Synaptic alpha 5 subunit-containing GABAA receptors mediate IPSPs elicited by dendrite-preferring cells in rat neocortex.* Cereb Cortex, 2008. **18**(6): p. 1260-71.
190. Crestani, F., et al., *Trace fear conditioning involves hippocampal alpha5 GABA(A) receptors.* Proc Natl Acad Sci U S A, 2002. **99**(13): p. 8980-5.
191. Collinson, N., et al., *Enhanced learning and memory and altered GABAergic synaptic transmission in mice lacking the alpha 5 subunit of the GABAA receptor.* J Neurosci, 2002. **22**(13): p. 5572-80.
192. Collinson, N., et al., *An inverse agonist selective for alpha5 subunit-containing GABAA receptors improves encoding and recall but not consolidation in the Morris water maze.* Psychopharmacology (Berl), 2006. **188**(4): p. 619-28.
193. Glykys, J. and I. Mody, *Hippocampal network hyperactivity after selective reduction of tonic inhibition in GABA A receptor alpha5 subunit-deficient mice.* J Neurophysiol, 2006. **95**(5): p. 2796-807.
194. Scimemi, A., et al., *Epileptogenesis is associated with enhanced glutamatergic transmission in the perforant path.* J Neurophysiol, 2006. **95**(2): p. 1213-20.
195. Houser, C.R. and M. Esclapez, *Downregulation of the alpha5 subunit of the GABA(A) receptor in the pilocarpine model of temporal lobe epilepsy.* Hippocampus, 2003. **13**(5): p. 633-45.

196. Vos, P., et al., *Infectious RNA transcripts derived from full-length DNA copies of the genomic RNAs of cowpea mosaic virus.* Virology, 1988. **165**(1): p. 33-41.
197. Howard, M.A., J.L. Rubenstein, and S.C. Baraban, *Bidirectional homeostatic plasticity induced by interneuron cell death and transplantation in vivo.* Proc Natl Acad Sci U S A, 2014. **111**(1): p. 492-7.
198. Stanley, E.M., J.R. Fadel, and D.D. Mott, *Interneuron loss reduces dendritic inhibition and GABA release in hippocampus of aged rats.* Neurobiol Aging, 2012. **33**(2): p. 431 e1-13.
199. Sanderson, J.L., J.A. Gorski, and M.L. Dell'Acqua, *NMDA Receptor-Dependent LTD Requires Transient Synaptic Incorporation of Ca(2)(+)-Permeable AMPARs Mediated by AKAP150-Anchored PKA and Calcineurin.* Neuron, 2016. **89**(5): p. 1000-15.
200. Arendt, K.L., et al., *Calcineurin mediates homeostatic synaptic plasticity by regulating retinoic acid synthesis.* Proc Natl Acad Sci U S A, 2015. **112**(42): p. E5744-52.
201. Sik, A., et al., *The absence of a major Ca2+ signaling pathway in GABAergic neurons of the hippocampus.* Proc Natl Acad Sci U S A, 1998. **95**(6): p. 3245-50.
202. Krzisch, M., et al., *Propofol anesthesia impairs the maturation and survival of adult-born hippocampal neurons.* Anesthesiology, 2013. **118**(3): p. 602-10.
203. Quadrato, G., et al., *Modulation of GABAA receptor signaling increases neurogenesis and suppresses anxiety through NFATc4.* J Neurosci, 2014. **34**(25): p. 8630-45.
204. Strom, C. and L.S. Rasmussen, *Challenges in anaesthesia for elderly.* Singapore Dent J, 2014. **35C**: p. 23-29.
205. Roehrl, M.H., et al., *Selective inhibition of calcineurin-NFAT signaling by blocking protein-protein interaction with small organic molecules.* Proc Natl Acad Sci U S A, 2004. **101**(20): p. 7554-9.
206. Franks, N.P. and W.R. Lieb, *Temperature dependence of the potency of volatile general anesthetics: implications for in vitro experiments.* Anesthesiology, 1996. **84**(3): p. 716-20.
207. Jenkins, A., N.P. Franks, and W.R. Lieb, *Effects of temperature and volatile anesthetics on GABA(A) receptors.* Anesthesiology, 1999. **90**(2): p. 484-91.
208. Smith, C., et al., *Leakage and absorption of isoflurane by different types of anaesthetic circuit and monitoring tubing.* Anaesthesia, 2002. **57**(7): p. 686-9.